GRI-93/0050

SAND93-7039

Topical Report

Multi-Site Project Seismic Verification Experiment and Assessment of Site Suitability

Prepared by:
CER Corporation
Sandia National Laboratories
Resources Engineering Systems

Gas Research Institute

Tight Sands and Gas Processing Research Department
February 1993

214p.

GRI-93/0050

Topical Report

Multi-Site Project Seismic Verification Experiment and Assessment of Site Suitability

Prepared by:

CER Corporation
950 Grier Drive
Las Vegas, NV 89119

Sandia National Laboratories
Advanced Technology Department 6114
Albuquerque, NM 87185-5800

Resources Engineering Systems
One Cambridge Center
Cambridge, MA 02142

Prepared for:

Gas Research Institute
8600 W. Bryn Mawr Avenue
Chicago, IL 60631

Tight Gas Sands Project Area
Contract No. 5091-221-2130
February 1993

GRI DISCLAIMER

LEGAL NOTICE: This publication was prepared as an account of work sponsored by the Gas Research Institute (GRI), and other organizations. Neither GRI, members of GRI, nor any person acting on behalf of either:

- makes any warranty or representation, express or implied, with respect to the accuracy, completeness, or usefulness of the information contained in this report, or that the use of any information, apparatus, method, or process disclosed in this report may not infringe privately-owned rights; or
- assumes any liability with respect to the use of, or for damages resulting from the use of, any information, apparatus, method, or process disclosed in this report.

Reference to trade names or specific commercial products, commodities, or services in this report does not represent or constitute an endorsement, recommendation, or favoring by GRI of the specific commercial product, commodity, or service.

CER CORPORATION DISCLAIMER

In the preparation of this report, CER Corporation has provided GRI with the benefit of its best judgement. However, because of the many variables and uncertainties inherent in drilling operations, CER Corporation cannot and does not guarantee results in utilizing the recommendations herein expressed and shall not be liable for any loss, cost or damage resulting from reliance upon its judgement.

Sandia National Laboratories

Albuquerque, New Mexico 87185

date: May 19, 1993

to: Distribution:

N.R. Warpinski

from: N.R. Warpinski, 6114

subject: Report Distribution

Enclosed are reports with a SAND number (SAND 93-7039) that have been printed by an outside printer to meet contract requirements.

Internal Distribution:

7141	Technical Library (5)
7613-2	Document Processing for DOE/OSTI (10)
7151	Technical Publications
8523-2	Central Technical Files

50272-101

REPORT DOCUMENTATION PAGE	1. REPORT NO. GRI-93/0050	2.	3. Recipient's Accession No.

4. Title and Subtitle Multi-Site Project Seismic Verification Experiment and Assessment of Site Suitability	5. Report Date February 1993 6.
7. Author(s) M. Middlebrook, R. Peterson/CER; N. Warpinski, B. Engler, G. Sleefe/SNL; M Cleary, T. Wright/RES; P. Branagan/Branagan & Assoc.	8. Performing Organization Rept. No.
9. Performing Organization Name and Address CER Corporation 950 Grier Drive Las Vegas, NV 89119	10. Project/Task/Work Unit No. 11. Contract(C) or Grant(G) No. (C) 5091-221-2130 (G)
12. Sponsoring Organization Name and Address Gas Research Institute 8600 W. Bryn Mawr Avenue Chicago, IL 60631	13. Type of Report & Period Covered Topical 14.

15. Supplementary Notes

Report prepared in coordination with Sandia National Laboratories and Resources Engineering Systems.

16. Abstract (Limit: 200 words)

The Multi-Site Project (M-Site No. 1) has been proposed as a means of resolving the significant unknowns associated with measuring and modeling the dimensions of hydraulic fractures. The proposed project would be performed using three existing wellbores associated with the former DOE Multiwell Experiment (MWX), as well as new wellbores drilled on the same site. The site initially appeared attractive because of: 1) multiple thick, laterally-continuous sandstone units present in the upper Mesaverde Group; 2) comprehensive, existing data sets which resulted from the MWX project; 3) the availability of the MWX wellbores for continued research; and 4) existing infrastructure which would facilitate the implementation of the project. However, before proceeding with full-scale project development, a series of assessments were necessary to definitively determine the suitability of the site from various perspectives. These perspectives included: 1) evaluation of confining stresses of the sandstone units; 2) assessment of wellbore (cement and casing) integrity; and 3) capability of remotely detecting seismic signals during a mini-frac. The site suitability assessments performed involved the use of existing stress data from the MWX wells and the acquisition of new seismic and fracture treatment data collected during field operations conducted in September and October 1992. These assessments concluded that the mechanical wellbore conditions, background seismic noise, seismic signal attenuation, remote seismic signal detection, stress contrast and hydraulic fracture pressure response clearly show that the MWX site is suitable for future fracture diagnostics experimentation to be conducted by GRI and DOE.

17. Document Analysis a. Descriptors

b. Identifiers/Open-Ended Terms

c. COSATI Field/Group

18. Availability Statement	19. Security Class (This Report)	21. No. of Pages
Unlimited	Unclassified	50 + app.
	20. Security Class (This Page)	22. Price
	Unclassified	

(See ANSI-Z39.18) *See Instructions on Reverse* OPTIONAL FORM 272 (4-77) (Formerly NTIS-35) Department of Commerce

Research Summary

Title Multi-Site Project Seismic Verification Experiment and Assessment of Site Suitability

Contractors CER Corporation
Sandia National Laboratories
Resources Engineering Systems

Principal Investigators M. Middlebrook, R. Peterson; CER
N. Warpinski, B. Engler, G. Sleefe; SNL
M. Cleary, T. Wright; RES
P. Branagan; Branagan & Associates

Report Date February 1993

Objective The objective of the seismic verification and site suitability assessment was to definitively determine the adequacy of the former U.S. Department of Energy (DOE) Multiwell Experiment site for continued fracture diagnostics and fracture modeling research to be jointly conducted by the Gas Research Institute (GRI) and DOE. The several evaluation perspectives included: 1) evaluation of confining stresses of the target sandstone units; 2) assessment of wellbore (cement and casing) integrity; and 3) capability of remotely detecting seismic signals during a mini-frac. The results of these assessments would provide the basis for selecting or rejecting this site for GRI/DOE research.

Technical Perspective Research work performed by GRI and DOE over the past several years has been directed at acquiring comprehensive data sets before, during and after hydraulic fracture treatments on a number of wells. Researchers have made significant advancements in several areas from these data, including evaluating formations, modeling fracture propagation processes, diagnosing the azimuth and height of the created fracture, and modeling production from a hydraulically fractured natural gas reservoir.

Significant advancements have been also made in developing and applying technology to define the stress characteristics of various rock layers, measure important parameters before, during and after a fracture treatment, and use that information in a hydraulic fracture propagation model to predict the shape and extent of the resulting hydraulic fracture. Based on these efforts, GRI and others have concluded that hydraulic fractures tend to be taller, wider and shorter in length than conventional models would predict.

Although considerable advances have been made, some important questions remain. Fracture propagation models in use in industry today can vary widely in their results for given input parameters due to various assumptions about the in-situ hydraulic fracturing process. In addition, diagnostic systems developed thus far are capable of determining only fracture azimuth and height. There is no technique available for accurately determining fracture length.

Technical Approach

GRI and DOE determined that a joint effort was necessary to focus on resolving the significant unknowns associated with measuring and modeling the dimensions of hydraulic fractures. The first site proposed for the hydraulic fracture experimentation is the former DOE MWX site located near Rifle, Colorado. This site, termed the Multi-Site (M-Site) No. 1, includes three closely-spaced wells (MWX-1, MWX-2 and MWX-3). The need for and location of future sites for the Multi-Site Project will be determined after an assessment of the results from this first site.

Results

The site suitability assessments performed involved the use of existing stress data from the MWX wells and the acquisition of new seismic and fracture treatment data collected during field operations conducted in September and October 1992. These assessments indicated the following:

- Wellbore and cement conditions of the MWX-2 and MWX-3 wells were suitable for acquiring high-quality seismic signals with low ambient noise levels.

- Log-derived stress data calibrated with in-situ stress test data indicate that a stress contrast ranging from 500 to 1,000 psi exists between the target sandstone units and the bounding lithologies. This stress contrast was considered suitable for limiting excessive fracture height growth.

- There were no unusual occurrences (e.g., near-wellbore effects) in pressure responses which inhibited 3-D modeling of the mini-frac treatment.

- Remote-wellbore monitoring during the mini-fracs was clearly able to identify over 1,000 microseisms during the hydraulic fracture injections. Limited analysis of these data indicated that the seismic signals can be spatially located and used for mapping the hydraulic fracture.

Based on these positive assessments, it is concluded that the MWX site is suitable for conducting additional comprehensive M-Site No. 1 fracture diagnostics and fracture model verification experiments.

Contents

Figures

Tables

1.0 Executive Summary

The Multi-Site Project (M-Site No. 1) has been proposed as a means of resolving the significant unknowns associated with measuring and modeling the dimensions of hydraulic fractures. The proposed project would be performed using three existing wellbores associated with the former DOE Multiwell Experiment (MWX), as well as new wellbores drilled on the same site. The site initially appeared attractive because of: 1) multiple thick, laterally-continuous sandstone units present in the upper Mesaverde Group; 2) comprehensive, existing data sets which resulted from the MWX project; 3) the availability of the MWX wellbores for continued research; and 4) existing infrastructure which would facilitate the implementation of the project.

However, before proceeding with full-scale project development, a series of assessments were necessary to definitively determine the suitability of the site from various perspectives. These perspectives included: 1) evaluation of confining stresses of the sandstone units; 2) assessment of wellbore (cement and casing) integrity; and 3) capability of remotely detecting seismic signals during a mini-frac.

The site suitability assessments performed involved the use of existing stress data from the MWX wells and the acquisition of new seismic and fracture treatment data collected during field operations conducted in September and October 1992. These assessments indicated the following:

- Wellbore and cement conditions of the MWX-2 and MWX-3 wells were suitable for acquiring high-quality seismic signals with low ambient noise levels.

- Log-derived stress data calibrated with in-situ stress test data indicate that a stress contrast ranging from 500 to 1,000 psi exists between the target sandstone units and the bounding lithologies. This stress contrast was considered suitable for limiting excessive fracture height growth.

- There were no unusual occurrences (e.g., near-wellbore effects) in pressure responses which inhibited 3-D modeling of the mini-frac treatment.

- Remote-wellbore monitoring during the mini-fracs was clearly able to identify over 1,000 microseisms during the hydraulic fracture injections. Limited analysis of these data indicated that the seismic signals can be spatially located and used for mapping the hydraulic fracture.

Based on these positive assessments, it is concluded that the MWX site is suitable for conducting additional comprehensive M-Site No. 1 fracture diagnostics and fracture model verification experiments.

2.0 Introduction

2.1 CONCEPT OF A HYDRAULIC FRACTURE DIAGNOSTICS SITE

Research work performed by the Gas Research Institute (GRI) and the U.S. Department of Energy (DOE) over the past several years has been directed at acquiring comprehensive data sets before, during and after hydraulic fracture treatments on a number of wells. Researchers have made significant advancements in several areas from these data, including evaluating formations, modeling fracture propagation processes, diagnosing the azimuth and height of the created fracture, and modeling production from a hydraulically fractured natural gas reservoir.

Significant advancements have been also made in developing and applying technology to define the stress characteristics of various rock layers, measure important parameters before, during and after a fracture treatment, and use that information in a hydraulic fracture propagation model to predict the shape and extent of the resulting hydraulic fracture. Based on these efforts, GRI and others have concluded that hydraulic fractures tend to be taller, wider and shorter in length than conventional models would predict.

Although considerable advances have been made, some important questions remain. Fracture propagation models in use in industry today can vary widely in their results for given input parameters due to various assumptions about the in-situ hydraulic fracturing process. In addition, diagnostic systems developed thus far are capable of determining only fracture azimuth and height. There is no technique available for accurately determining fracture length.

2.2 PROPOSED MULTI-SITE PROJECT

GRI and DOE determined that a joint effort was necessary to focus on resolving the significant unknowns associated with measuring and modeling the dimensions of hydraulic fractures. The first site proposed for the hydraulic fracture experimentation is the former DOE Multiwell Experiment (MWX) site located near Rifle, Colorado, as shown in Figure 1. This site, termed the Multi-Site (M-Site) No. 1, includes three closely-spaced wells (MWX-1, MWX-2 and MWX-3), as shown in Figure 2. The need for and location of future sites for the Multi-Site Project will be determined after an assessment of the results from this first site.

All of the proposed M-Site No. 1 experimentation will occur in several sandstone units present in the upper Mesaverde Group between 4,130 and 5,500 ft. These shallower sandstone units are desirable for multiple reasons:

1) the previous MWX project did not perform any hydraulic fracture stimulations above 5,500 ft;

2) few (if any) wellbore obstructions (e.g., bridgeplugs) exist above 5,500 ft;

3) shallower target intervals decrease operational costs associated with conducting experiments;

4) shallower depths promote the acquisition of higher quality data from surface-deployed instrumentation; and

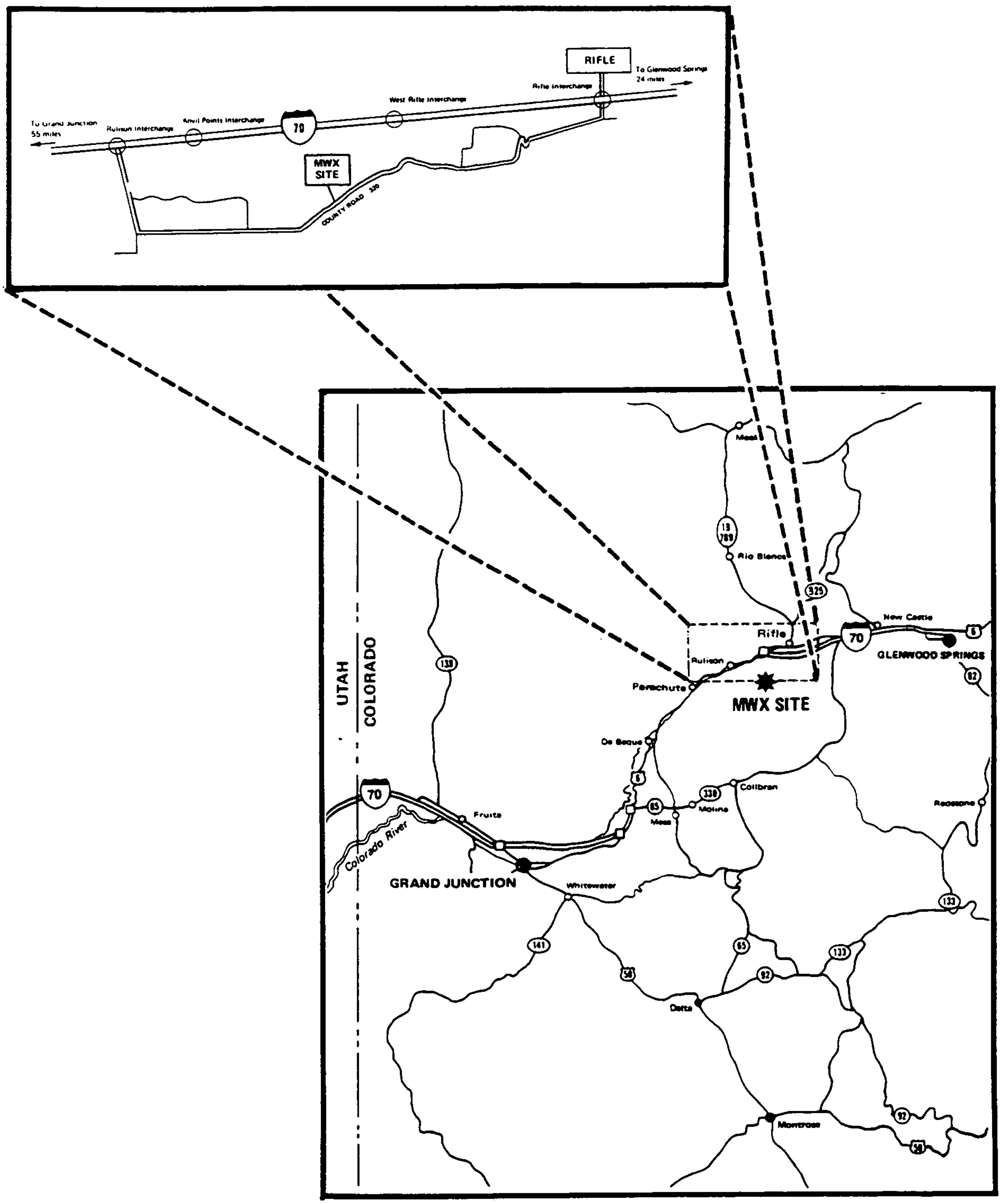

Figure 1 Geographic Location of the Multiwell Experiment Site

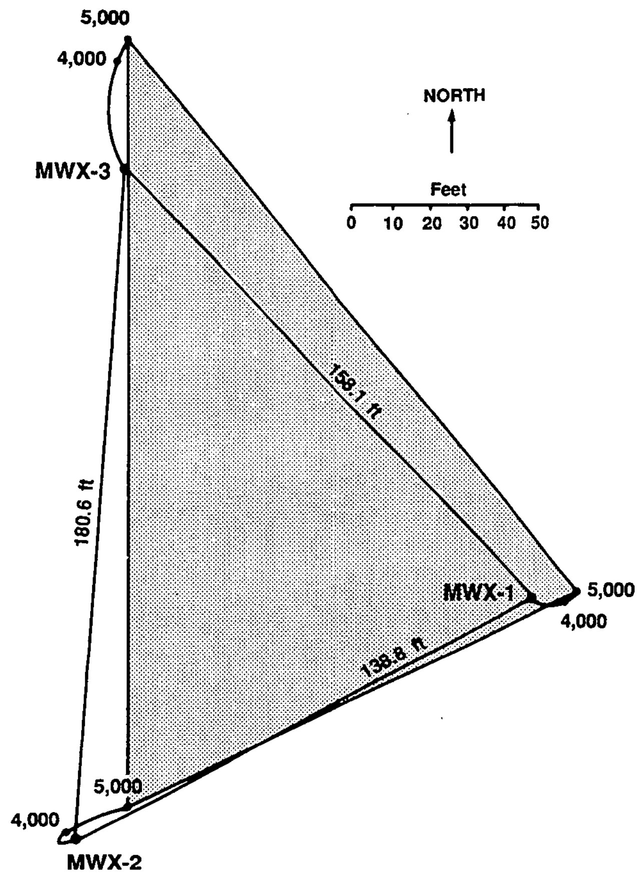

Figure 2 Closely-Spaced Wells of the MWX Project

5) the fluvial and paralic depositional environments of the upper Mesaverde were conducive to deposition of thick, laterally-continuous sandstone bodies.

Within the gross interval of 4,130 to 5,500 ft, there are three sandstone units which are proposed for diagnostic and modeling experimentation. These units are shown in Figure 3 and are referred to in this report as the A, B and C sands.

The fluvial and paralic sections of the upper Mesaverde, which includes the A, B and C sands, is characterized by thick, blanket-like (i.e., laterally continuous), low-permeability sandstone units. For example, the average dry core permeability of the sandstone unit between 4,290 and 4,366 ft in MWX-2 is 0.107 md and the average porosity is 5.2 percent as determined from core analyses. These upper Mesaverde sands have high water saturations (up to 100 percent) but gas saturations begin to increase below 4,500 ft as determined from existing core and log analyses.

Within the proposed test interval, there are abundant data which currently exists as a result of MWX research:

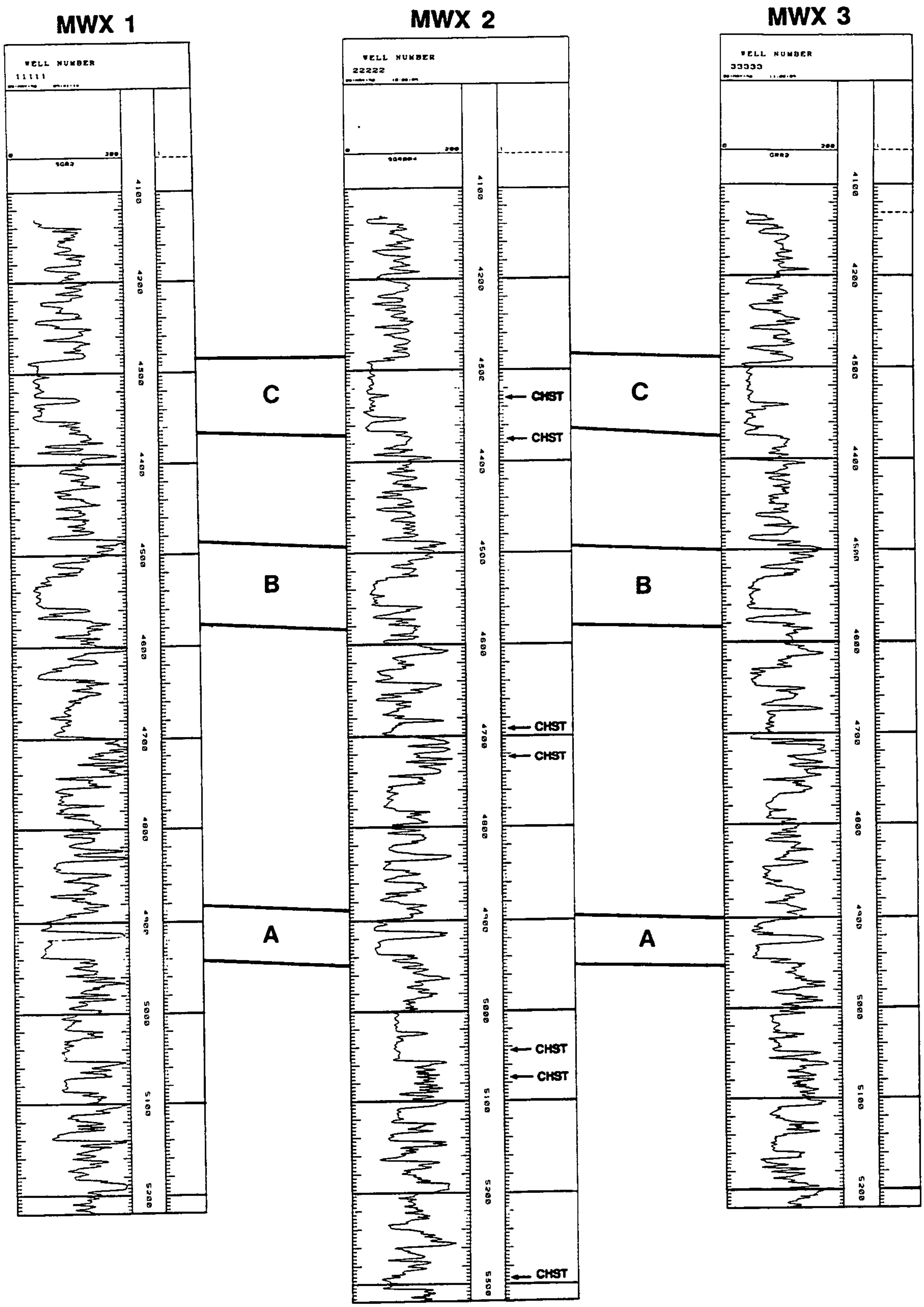

Figure 3 Upper Mesaverde Sandstone Units Proposed for M-Site No. 1 Research

- This entire proposed interval, from 4,170 to 5,550 ft, was continuously cored in the MWX-1 well. This core is now stored at Sandia and is available for continued analysis, if required. Routine and special core analyses have already been performed on much of this core to determine rock mechanical and reservoir properties. Mineralogic, petrographic and sedimentological analyses have also already been performed and results documented. The MWX-2 well was also cored in select intervals of the upper Mesaverde.

- Thirteen cased-hole stress tests have already been performed in the MWX-2 well between 4,170 ft and 5,502 ft. The depths of these intervals are graphically shown in Figure 3.

- Multiple overlapping runs of high-quality wireline log data exists for this interval and are archived at CER. The log and core data have been compiled into a depth-shifted, digital database which is also maintained at CER.

- Seismic data in the form of high-resolution 3-D, vertical seismic profile and cross-borehole is available.

Below the proposed test interval, there are additional data and information which will be useful to M-Site No. 1 research. These data and information include the following:

- Hydraulic fracture azimuth was determined to be N78°W based on 7 techniques in the deeper Mesaverde in the MWX wells.

- 3-D fracture modeling was previously performed on a hydraulic fracture treatment at 5,530 ft, so there is information on model behavior.

- Natural fractures and the associated onset of over-pressuring are known to occur primarily below 5,500 ft (below the proposed interval).

- Through work in 10 separate completion intervals, there were no indications of any near-wellbore effects during fracturing experiments. Thus, fracture treatment modeling is not expected to be hindered.

Appendix 1 includes a document that summarizes the accomplishments of the MWX project and gives a bibliography of the reports and technical papers which resulted from MWX research.

The proposed M-Site No. 1 is located 9 miles from Rifle, Colorado (see Figure 1). Access to the site is by paved road maintained by Garfield County. The site itself has all utilities (power, water, phone) existing for immediate hookup of a field facilities (offices, data acquisition systems). Surface use agreements have been previously negotiated with the landowner and future agreements are expected to be available.

2.3 OBJECTIVES OF SITE VERIFICATION

A series of analyses and field operations were required before proceeding with the full-scale project to verify that the M-Site No. 1 was technically suitable for hydraulic fracture experiments. The objectives of these verification efforts are described in the following sections.

2.3.1 Evaluate Cement and Wellbore Integrity

Cement and casing conditions, including pipe to formation bond, are crucial to conducting meaningful hydraulic fracture and seismic experiments in any of the wells located on the MWX site. The three MWX wells were drilled and cased between 1981 and 1985. Each used high-quality casing and were cemented to surface. However, since the MWX fracturing experiments focused on the deeper portions of the Mesaverde Group, evaluation of the cement bond in the upper sections may not have been a priority. Thus, an objective of the site verification was to evaluate existing cement bonding data to determine the quality of the cement to formation bond between 5,500 and 4,170 ft.

Accomplishing this objective would require a workover rig to drill out cement and an existing bridge plug at approximately 4,310 ft in the MWX-2 well. After this plug is drilled, a casing/scraper and gauge ring would be run in both wells to confirm that there are no obstructions or restrictions in either wellbore. A crosswell seismic monitoring survey would then be conducted between MWX-2 and MWX-3 to confirm that current wellbore conditions (e.g., cement bonding) are acceptable for conducting microseismic fracture diagnostics experiments.

2.3.2 Assess Confining Stresses

Data acquired during MWX is currently available to construct a calibrated stress profile. This data consists of multiple digital sonic logs, 12 in-situ stress tests, pore pressure measurements and rock mechanical properties core analyses. A calibrated stress profile would be constructed in the site verification process to assess the relative degree of stress contrast which can be expected in the upper Mesaverde Group.

2.3.3 Evaluate Background Seismic Noise Levels and Remote Detection of Microseism

After the integrity of the cement has been confirmed in both MWX-2 and MWX-3, small mini-frac injections would be performed in the A sand unit of MWX-3. While the injections are being pumped, a wireline seismic receiver locked into the MWX-2 well would collect data which would be transmitted and recorded by a surface high-speed data acquisition system. The objective of this effort would be to determine if analyzable microseisms would be generated in sufficient numbers so that hydraulic fracture geometry could be determined as a part of any experiment test plan.

3.0 Field Operations and Data Acquisition

3.1 WELLBORE PREPARATION

Upon initiating the site suitability assessments, the MWX-2 and MWX-3 wellbores had been shut-in for several years following the conclusion of the MWX experiment. The following operations were performed between August 25 and September 21, 1992, to prepare the wellbores for subsequent testing:

1) Each of the two wellbores were filled with 2 percent KCl water.

2) A bridgeplug and cement plug located at 4,310 ft in the MWX-2 well were drilled out and a new cast-iron bridgeplug was set at 5,020 ft. Re-setting the bridgeplug permitted the access to deeper portions of the wellbore and acquisition of seismic data in the A sand interval.

3) A gauge ring run in both MWX-2 and MWX-3 confirmed the fullbore diameter of the casing and that the wellbores were mechanically suitable for running instruments downhole.

The wellbore sketches for MWX-2 and MWX-3 at the completion of the operations described above are shown in Figures 4 and 5.

3.2 BACKGROUND NOISE AND WELLBORE CONDITION SEISMIC TEST

During the week of September 21, 1992, M-Site No. 1 suitability testing focused on determining if: 1) the ambient noise level at the site (primarily due to production in two proximal wells) is low enough that microseisms could be detected; and 2) the MWX-2 and MWX-3 wellbores are in sufficiently good condition that seismic signals will not be distorted or attenuated by poor cement bonding or behind-pipe, microannuli gas bubbling.

3.2.1 Seismic Receiver Instrumentation

Seismic data were acquired during the background noise testing and subsequent testing during the mini-frac with a new-generation seismic receiver developed by Sandia National Laboratories. Current seismic receivers used by industry exhibit significant resonances above about 200 to 400 Hz. The new receiver was designed using modal analysis and advanced accelerometer technology with the result that no resonances below 2,000 Hz are present and the electronic noise floor is extremely low. The receiver provided a signal quality that is superior to any results obtained previously with a wireline receiver.

3.2.2 Data Acquisition

On September 22, 1992, the seismic receiver was placed in MWX-2 at a depth of 4,800 ft and a background noise test was performed. Although some 60 cycle noise problems were occurring, the general noise background was about -150 db relative to 1 g/$\sqrt{\text{Hz}}$, extremely quiet compared to past microseismic experiments.

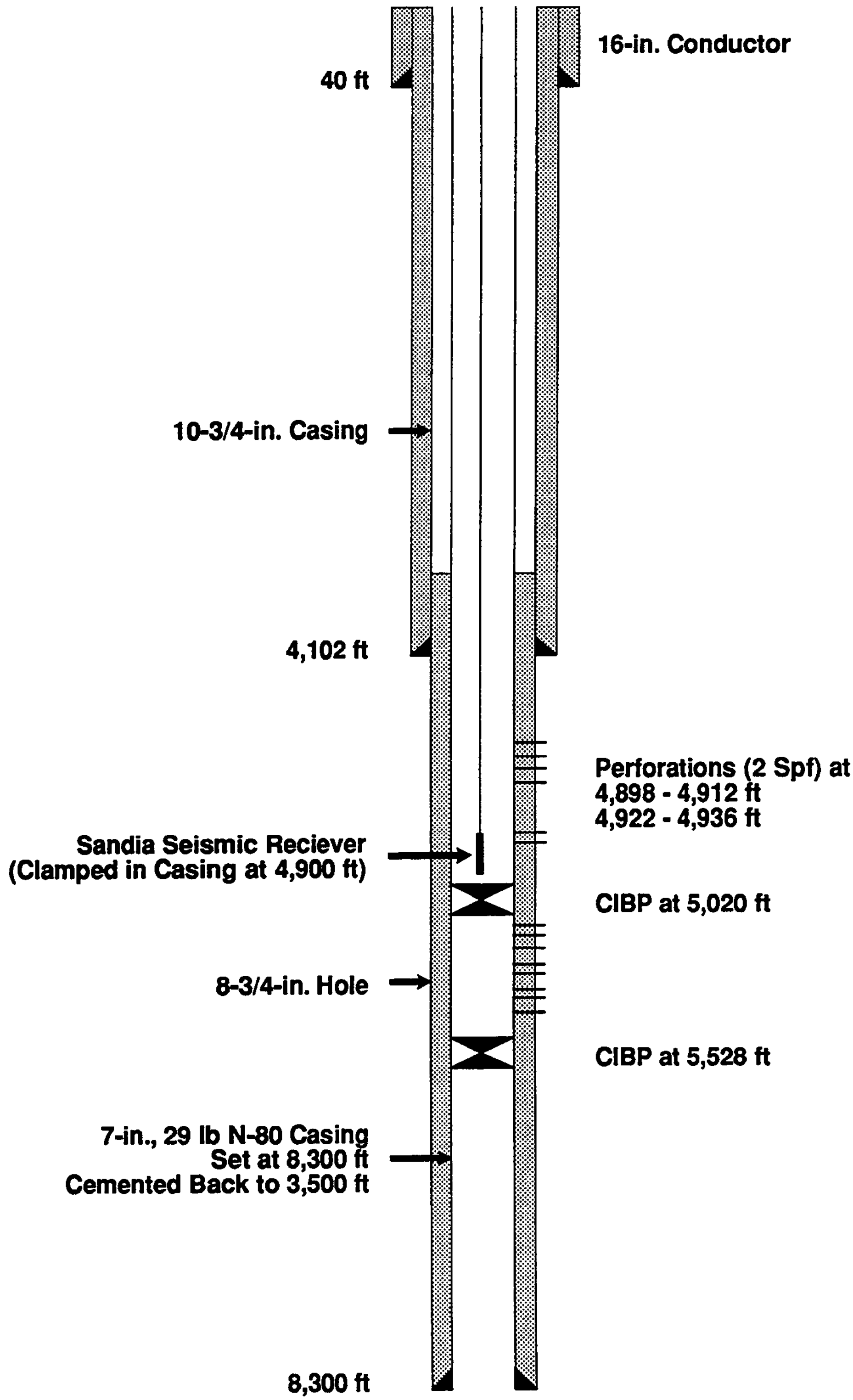

Figure 4 MWX-2 Wellbore Sketch

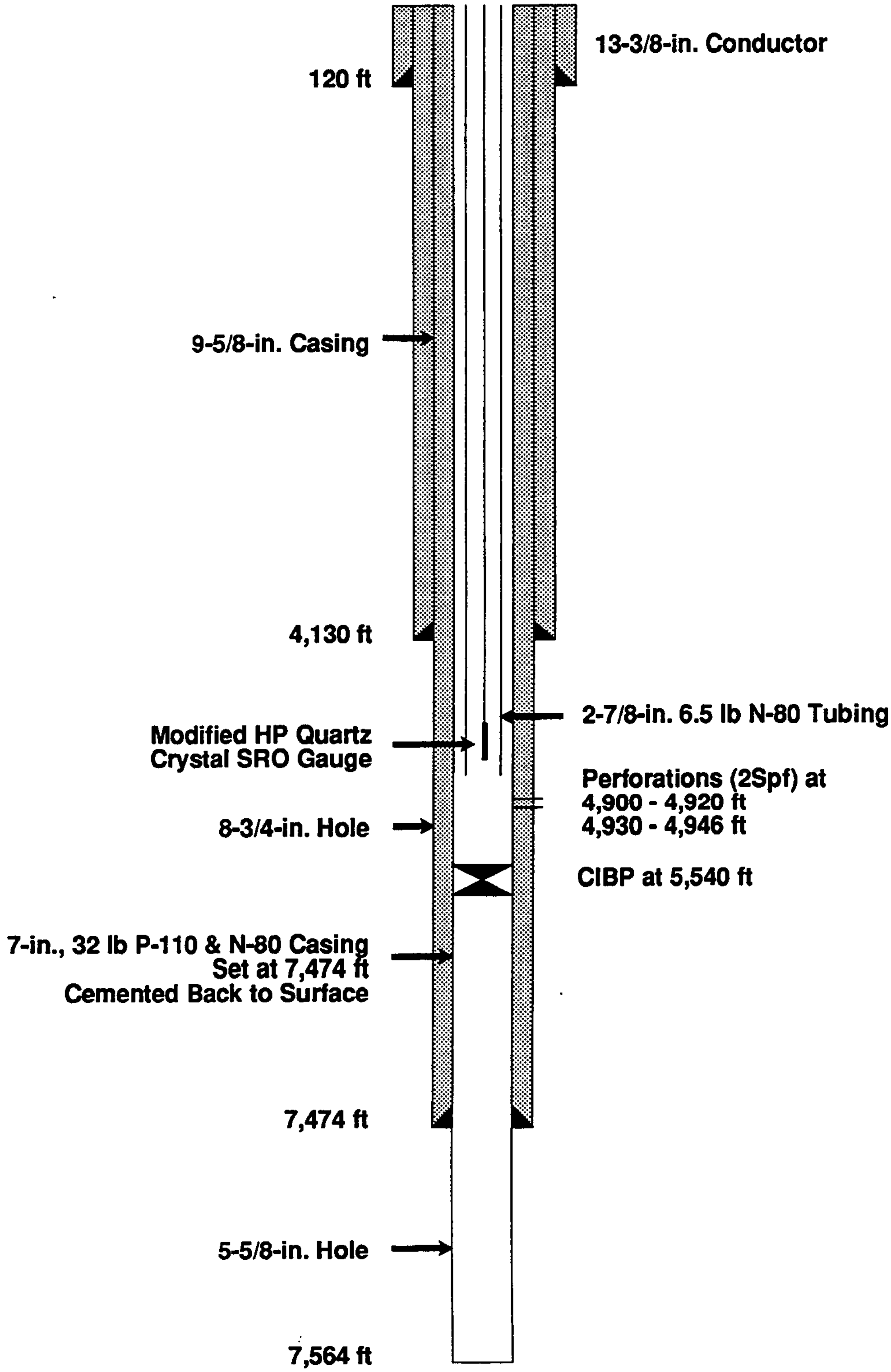

Figure 5 MWX-3 Wellbore Sketch

It should be noted here that there was a depth shift problem that was not reconciled until after these MWX-2 tests were completed. An uncertainty in depth in MWX-2 arose after tagging bottom at what was thought to be 5,006 ft. Although the wireline depth registered 4,908 ft when bottom was apparently tagged, it was suspected that the depth counter on the 7-conductor wireline may not have been accurate. As a result, all receiver depths in this well were set at [(100 ft) + (wireline depth)]. However, after this series of tests was completed, other tools were run in the hole and it was determined that there was likely an obstruction in MWX-2 just below 4,900 ft and the wireline depth was essentially correct. Thus, all receiver locations in this well were incorrectly set 100 ft higher than actually desired. This depth problem only occurred during this preliminary noise test. All depths were correct during the subsequent microseismic monitoring.

With the receiver set at 4,800 ft (and not 4,900 ft, as desired), small decoupled perforations (about 3.5 gm) were shot in MWX-3 at several depths, as shown in Table 1, and the signals were detected with the receiver in MWX-2. During these tests, the sampling rate was 0.25 msec, which should have been sufficient for signal frequencies in the 400 Hz range, the frequency range typical of most previous microseismic experiments. The perforation shots were clearly seen in MWX-2.

Table 1 Receiver (MWX-2) and Perforation (MWX-3) Locations

Receiver Depth, ft	**Perforation Depth, ft**
4,800	4,900
4,800	4,950
4,800	5,000
4,800	4,850
4,800	4,800
4,800	4,750
4,800	5,050
4,440	4,540
4,200	4,310
4,200	4,360

The seismic energy associated with the perforations exhibited a broad band energy spectrum from 200 to 1,500 Hz (1,500 Hz was the maximum capability of the recording system used on this test). Figure 6 shows an example perforation from the shot at 4,900 ft with the receiver at 4,800 ft. This figure includes traces from each of the accelerometers with all three channels scaled by the same factor. The first arrival of the p-wave is clear, and the primary energy is arriving on the y channel. Figure 7 shows an overlay of the two horizontal channels and the polarization plot, indicating the relative orientations in the horizontal and vertical planes. The hodogram clearly shows that the y channel is pointing almost directly north, which is the orientation of MWX-3 (the perforation well) relative to MWX-2.

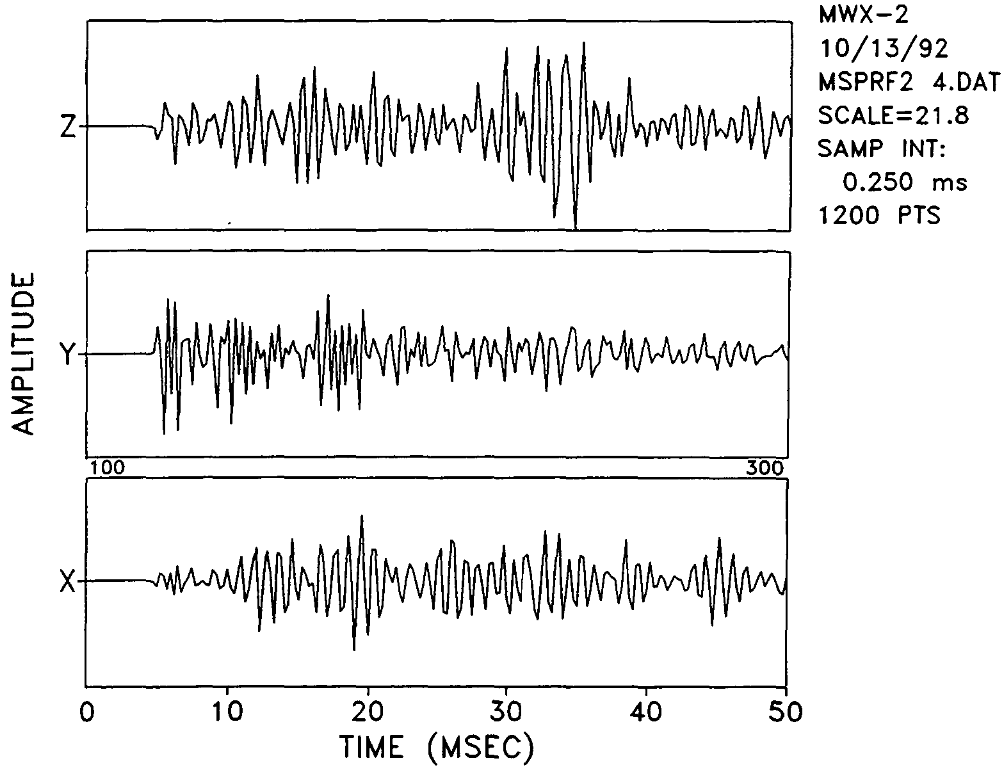

Figure 6 Example of Seismic Energy Generated from a Perforation Shot in MWX-2

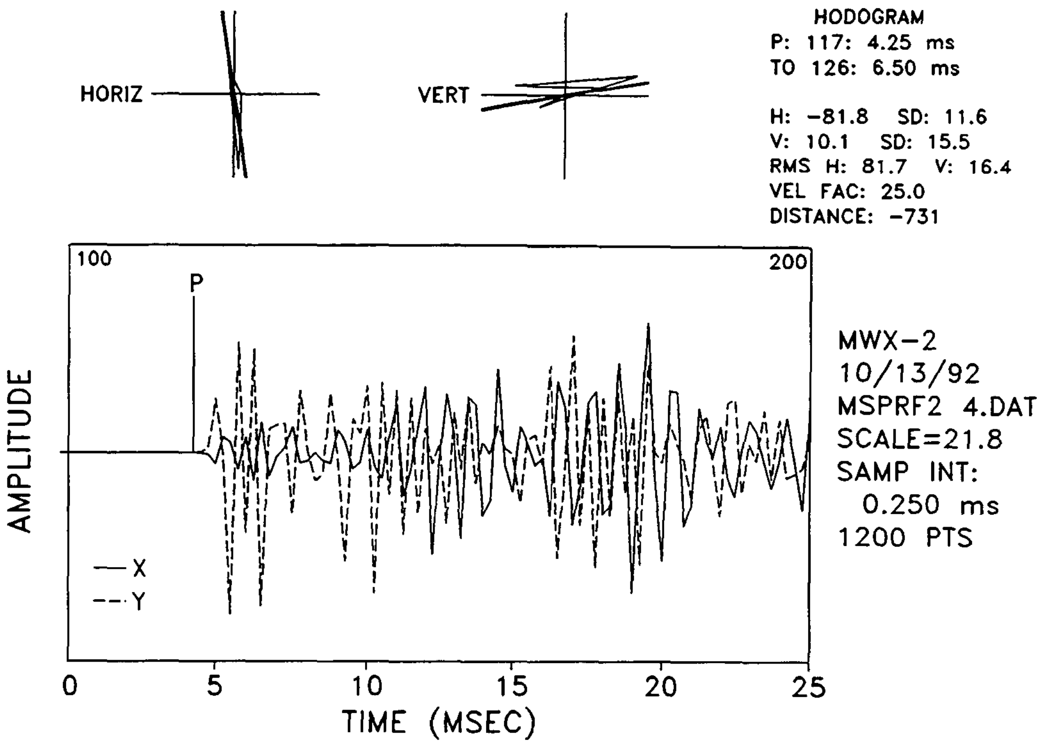

Figure 7 Overlay of X and Y Components and Hodogram, Perf Shot No. 1 in MWX-2

The only problem with these data is that the sampling rate is too slow relative to the event spectral content. Figure 8 shows an expanded view of the three separate channels. It can be seen in this figure that most cycles have only 3 to 5 points; this limited number of points is particularly a problem in the polarization plots where the hodogram of the first one or two cycles is used to determine orientation. (After the first cycle or two, other reflected, refracted, shear, or tube waves may begin to interfere.) Typically, only 6 to 10 points can be used for polarization analysis, which limits the ability to generate full statistics. Nevertheless, the available data shows that 1) the initial cycles of the events are highly polarized, so that event orientation can be determined, and 2) the first arrivals have a high signal-to-noise ratio.

The shear wave from these perforations is not easily determined, as can be seen in Figures 6, 7 and 8, but this difficulty is probably a function of the source, rather than the medium, the receiver wellbore, or the receiver itself. The perforation was purposely decoupled from the wellbore to avoid putting holes in the pipe. As a result, shear waves are only formed by conversion when the fluid compressional wave inside the wellbore strikes the pipe, cement annulus, and rock. It is not expected that this shear wave would necessarily be distinct under such conditions.

On September 23, 1992, the configuration was switched, with the receiver run in MWX-3 and the perforations shot in MWX-2. Table 2 shows the shot and receiver locations for these tests. Results from this reverse configuration were essentially the same as the first case, with either MWX-2 or MWX-3 appearing to be acceptable for monitoring.

3.2.3 Conclusions of Wellbore Condition Testing

In summary, the initial background and wellbore condition testing demonstrated that:

1) ambient noise levels at the site were low;

2) MWX-2 and MWX-3 wellbores are both suitable for microseismic monitoring;

3) clear first arrivals and well-defined polarizations can be obtained; and

4) higher sampling rates would be needed for microseismic monitoring.

3.3 MINI-FRAC TREATMENTS

The final phase of the M-site suitability experiments were conducted during the week of October 13, 1992, and involved the pumping of a breakdown/ballout treatment, step-rate test and two mini-frac injections in the MWX-3 well while collecting seismic data in the MWX-2 well. Figure 4 showed the wellbore configuration of the MWX-2 well, as a seismic monitor well, during the mini-frac testing. MWX-3 was perforated in the "A" sand at 4,900 to 4,920 ft and 4,930 to 4,946 ft with 72 holes (0.4 in.) at 2 shots per foot (SPF) and 120° phasing. Subsequently, a 2-7/8-in. tubing string was run and set at 4,879 ft.

Each of the treatments (except for the breakdown) were pumped down the 2-7/8- by 7-in. annulus. A surface readout pressure gauge was lowered to the end of the tubing to provide real-time bottomhole pressure data during the treatments. Figure 5 showed the wellbore configuration for MWX-3 during all of the injections except for the breakdown/ballout treatment.

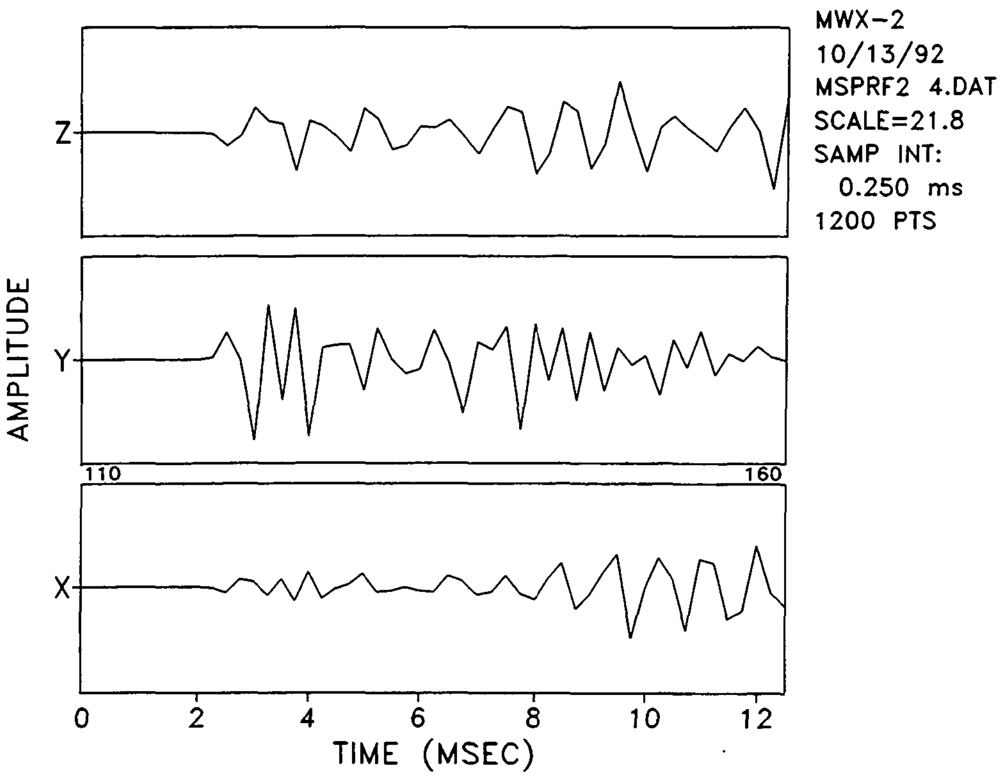

Figure 8 All Traces for Perf Shot No. 1 in MWX-2, Expanded View

Table 2 Receiver (MWX-3) and Perforation (MWX-2) Locations

Receiver Depth, ft	**Perforation Depth, ft**
4,935	4,995
4,935	4,975
4,935	4,955
4,935	4,935
4,935	4,915
4,935	4,895
4,935	4,875
4,540	4,540
4,310	4,310
4,310	4,310

The breakdown treatment was pumped down the 2-7/8-in. tubing while utilizing the annulus as a dead string measurement of bottomhole pressure.

The breakdown treatment consisted of spotting crosslinked gel at the end of the tubing and pumping approximately 78 bbl through the perforations. One hundred ball sealers were dropped in the last 25 bbl (of crosslinked gel) and the gel was over displaced with KCl water. Although no ball action was observed, the well was surged to allow the balls to fall.

A step-rate test was pumped about 5 hours after the breakdown treatment. The test included pumping 99 bbl of 2 percent KCl water at rates of 1, 2, 5, 8, 10 and 20 barrels per minute (BPM). The step-rate test was followed 2 hours later by a KCl mini-frac which consisted of pumping 304 bbl of KCl water at rates ranging from 0 to 30 BPM. The pump rates were intentionally varied to aid in the evaluation of near-wellbore friction pressure. Following the mini-frac, pressure decline data was acquired through the night to verify fracture closure pressure.

The final mini-frac consisted of pumping 634 bbl of 40-lb linear gel through the perforations at rates ranging from 0 to 25 BPM. The pressure decline was monitored for two hours following shutdown. All treatments were pumped by the Western Company.

3.4 MICROSEISMIC VERIFICATION TESTS

The microseismic monitoring part of the experiment was conducted in conjunction with the mini-frac treatments during the week of October 13. The receiver was placed in MWX-2 at 4,900 ft, just above the A sand; several 3.5-gm decoupled perforations were shot in MWX-3 to orient the tool. Perforation hodograms were similar to those observed in the background noise tests, with the y channel again pointing nearly north. Table 3 gives the receiver depths and perforation depths during orienting. The first three depths did not provide acceptable microseisms, so the tool was moved and reclamped until a suitable location (4,881 ft) was found.

Table 3 Orientation Results for Microseismic Monitoring

Receiver Depth, ft	Perforation Depth, ft	Comments
4,910	4,910	Poor Hodogram
4,897	4,910	Poor Hodogram
4,901	4,910	Poor Hodogram
4,881	4,910	
4,881	4,970	Perforation Misfire
4,881	4,940	
4,881	4,880	
4,881	4,840	
4,881	4,810	
4,881	4,970	

Prior to monitoring microseisms during the mini-fracs, breakdown and step-rate tests, a new recording system (Sony audio-digital cassette recorder) with a greater band width (0 to 5,000 Hz) and dynamic range (90 db) was purchased. Microseismic activity was monitored continuously on this system (no event detector was used), and individual signals were selected during playback at a later time. A direct computer interface to the Sony was not available at the time these tests were conducted and analyzed, so the data were played back into a manually-triggered EG&G recording device at a sampling rate of 0.05 msec. These raw data sets were used for determination of first arrivals, but any amplitude processing was performed using data that were low-pass filtered at 2,000 Hz. This filtering procedure eliminated the accelerometer resonances at 2,200 Hz.

Figures 9 through 12 show the number of signals obtained during the four injections, with each bar interval being 30 seconds. Only signals greater than 40μg's are included in these histograms. For reference the background noise levels are a few μg's, so these signals are at least ten times the noise level. After breakdown, as shown in Figure 9, there are approximately 20 microseisms per 30 second interval during the pumping, with the number of signals tapering off quickly after shut-in. Several hundred large signals were recorded during this short injection.

As seen in Figure 10, fewer signals were recorded during the step-rate test, with most of the signals observed during the high flow-rate periods. Approximately 300 signals were observed during this injection. The KCl injection, shown in Figure 11, also had fewer signals than the previous pump, with about 300 signals observed over a considerably longer time period. The gel mini-frac, a slightly larger volume than the KCl mini-frac, resulted in nearly double the number of microseisms, as can be seen in Figure 12. The most important point is that conditions at this site are such that large numbers of microseisms are generated by hydraulic fractures of even modest size (e.g., the breakdown or the step-rate test).

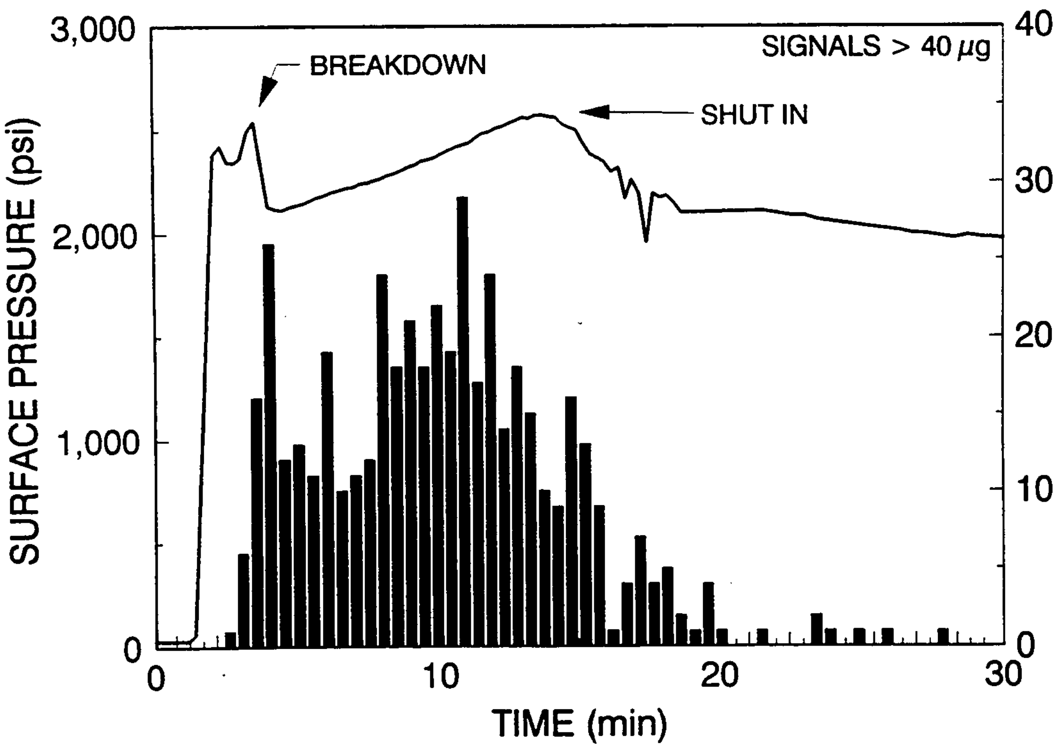

Figure 9 Histogram of Microseisms During Breakdown

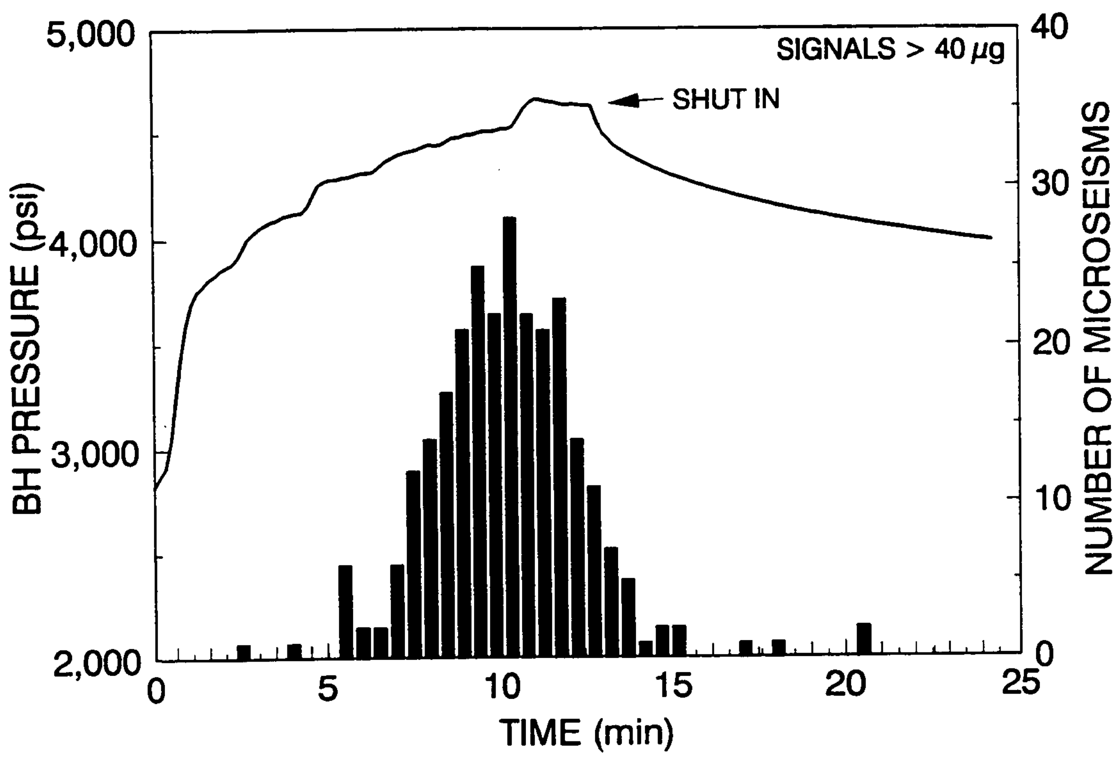

Figure 10 Histogram of Microseisms During Step-Rate Test

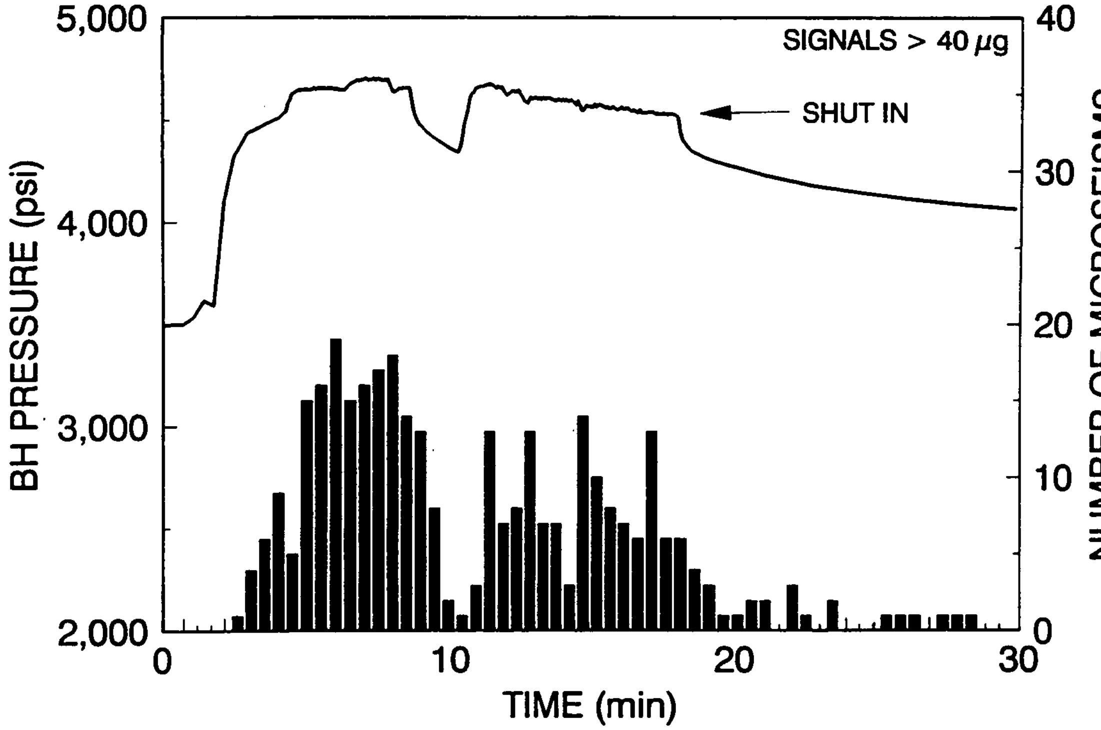

Figure 11 Histogram of Microseisms During KCl Mini-Frac

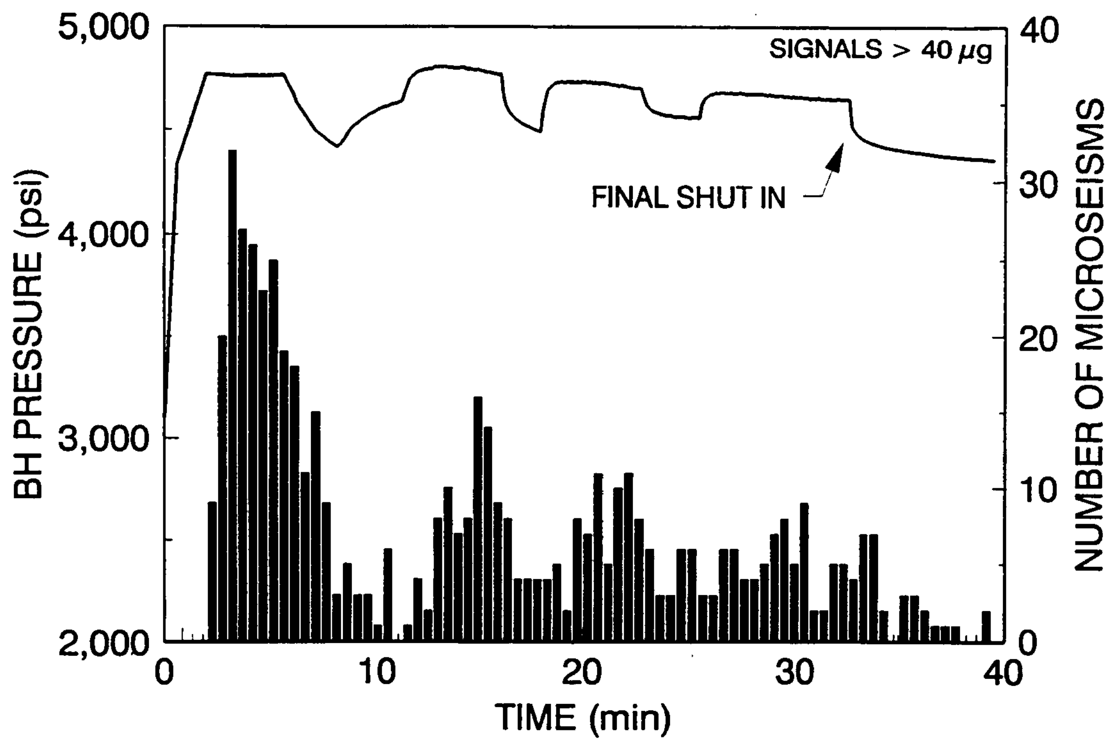

Figure 12 Histogram of Microseisms During Gel Mini-Frac

4.0 Results and Analyses

4.1 STRESS TESTING AND STRESS PROFILING

Log-derived stress profiles were constructed for the MWX-2 and MWX-3 wells over the interval 4,130 to 5,500 ft to verify the stress contrast between upper Mesaverde lithologic units. These profiles were normalized to MWX-2 stress test measurements.

4.1.1 Stress Data and Summary of Log Analysis Results

Eleven measurements of the minimum horizontal stress were made above 5,500 ft in the MWX-2 well. This stress test data was previously reported by Warpinski, 1990. For log-derived stress, the Amoco Long Spaced Sonic Log was used to analyze MWX-2 and the Schlumberger Long Spaced Sonic Log was used to analyze MWX-3. Both sets of log data have limitations. The Amoco data is more coherent; however, no Amoco acoustic data is available over the intervals 4,323 to 4,387 ft and 4,558 to 4,670 ft of MWX-2. The Schlumberger acoustic data was incoherent above 4,171 ft and below 5,300 ft; therefore, no analysis was performed above and below these respective depths in MWX-3. Incoherent Schlumberger acoustic data was also discriminated by hand within the analyzed interval as needed. Since all of the stress test data is from MWX-2, and since the MWX-2 Amoco log data in discontinuous, it was necessary to compare portions of the MWX-2 stress test data to correlative intervals of MWX-3.

The stress test data is combined with log-derived stress calculations in Table 4. Stress profile logs of MWX-2 and MWX-3 are included in Appendix 2. Figures 13 and 14 are crossplots comparing log-derived stress with stress test data. Figure 13 presents all data, and Figure 14 excludes one anomalous stress test point. Figure 14 shows satisfactory agreement between log-derived stress and stress test data.

4.1.2 Discussion of Log Analysis Model and Assumptions

The equation used to compute log-derived stress has been routinely used on many GRI Tight Gas Sand Program co-op wells and staged field experiments. It is presented here:

$$\sigma_h = \frac{\nu}{1-\nu}(\sigma_v - \alpha P_{pore}) + \alpha P_{pore}$$

$$\nu = \frac{0.05\,(\Delta_{ts} / \Delta_{tc})^2 - 1}{(\Delta_{ts} / \Delta_{tc})^2 - 1}$$

Poisson's Ratio (ν) is computed from the acoustic travel time log data (Δ_{ts} and Δ_{tc}). Overburden stress is assumed to have a gradient of 1.04 psi/ft. The Biot poro-elastic constant (α) is assumed to be 1.0. Pore pressure (P_{pore}) is based upon high quality well test data in deeper horizons. Pore pressure is fairly predictable at the M-Site No. 1, as shown in Figure

Table 4 Stress Test Data and Log-Derived Stresses

Interval, ft	Lithology	σ_{min}, psi	Log-Derived Stress, psi	Log-Derived Poisson's Ratio	Log-Derived Clay Volume, %
5,480 - 5,482	Sandstone	4,520 ± 20	4,669.6	0.230	7.4
5,450 - 5,452	Mudstone	4,715 ± 135	5,050.4	0.276	55.4
5,414 - 5,416	Mudstone	4,450 ± 100	4,675.0	0.244	56.2
5,320 - 5,322	Mudstone	4,800 ± 100	4,721.4	0.264	66.0
5,294 - 5,296	Sandstone	4,530 ± 20	4,503.7	0.242	34.2
5,074 - 5,076	Mudstone	4,650 ± 20	4,610.1	0.270	60.4
5,044 - 5,046	Sandstone	4,460 ± 30	4,094.2	0.206	26.4
4,714 - 4,716	Mudstone	5,250 ± 30	4,450.0	0.286	78.4
4,692 - 4,694	Sandstone	3,730 ± 50	3,945.9	0.260	22.4
4,376 - 4,378	Mudstone	4,050 ± 30	4,140.5*	0.256*	58.0*
4,330 - 4,332	Sandstone	3,350 ± 75	3,315.4*	0.192*	11.0*

*Log-derived stress for 4,376-4,378 ft and 4,330-4,332 ft are from correlated depths of MWX-3

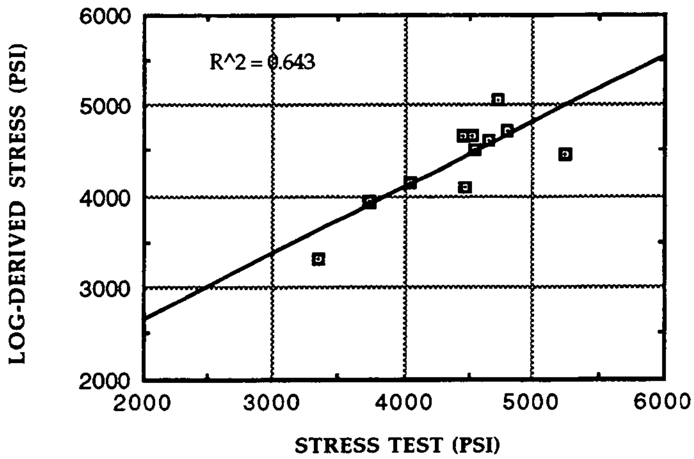

Figure 13 Normalized Log-Derived Stress (All Data)

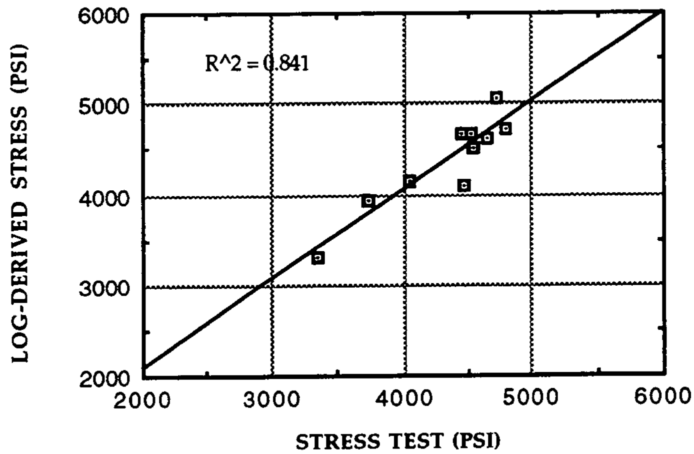

Figure 14 Normalized Log-Derived Stress (Minus One Data Point

15. The pore pressure data were extrapolated to the bottom of the gas-water transition interval at 4,850 ft. The water-bearing interval from 4,130 to 4,500 ft was assumed to have a pore pressure gradient of 0.433 psi/ft. From 4,850 to 4,500 ft the change in pressure gradient was made linear. The determination of residual tectonic stress ($\sigma_{tectonic}$) was less straightforward. Log-derived stress (σ_h) was first computed assuming that the residual tectonic stress is 0.0. Then the difference of the correlative stress test (σ_{min}) and "unnormalized" log-derived stress were assumed to be equivalent to the residual tectonic stress for each stress test interval. These results are shown in Figure 16.

It is clear that there is no predictable constant residual stress or residual stress gradient for all lithologies. The computed difference attributable to residual tectonic stress varies between 650.4 to 1,264.7 psi (and as much as 2,033.4 when the one anomalous stress test data point is included). The Figure 16 data were reduced to determine whether the residual tectonic stress varies with lithology. The average residual tectonic stress of sandstones is about 800 psi. The residual tectonic stress of mudstones would appear to vary with depth, as shown in Figure 17. Since the goal of this study was to empirically match the stress test data using log data, the log analysis model treats the residual tectonic stress of mudstones as a variable with depth. The log analysis uses the equation presented in Figure 17 to correct mudstones for the effects of residual tectonic stress when log-derived clay volume is greater than 55 percent. When log-derived clay volume is less than 35 percent, residual tectonic stress is treated as a constant. From 35 to 55 percent, the residual tectonic stress is weighted from a constant to a variable based on the log-derived clay volume.

4.1.3 Conclusions of Stress Profiling

The determination of log-derived stress in the upper Mesaverde Group at the M-Site No. 1 is not without some degree of uncertainty. As might be expected, the selection of a constant residual tectonic stress or stress gradient for varying lithologies is not so straightforward. The computed difference in residual tectonic stress varies between 650 to 1,265 psi for the combined lithologies. When taken separately, the residual tectonic stress for the sandstones is found to be a constant 800 psi while that for the mudstones appears to be best defined by a varying depth dependent stress gradient (see Figure 17).

However, the empirical approach used to predict log-derived in-situ stresses was useful. This stress profile, with only slight modifications, was used to produce a reasonable pressure match in the fracture modeling effort, as described in the Section 4.3. Improved interpretations of log-derived stress, however, may be derived by acquiring shear wave data from new-technology tools (e.g., Schlumberger Dipole Shear Wave Sonic Imager). It is recommended that acquisition of this data be considered when additional wells are drilled in the M-Site No. 1 project.

4.2 CALCULATION OF FRACTURE CLOSURE PRESSURE

As previously described, bottomhole pressure measurements were acquired during the execution of the mini-frac treatments. These pressure data were gathered using a quartz pressure gauge placed at or near the bottom of the tubing, as close as possible to the perforated fracturing interval. The resulting measurements provide the most accurate data set from which to assess true bottomhole fracturing pressures due to the close proximity of the pressure gauge to the fracturing interval. FRACPRO made use of this real-time data in modeling and assessing each of the treatments.

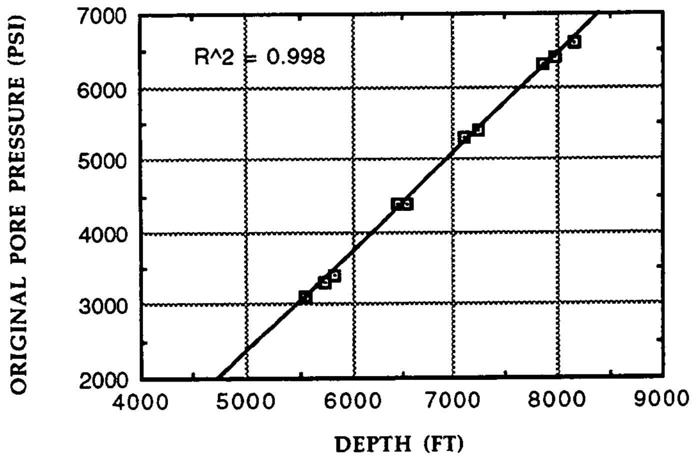

Figure 15 Original Pore Pressure Versus Depth

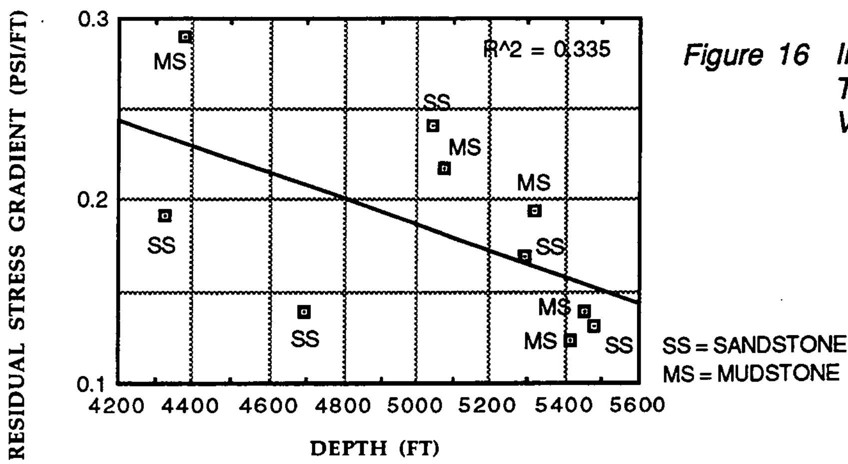

Figure 16 Interpreted Residual Tectonic Stress Gradient Versus Depth

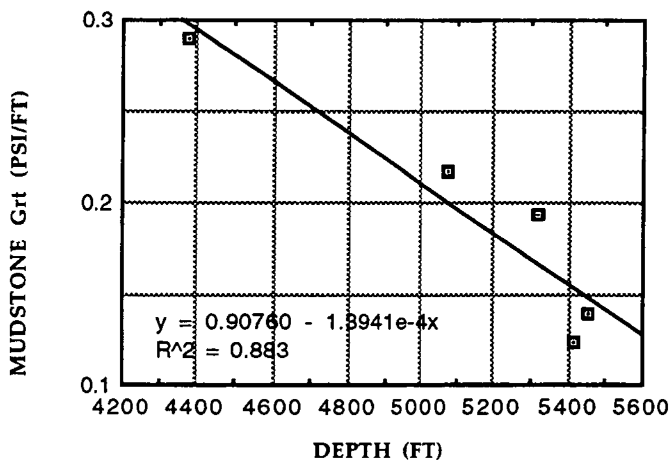

Figure 17 Mudstone Residual Tectonic Stress Gradient Versus Depth

A corollary to the acquisition of real-time fracture treatment pressure is the observation of the post-fracture or fall-off pressure. Analysis of this fall-off pressure can provide critical information regarding fracture closure pressure.

Fall-off pressure acquired following the KCl step-rate and the KCl mini-frac furnished an excellent data set from which to assess fracture closure pressure. However, the fall-off pressure that followed the gelled mini-frac was sporadic as viewed in the sensitive derivative analysis and thus was not used in assessing fracture closure. Bottomhole pressure could not be obtained during the ballout/breakdown procedure because of the nature of the test and the requisite configuring of the well.

4.2.1 KCl Step-Rate Pressure Fall-Off Analysis

Figure 18 is a log/log and derivative group plot of the bottomhole fall-off pressure that followed the KCl step-rate injection test. The log/log pressure plot is actually the difference pressure measured from the initial shut in and plotted in log/log coordinates, shown as stars. Initial shut-in pressure was taken to be 4,620 psi. As shown in Figure 18, the early portion of the shut in (up to 13 minutes) exhibits a straight line which subsequently shifts to a second straight line of much smaller slope. These two straight line portions suggest specific fluid flow regimes, such as linear, bilinear or radial.

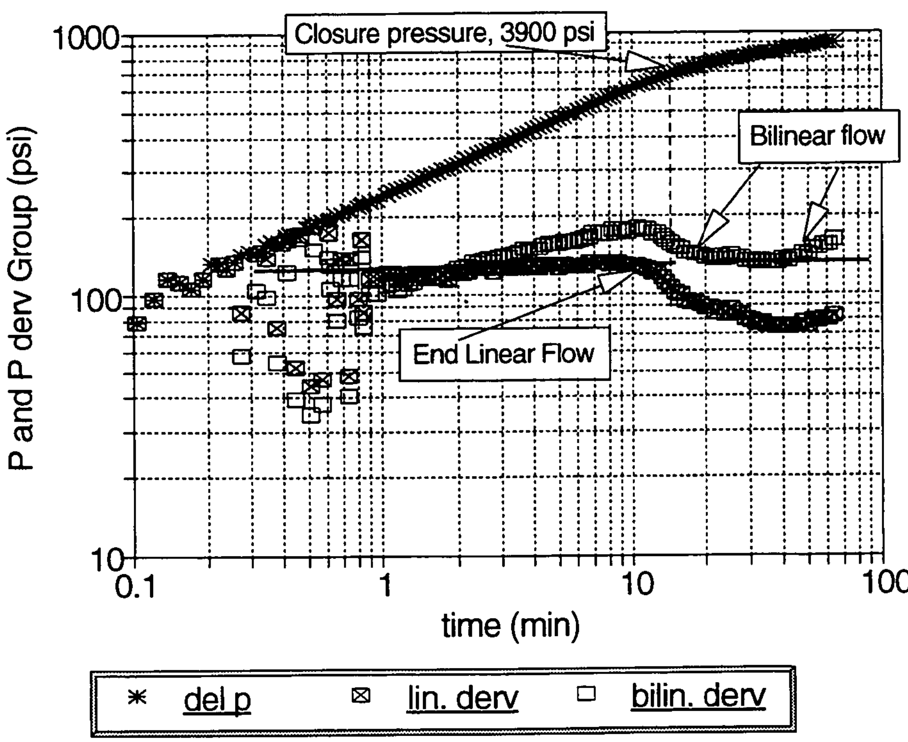

Figure 18 Log/Log and Derivative Group Plot of the Bottomhole Fall-Off Pressure Following the KCl Step-Rate Injection Test

The derivative group analysis are shown for linear and bilinear flow periods and assume that these flow regimes exist at some time during the falloff. When a pressure derivative exhibits a flat line, it suggests that the fluid movement is best described by that flow regime. The radial derivative is not shown for either test since radial flow was not expected nor did it appear to manifest itself during this short fall-off period. This is not surprising since the creation of an extended linear hydraulic fracture would normally induce some form of linear flow.

Note in this case that the linear group derivative, shown as a crossed square, is flat from about the first minute following shut in until about 12 minutes. It is assumed that this indicates fracturing fluids residing in the open frac are continuously being forced or imbibed into the reservoir rather uniformly along the entire length of the fracture, thus, resulting in the linear flow regime and subsequent pressure domain. The linear derivative begins to fall after about 12 minutes, suggesting a transition to a different flow regime.

At about 18 minutes after shut in, the bilinear derivative (shown as open squares) tends toward becoming flat, indicating that fluid movement can now be described as bilinear. In this case, it is assumed that the fracture is closing, thus creating a significant pressure drop along the axis of the fracture. This pressure drop establishes linear fluid flow along the fracture axis in addition to the continuing linear fluid flow that exists between the frac face and into the reservoir; thus, the term bilinear. Note the apparent bilinear flow period lasts about 30 minutes.

This analysis indicates that closure begins some time between the end of the linear flow and the beginning of the bilinear flow regimes. Taking the mid-point in time between these flow regimes (i.e., 15 minutes), the resulting closure pressure is, p_c = 3,900 psi.

4.2.2 KCl Mini-Frac Fall-Off Analysis

Figure 19 is a log/log and derivative group plot of the bottom hole fall off pressure that followed the KCl mini-frac injection test. This analysis follows that previously described for the KCl step-rate test. Note, however, that although the linear flow regime is established during the early part of the falloff, bilinear flow does not appear to manifest itself at any time during the lengthy 1.5-hour shut-in period.

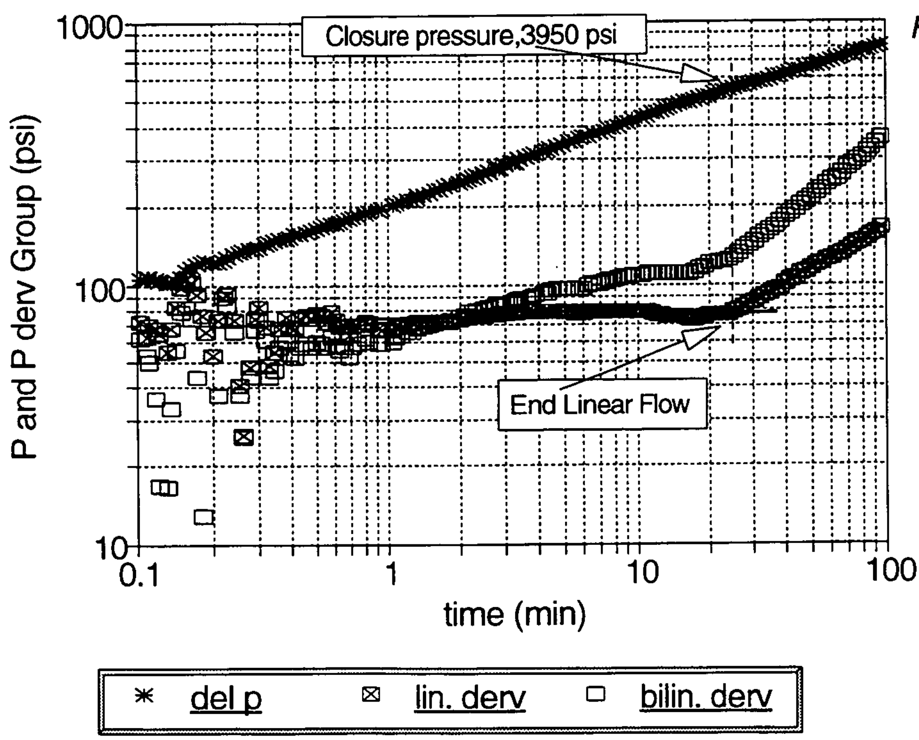

Figure 19 Log/Log and Derivative Group Plot of the Bottomhole Fall-Off Pressure Following the KCl Mini-Frac Injection Test

In this case, the difference pressure shows only small transitions that make the selection of flow regime changes difficult. Thus, the simple log/log analysis does not provide even qualitative information concerning flow behavior. Initial shut-in pressure was taken to be 4,520 psi.

The linear derivative group on the other hand displays a well-defined flat response from the first minute following shut in until about 23 minutes, suggesting linear flow and an open, highly-conductive fracture. The subsequent transition away from the linear flow regime seen at 23 minutes is abrupt, positive and exhibits a sharp increasing slope. This signifies that later-time fluid-flow regimes are probably not readily defined.

The bilinear derivative, shown as open squares, never displays a clearly-defined flat period. This implies that fluid flow along the fractures length may never reach the point of being substantively impeded, thus creating little if any pressure drop. So although the fracture may be closing, the dimensionless fracture conductivity may be sufficiently high enough to create the appearance of high fracture conductivity with negligible pressure drop. The continuous rise in slope supports the premise that the fluid flow regime is not readily defined.

Selecting closure time based on the transition point from linear flow seen at 23 minutes translates to a closure pressure (p_c) of 3,950 psi. This is about 50 psi higher than the p_c = 3,900 psi derived from the step-rate test. The cause of this increase may be rooted in elevated, near-wellbore reservoir pressure created by imbibed frac fluids that results in back stresses.

4.3 3-D FRACTURE MODELING OF THE MINI-FRAC TREATMENTS

GRI's 3-D hydraulic fracture model FRACPRO (Crockett and Okusu, 1986) was used to record and analyze the pressure and flow data in real time during all four injections. Data was collected via a serial connection to·CER's data acquisition computer which was receiving data from the Western Company. GRI's model was also used after the treatments to perform the analyses reported herein.

The pre-test closure stress profile generated by a stress-test-calibrated sonic log is shown in Table 5. As a result of the data measured during the four injections that are subsequently discussed in this report (namely, based on analyses of the pressure declines), it was decided that the closure stresses in the two sand intervals was slightly higher than predicted by logs (Table 5 also shows these corrections). Besides the sand intervals, the stress in the shale interval between the sands was changed (see Table 5) so the (model predicted) fracture would initiate in the middle of the gross sand interval. It is believed that this modification to the stress profile had little effect on the overall, final net pressure prediction and allowed for a more accurate prediction of the final fracture geometry.

4.3.1 Analysis of the X-Linked Gel Ball-Out

The formation was broken down using crosslinked gel that had been circulated to the perforations via an open-ended tubing string. Crosslinked gel was used for the breakdown with the hope that tortuous/multiple fractures would be minimized near the wellbore; such fractures are thought to cause high levels of tortuosity and the associated large pressure losses that can accompany them (Cleary and others, 1993).

Table 5 Stress Data Used in Fracture Modeling

Depth to Top of Layer, ft	Pre-Frac Estimate of Stress from Logs and Microfracs, psi	Value of Stress Used in GRI's 3-D Model, psi
4,700	4,500	4,500
4,770	4,000	4,000
4,800	4,400	4,440
4,844	4,000	4,000
4,870	4,500	4,500
4,900[1]	3,800	3,900
4,920[2]	4,500	3,900
4,920[3]	4,500	3,900
4,950	4,450	4,450
5,006	4,000	4,000
5,050	4,500	4,500

[1] Top interval of "A" sand
[2] Shale interval between top and bottom intervals of "A" sand
[3] Bottom interval of "A" sand

After crosslinked gel was circulated to the perforations, the treatment was pumped down the tubing with the live annulus used to measure bottomhole pressure. The tubing was flushed with KCl water. Seventy-eight barrels of crosslinked gel were pumped into the formation. The treatment data are shown in Figure 20. The maximum rate was 8 BPM. It is interesting to note that no ball action whatsoever was seen. The pressure was allowed to decline to well past the value expected for fracture closure in an attempt to determine closure stress. The well was surged after pumping to allow any balls to fall; data transmission was lost temporarily during surging.

Figure 21 shows the observed net pressure, which is measured bottomhole pressure minus perforation/tortuosity pressure losses and closure stress.

$$P_{\text{observed net}} = P_{\text{measured bottomhole}} - P_{\text{perforation/near-wellbore}} - P_{\text{closure}}$$

Perforation/tortuosity pressure losses were estimated to be approximately 100 psi at 7 BPM at shut in. (This data, though it agrees with that collected from subsequent injections, should be considered suspect for this injection since balls were pumped). Also shown in Figure 21 is the net pressure predicted by GRI's 3-D hydraulic fracture simulator. Figure 22 shows a schematic of one wing of the fracture at shut in. Also shown in Figure 22 are the permeability and stress profiles. From the pressure match, efficiency was estimated to be about 53 percent at shut in.

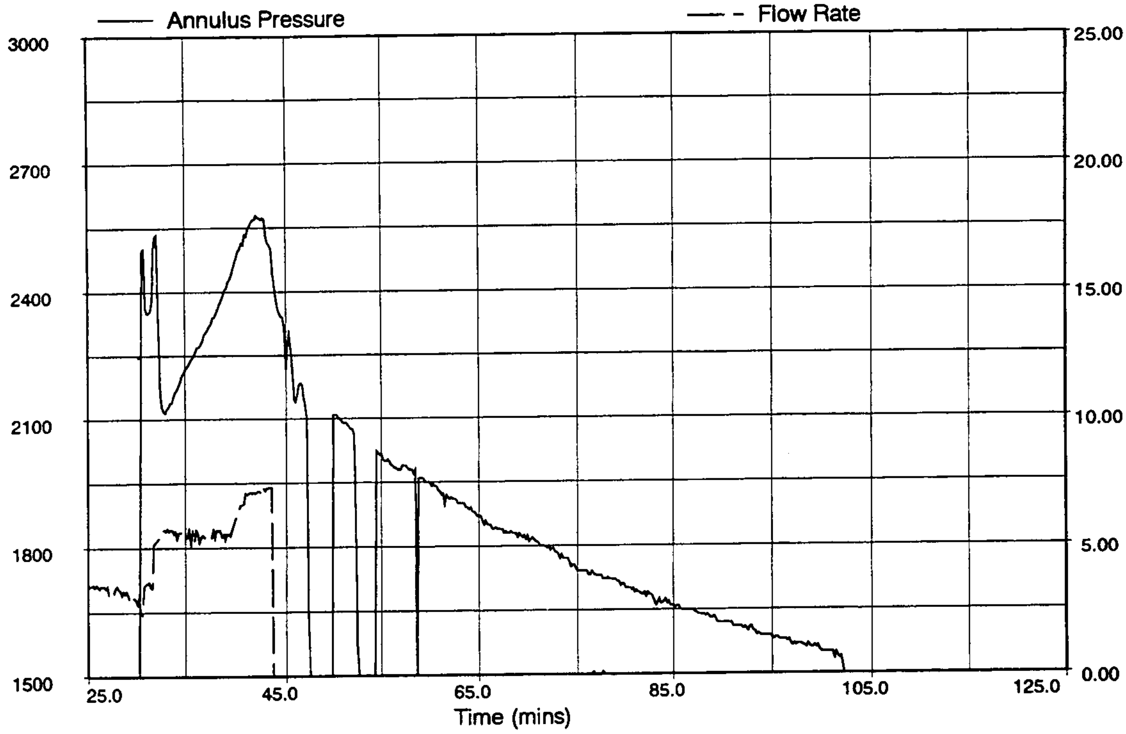

Figure 20 Treatment Data, X-Linked Gel Ball-Out

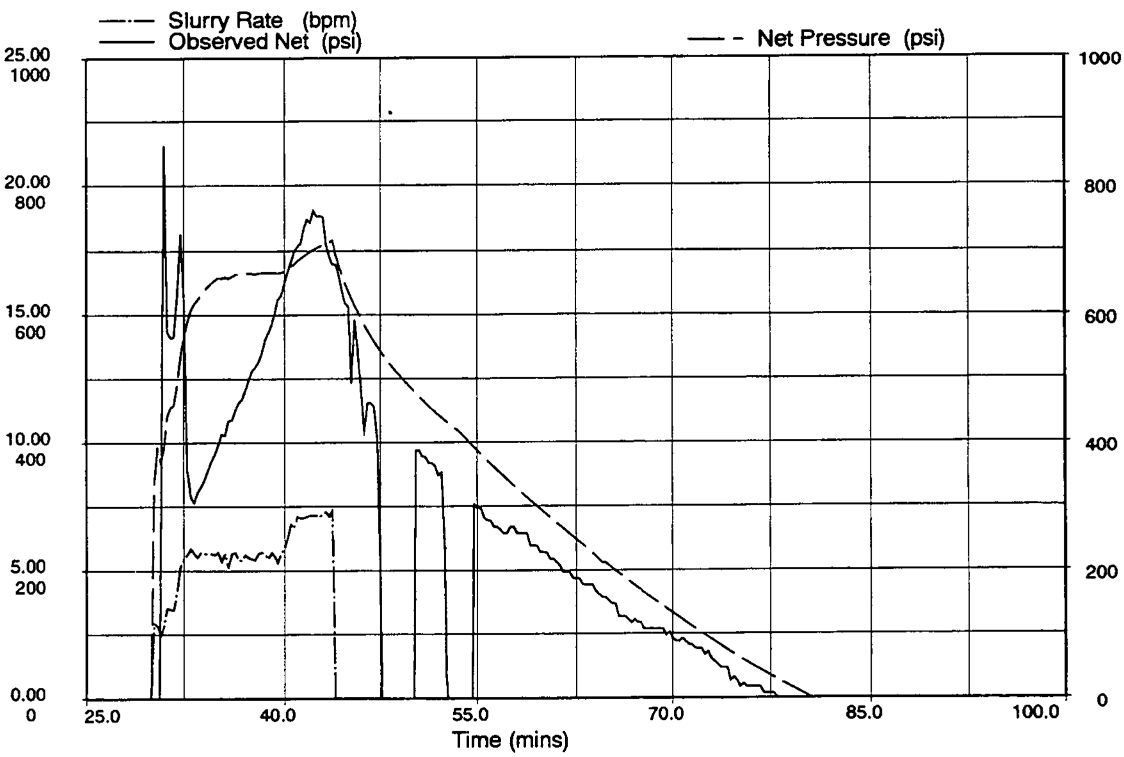

Figure 21 Net Pressure Match, X-Linked Gel Ball-Out

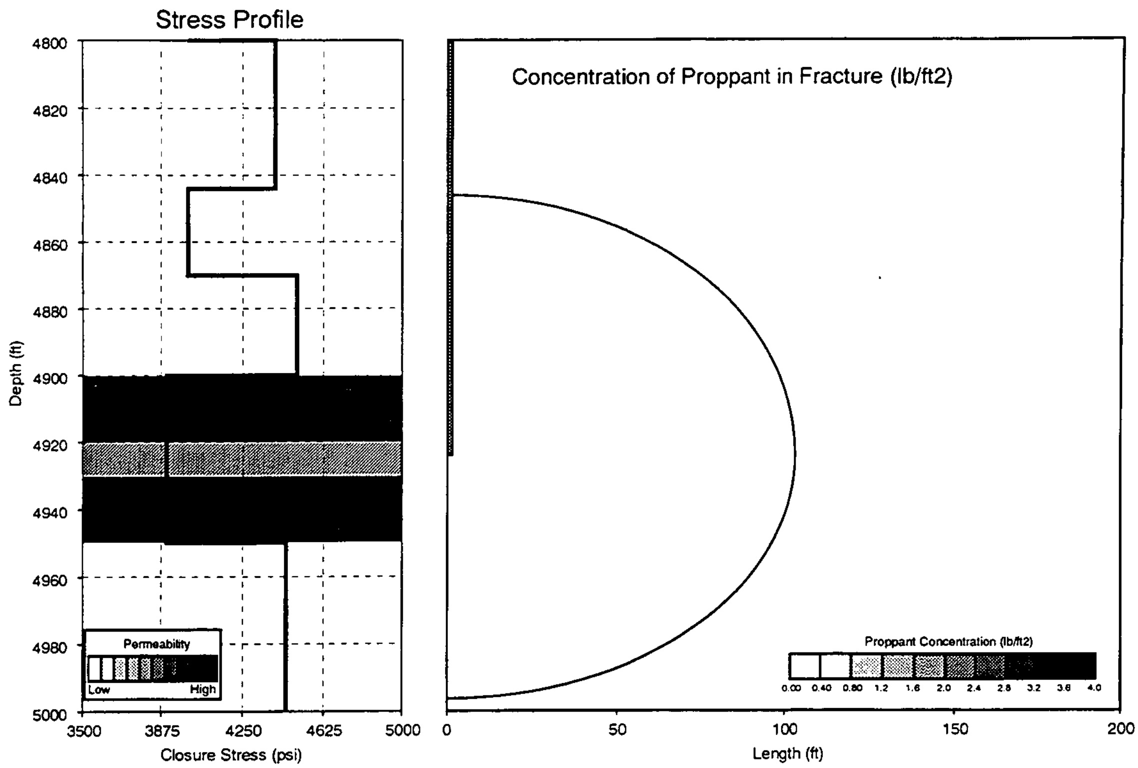

Figure 22 Stress Profile, Permeability Profile and Fracture Geometry for the X-Linked Gel Ball-Out

4.3.2 Analysis of the KCl-Water Step-Rate Test

After the ball-out test, 99 bbl of KCl water were pumped into the formation in a step-rate, reopening test. The treatment was pumped down the annulus with a wireline-conveyed downhole pressure gauge in the open-ended tubing string. It was hoped that both a maximum value of closure stress could be estimated from the reopening test and that closure stress could be verified/measured from the pressure decline.

The treatment data for the step-rate test are shown in Figure 23. Tortuosity pressure losses were measured to be approximately 125 psi at 20 BPM at shut in. The observed and model-predicted net pressures are shown in Figure 24, with the corresponding fracture size/shape at shut in shown in Figure 25. Efficiency was estimated to be 45 percent at the end of pumping.

4.3.3 Analysis of the KCl-Water Mini-Frac

The next injection consisted of 304 bbl of KCl water. The treatment was again pumped down the annulus with a downhole pressure gauge in the open-ended tubing. The treatment data from the KCl-water mini-frac are shown in Figure 26. Tortuosity pressure losses were measured to be 150 psi at 26 BPM about halfway through the treatment, and about 120 psi at 23 BPM at the end of pumping.

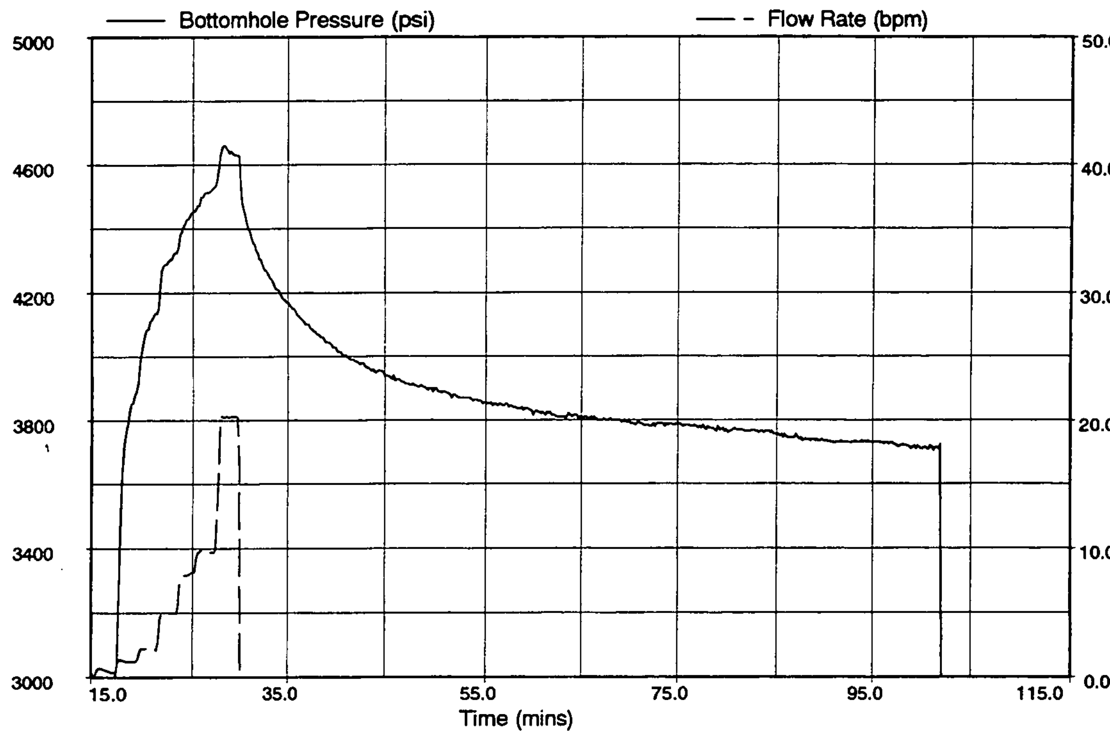

Figure 23 Treatment Data, KCl-Water Step-Rate Test

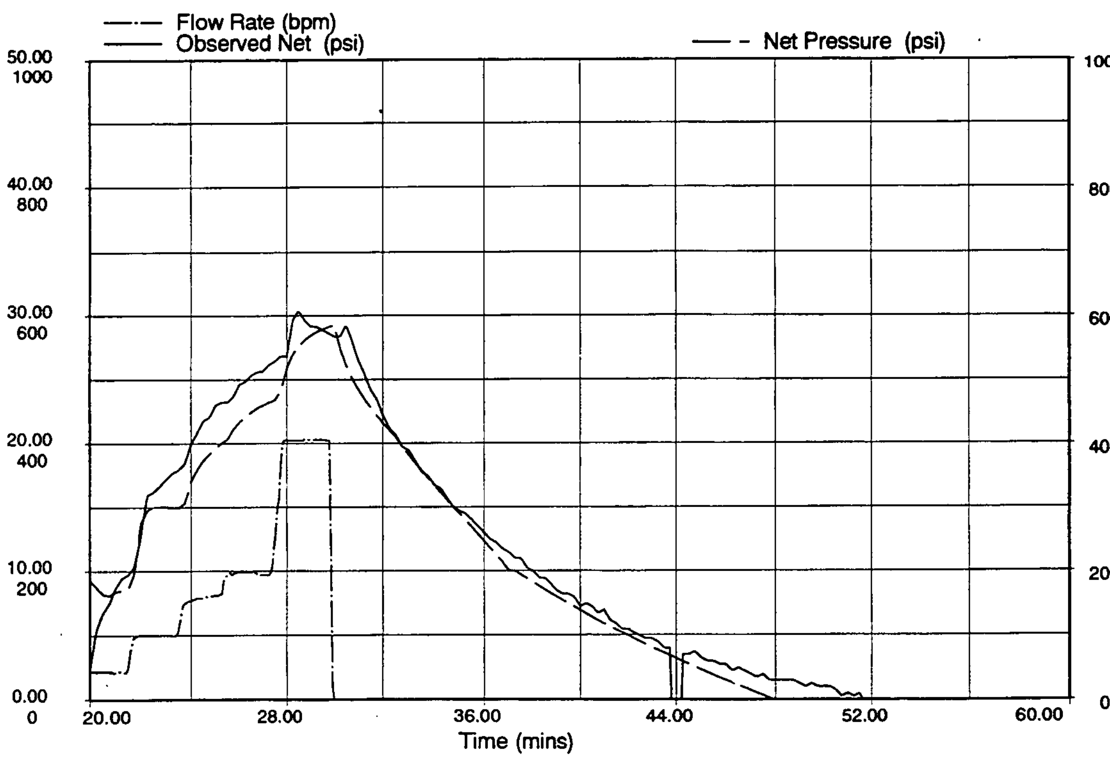

Figure 24 Net Pressure Match, KCl-Water Step-Rate Test

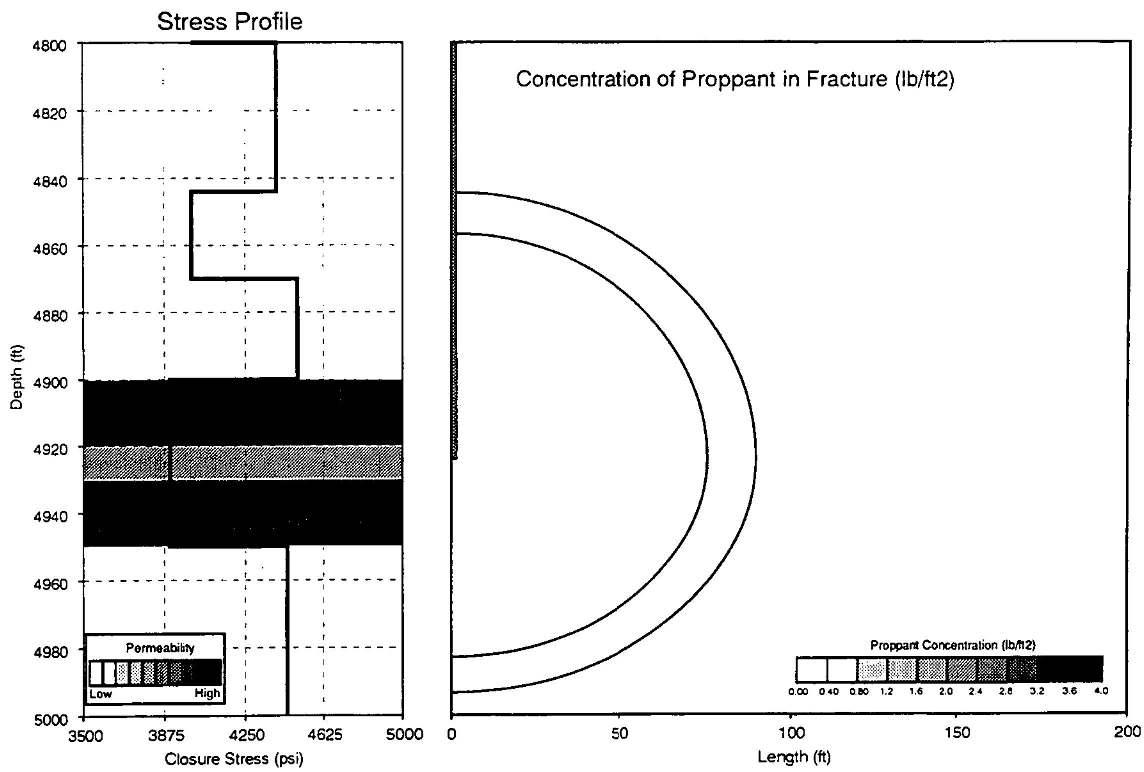

Figure 25 Stress Profile, Permeability Profile and Fracture Geometry for the KCl-Water Step-Rate Test

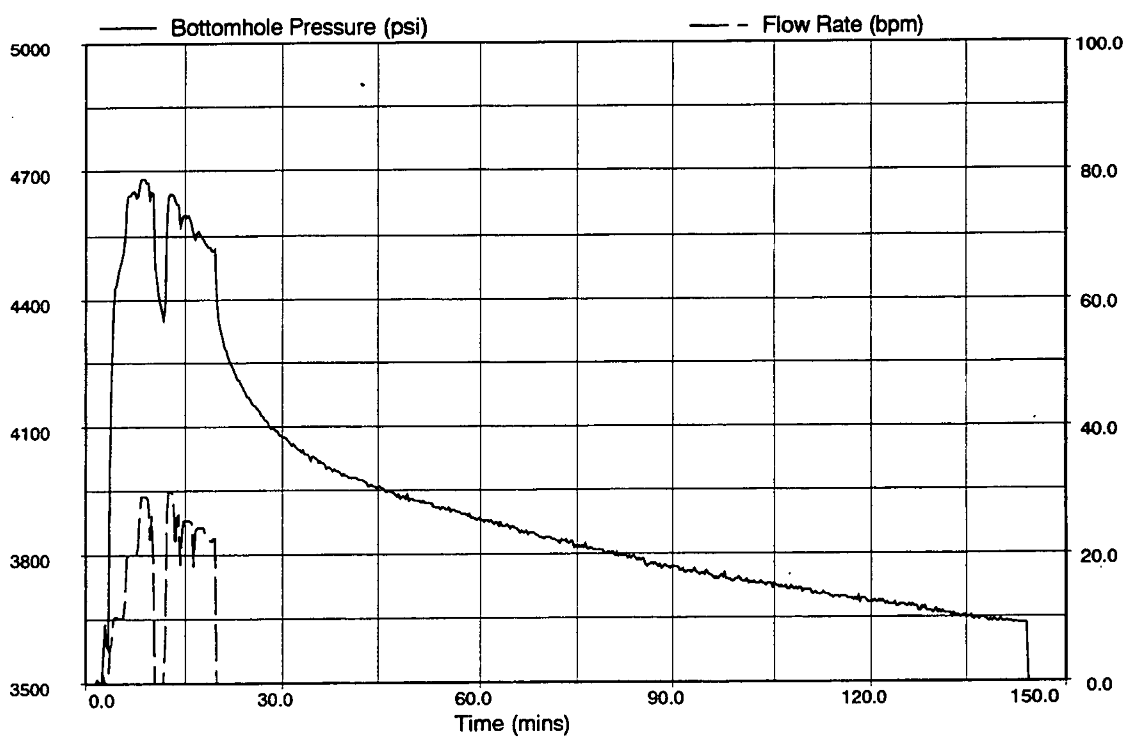

Figure 26 Treatment Data, KCl-Water Mini-Frac

The observed and model-predicted net pressures are shown in Figure 27. Figure 28 shows a schematic representation of the fracture corresponding to the model-predicted net pressure at shut in. The efficiency at the end of pumping was estimated to be 38 percent.

4.3.4 Analysis of the 40-lb Linear-Gel Mini-Frac

The final injection consisted of 634 bbl of 40-lb linear gel being pumped down the annulus with a downhole pressure gauge in the open-ended tubing string. The treatment data from the gel mini-frac are shown in Figure 29. Tortuosity pressure losses were measured to be 100 psi at 26 BPM.

The observed and model-predicted net pressures are shown in Figures 30 and 31 show the corresponding fracture geometry as predicted by the fracture model at shut in. The efficiency at the end of pumping was estimated to be 56 percent.

4.3.5 Conclusions of Fracture Modeling

The modeling of the seismic verification injections resulted in the following conclusions:

1) The log-derived stress profile, calibrated with stress-test data, were used in all four net pressure matches.

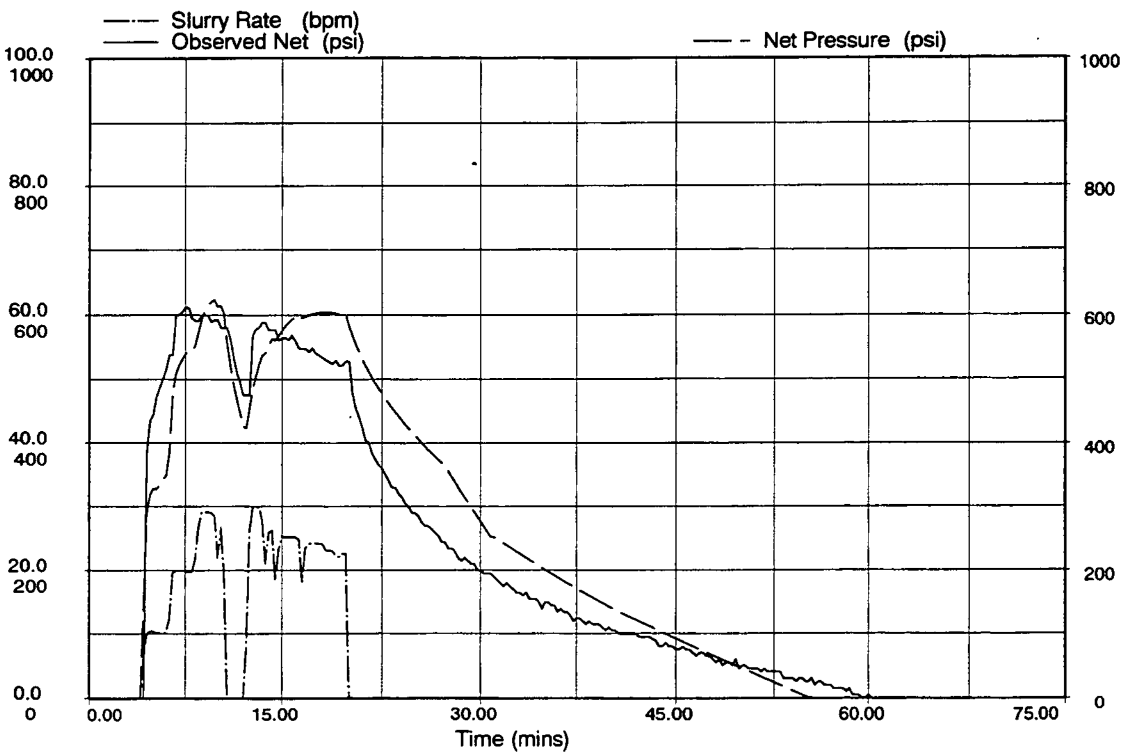

Figure 27 Net Pressure Match, KCl-Water Mini-Frac

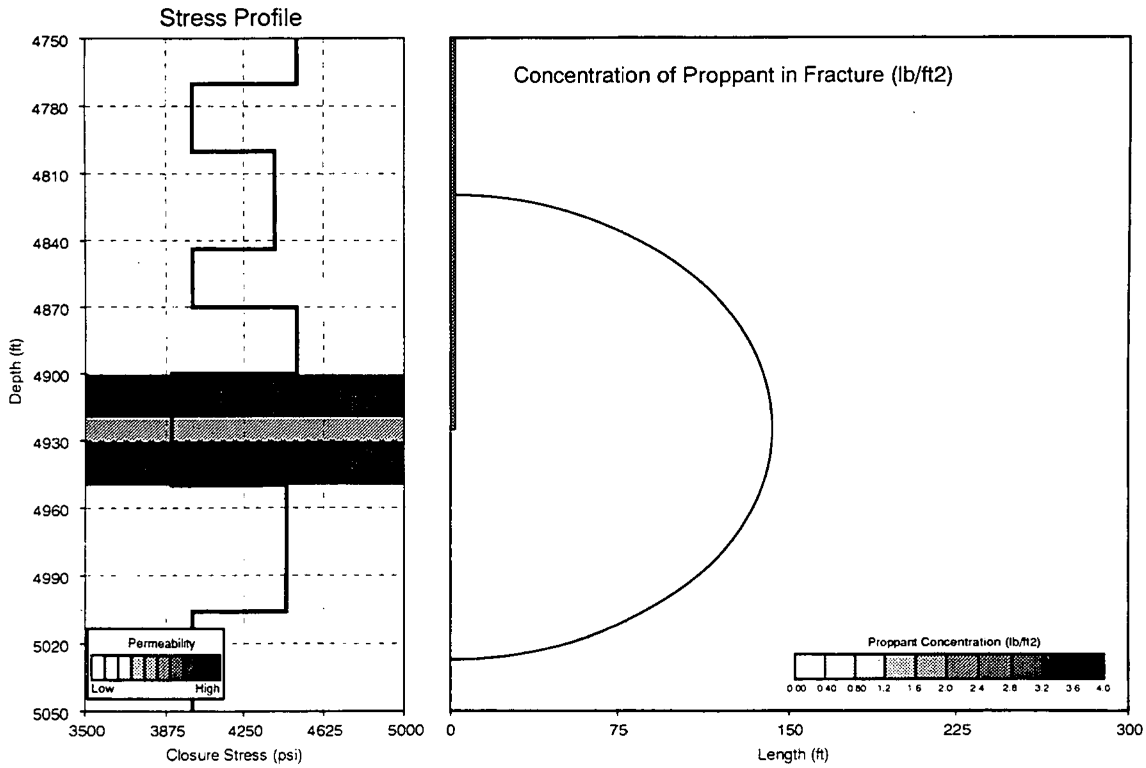

Figure 28 Stress Profile, Permeability Profile and Fracture Geometry for the KCl-Water Mini-Frac

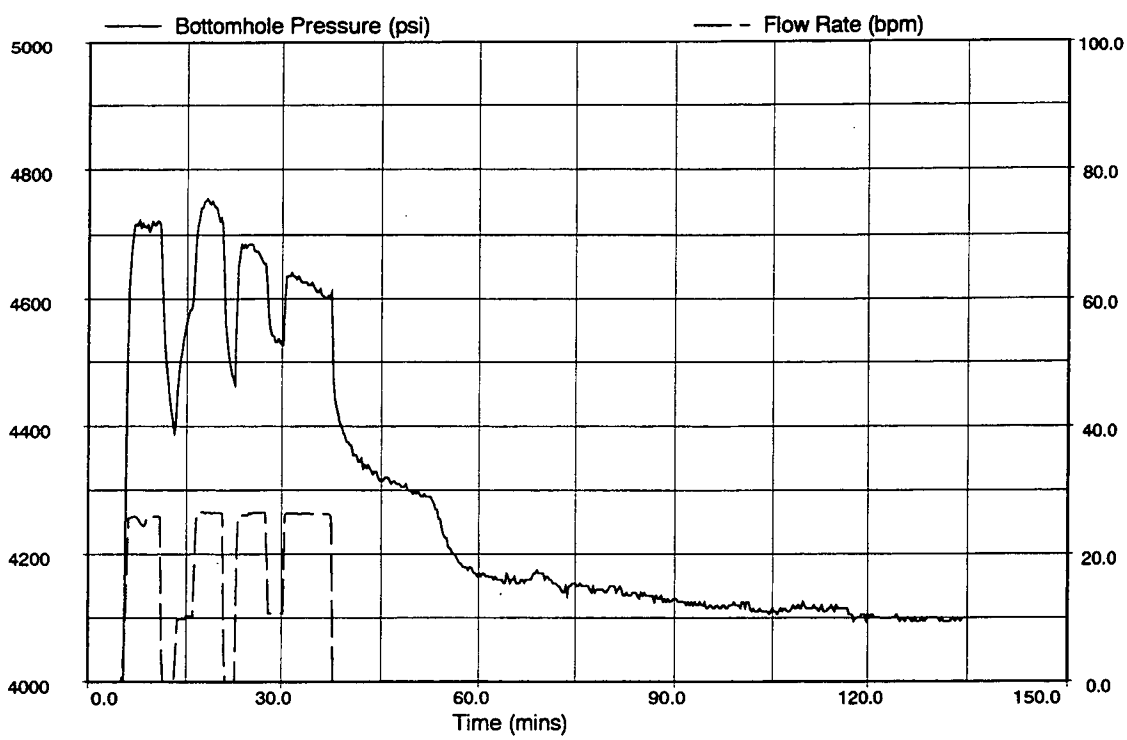

Figure 29 Treatment Data, Linear Gel Mini-Frac

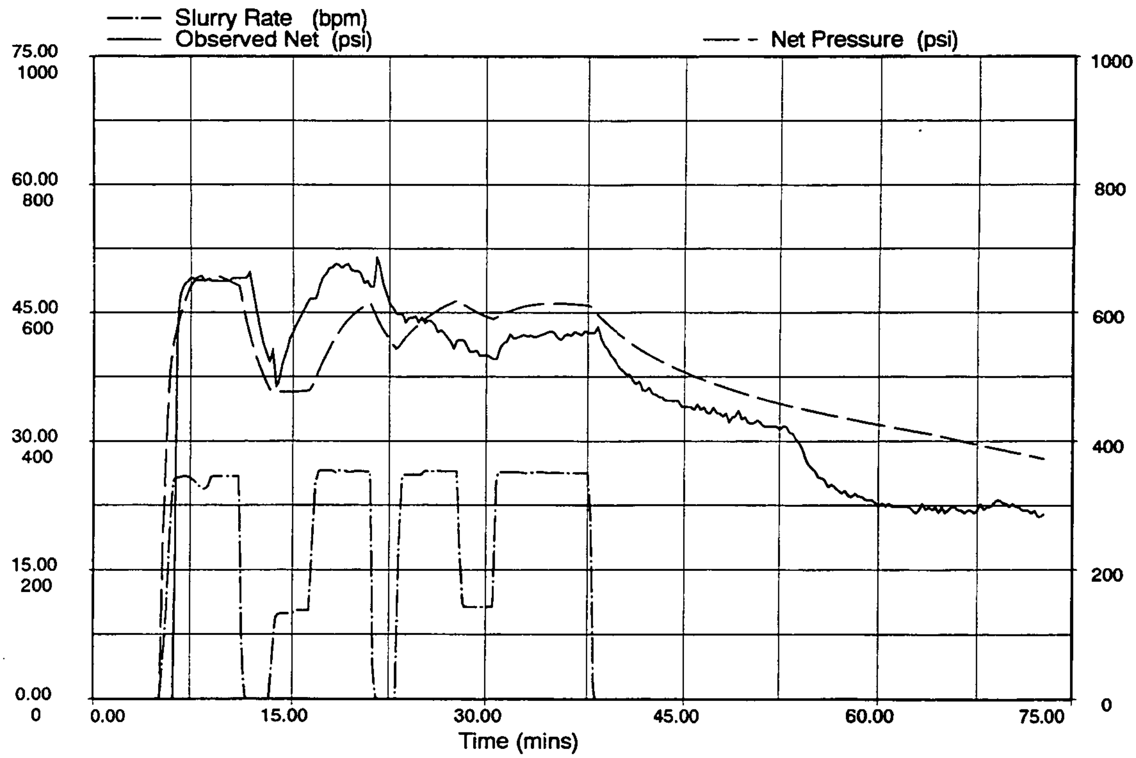

Figure 30 Net Pressure Match, Linear Gel Mini-Frac

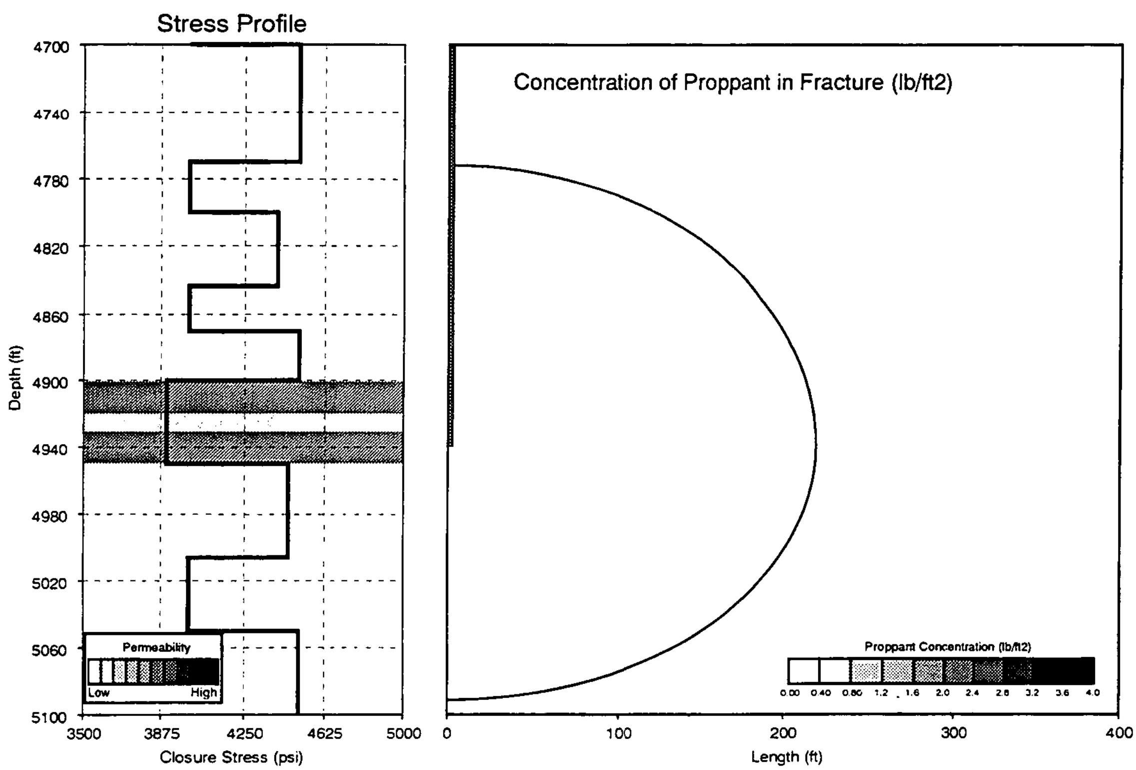

Figure 31 Stress Profile, Permeability Profile and Fracture Geometry for the Linear Gel Mini-Frac

2) Observed net pressures were very similar for all four injections, and they matched closely with those estimated by GRI's 3-D fracture model, as shown in Figure 32.

3) There were no indications of high near-wellbore tortuosity.

4) There were no indications of (parallel) multiple fractures being propagated.

5) Efficiencies ranged from 38 to 56 percent (the range is most likely due to the different fluids and volumes used).

6) The fracture geometry resulting from these injections was estimated to be essentially radial.

Assuming similar fracture behavior uphole in the zones proposed for fracture mapping experiments, M-Site No. 1 is deemed appropriate for future modeling research from the standpoint of the observed pressure responses.

4.4 REMOTE DETECTION AND VERIFICATION OF MICROSEISMIC SIGNALS

4.4.1 Maps of Microseisms

As mentioned in Section 3.4, separate signals were chosen for analysis by playing back the Sony and manually triggering to an EG&G model 2401 recorder. Sixty-seven different events were sampled in this manner, including events from all of the injections and the perforation of the treatment well. In general, the larger events were chosen because of their clear p-wave arrivals, but some smaller and some unusual signals were also selected. Initial analysis consisted of determination of p-wave and s-wave arrivals for each signal and the polarization of the first one-two cycles of the p-wave.

Figure 33 shows a plan view of the locations of the subset of analyzable microseisms taken from the 67 events extracted from the continuous recording. This map shows the approximate locations of signals from all four injections; it should be stressed that these locations are approximate because of the orientation errors associated with using perforations as well as the uncertainty in locating the microseism. The apparent azimuth of the hydraulic fractures is about N65°E, about the same orientation as was determined in previous hydraulic-fracture experiments at this site. The half length of the east wing appears to be at least 200 to 300 ft, with a possibility of being over 400 ft. (Since there is only one data point at 400 ft, there is not good confidence in this data point.) The east wing of the fracture is relatively well described, but the west wing has few points, possibly because of the distance but also possibly due to some attenuating effects of the formation (such as orientation of natural fractures). It is believed that the hydraulic fracture could be more completely described if additional microseisms are analyzed, but such an additional effort is outside of the scope of this suitability experiment.

A side view of the microseism locations is shown in Figure 34. Signals are observed within a 350 ft high band, but most of the signals are within a 200-ft high region. Because the velocity structure of the different layers within this region is not known, it is difficult to assess the uncertainty associated with this height map. Nevertheless, the ability to define a rough outline of one wing of the fracture (east wing) with such a limited data set (and all the uncertainties associated with using a single receiver and perforations for orientation) shows that hydraulic fractures can be mapped at this site.

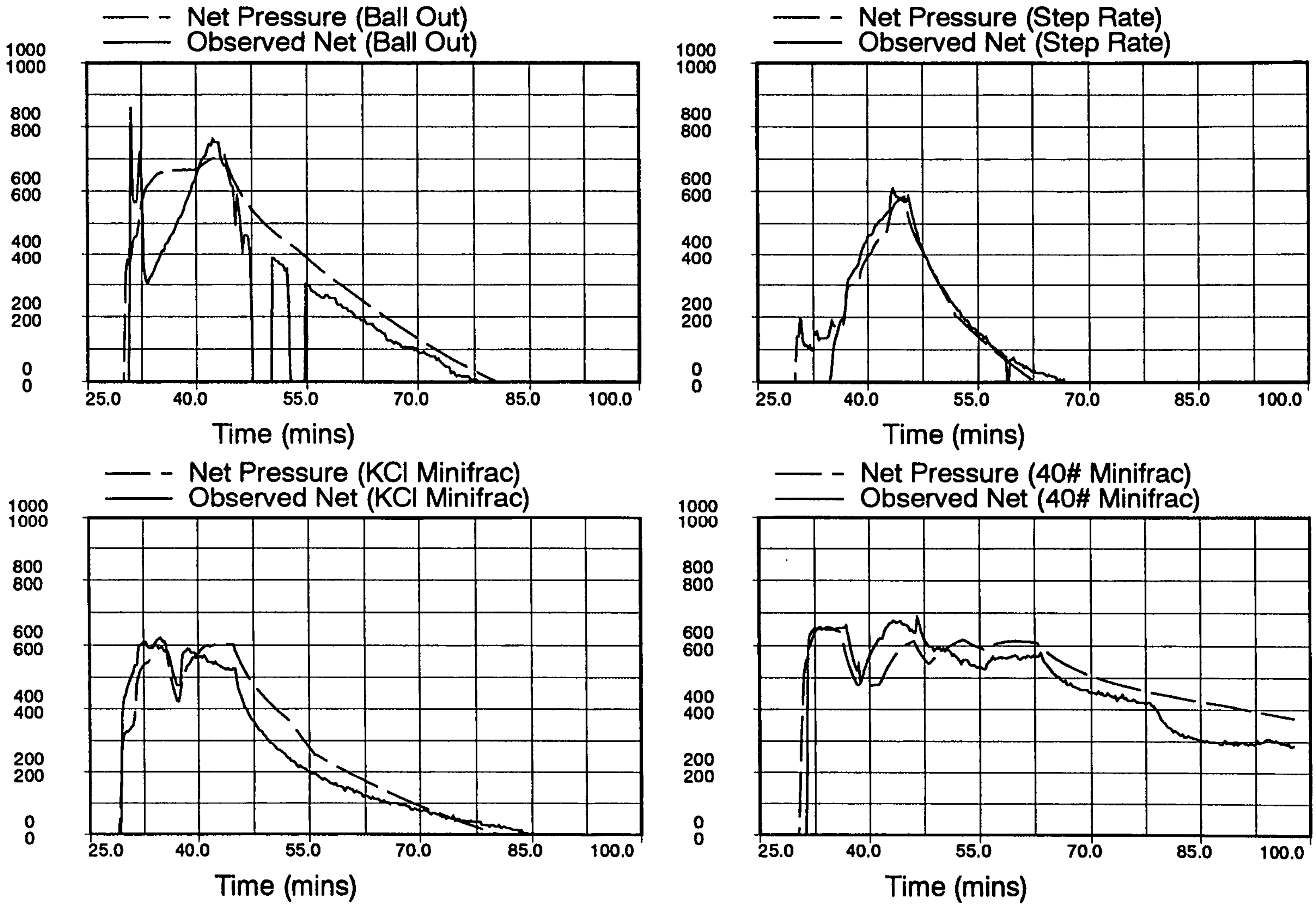

Figure 32 Net Pressure Matches, Comparison of All Injections

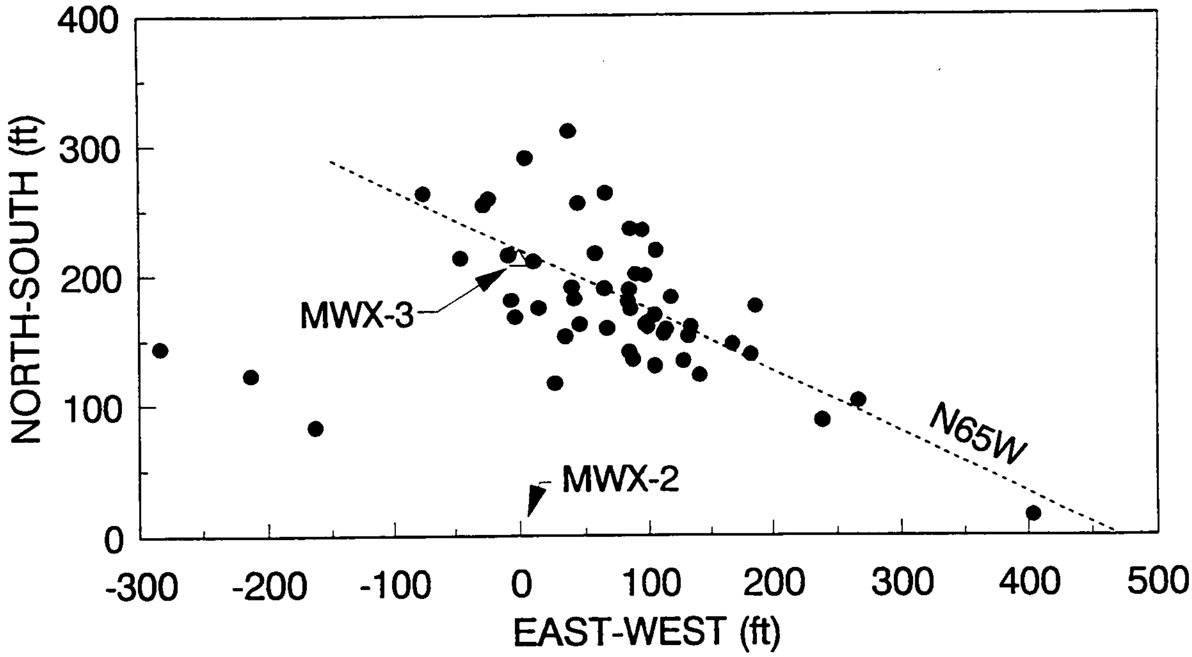

Figure 33 Plan View of Microseism Map

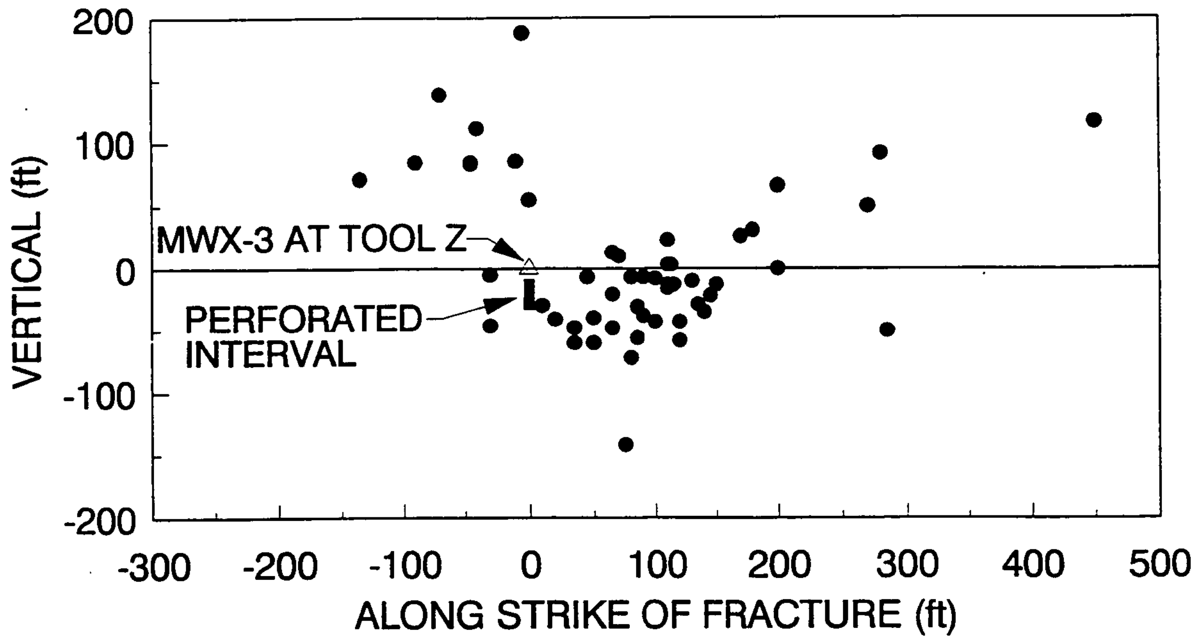

Figure 34 Side View of Microseism Map

4.4.2 Description of Microseisms

Examples of some of the observed microseisms and their notable features are given in this section. These results are useful for planning the type of instrumentation that will be required for full-scale microseismic monitoring at this site.

Figure 35 shows the three traces taken from Event No. 33 using the raw or unfiltered data. In this example the signal clearly rises from the background at about 6.5 msec. Figure 36 shows an overlay of the three unfiltered traces and the polarization plot for the initial cycle and a half of the p-wave. The azimuth is 68° counterclockwise from the x-axis (which is aligned with the east-west direction), with a standard deviation of 9° based on circular statistics. The vertical is down 9° with a standard deviation of 6°. The plot of the unfiltered data is best used for determining first arrivals.

Figure 37 shows the filtered data (low-pass filtered to 2,000 Hz, as discussed previously) for this same event. The orientation from the hodogram is essentially the same, with a slightly greater uncertainty. The s-wave, arriving at about 15 msec was determined using three techniques. First, hodograms of the traces were searched for the sections where the polarization shifted by approximately 90°; second, traces were searched for locations where amplitudes increased significantly; third, traces were searched for locations where the frequency of the signal decreased significantly. Using some combination of the three techniques, it was generally possible to choose a well-defined s-wave arrival. In this example, there is a polarization shift, a frequency decrease, and an amplitude increase. Other events were not always so clear.

Given a difference in the p- and s-wave arrivals (t_p - t_s), the distance to the event can be calculated from the two equations,

$$d = V_p\,(t_p - t_o) \quad \text{and} \quad d = V_s\,(t_s - t_o),$$

where V_p and V_s are the p-wave and s-wave velocities. Eliminating t_o, the time of origination of the microseism, the distance can be found as

$$d = \frac{V_p V_s}{V_p - V_s}\,(t_p - t_s),$$

where the factor multiplying (t_p - t_s) is about 25 ft/msec for the sandstone and siltstone rocks. This factor is called the velocity factor in this report and in the figures.

In Figure 37, the p-s separation is about 8.8 msec, yielding a distance of 221 ft from MWX-2. Thus, using the polarization and the p-s separation, the location of the microseism can be approximately determined.

Figure 38 shows Event No. 34 using the raw data. The unfiltered polarization plots are shown in Figure 39 and the filtered data in Figure 40. This event is an example of a microseism with greater uncertainty in the orientation (standard deviations of 16° and 18° in the horizontal and vertical planes, respectively), but a very clear s-wave arrival. It can be seen in this microseism that the unfiltered data provide a much clearer first arrival of the p-wave than the

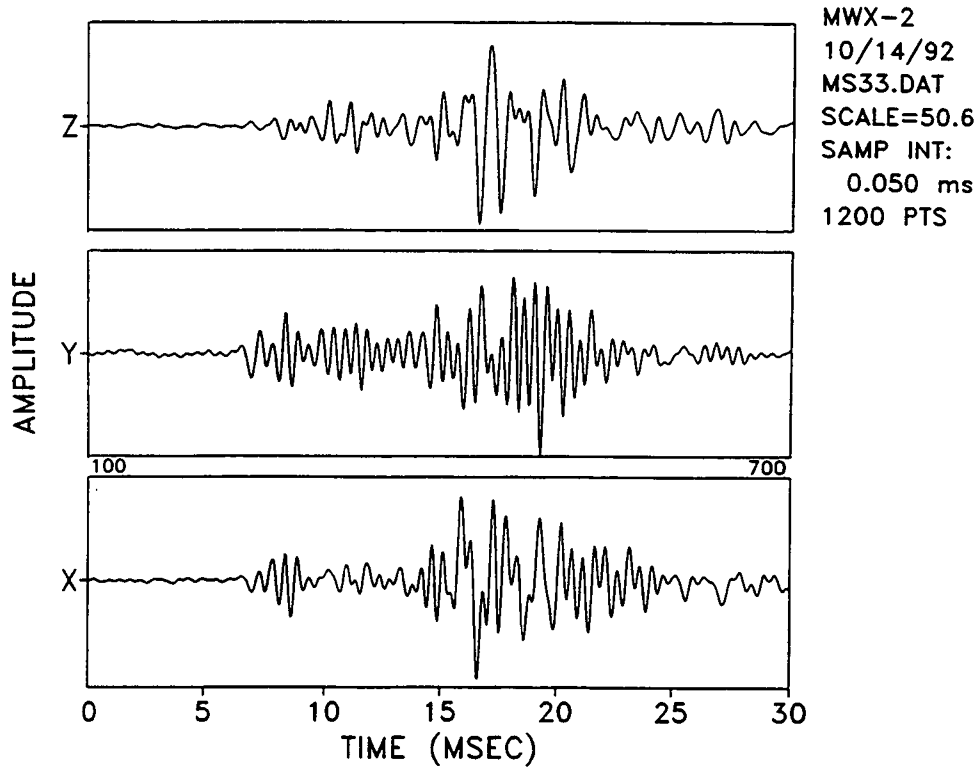

Figure 35 All Traces for Event No. 33, Unfiltered

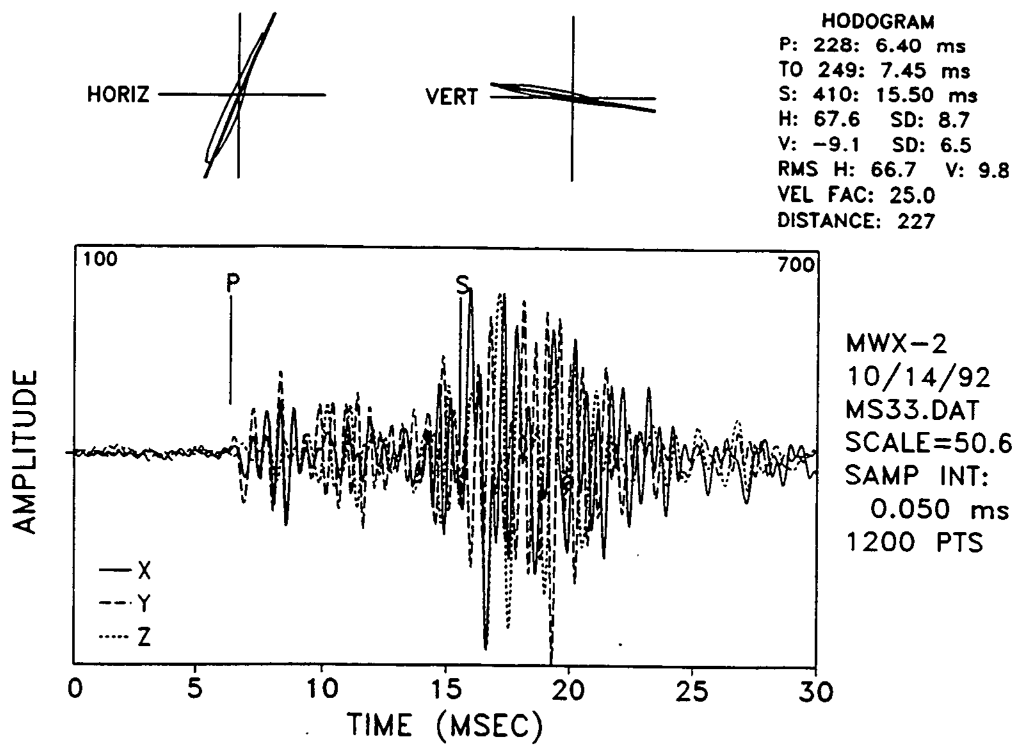

Figure 36 Overlay of Traces and Hodograms for Event No. 33, Unfiltered

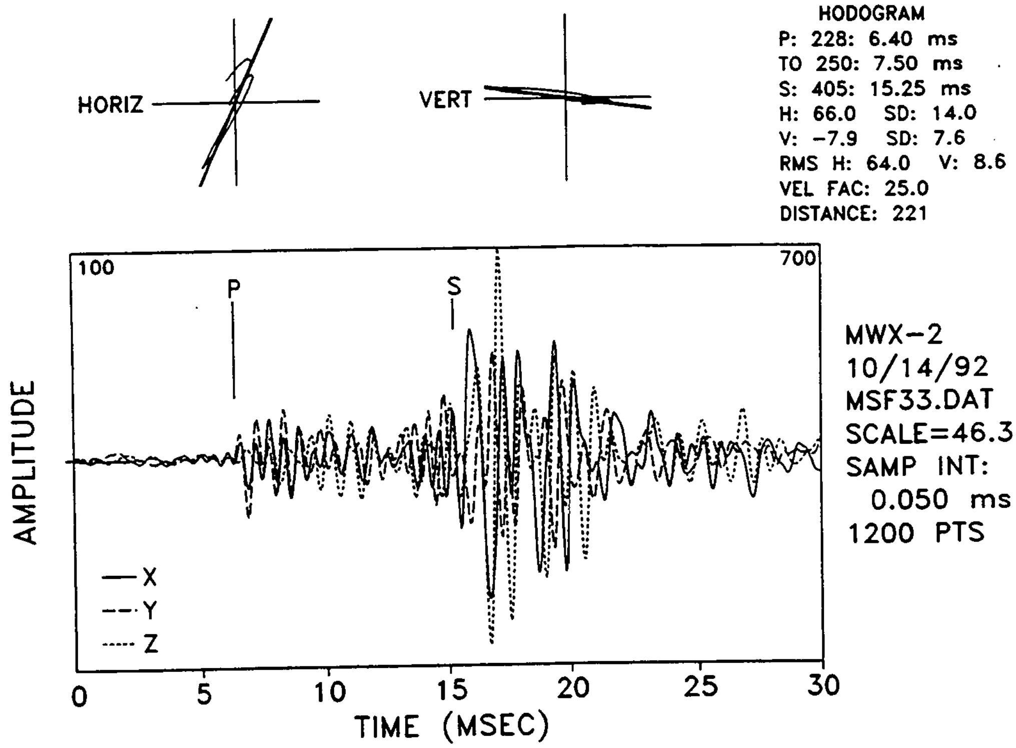

Figure 37 Overlay of Traces and Hodograms for Event No. 33, Filtered

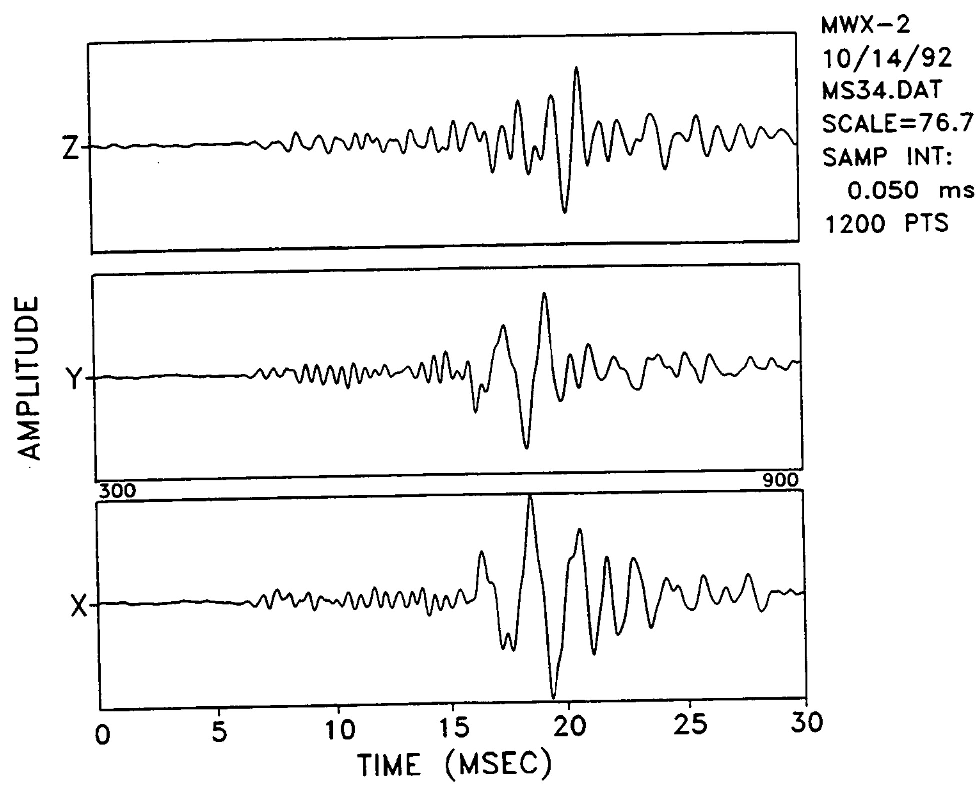

Figure 38 All Traces for Event No. 34, Unfiltered

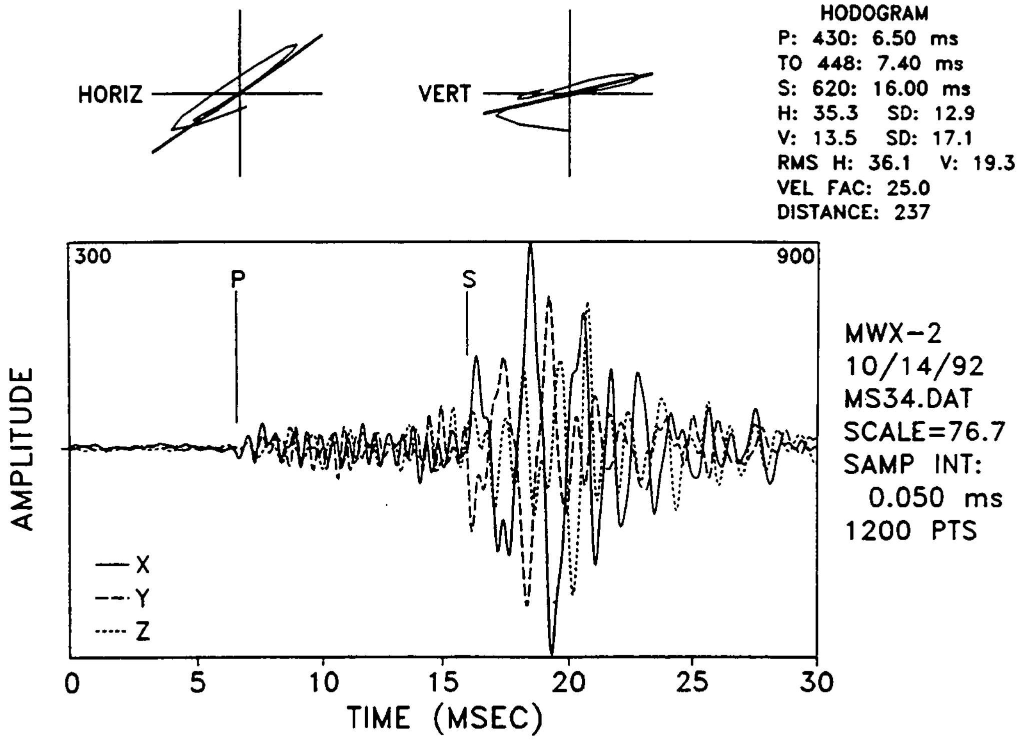

Figure 39 Overlay of Traces and Hodograms for Event No. 34, Unfiltered

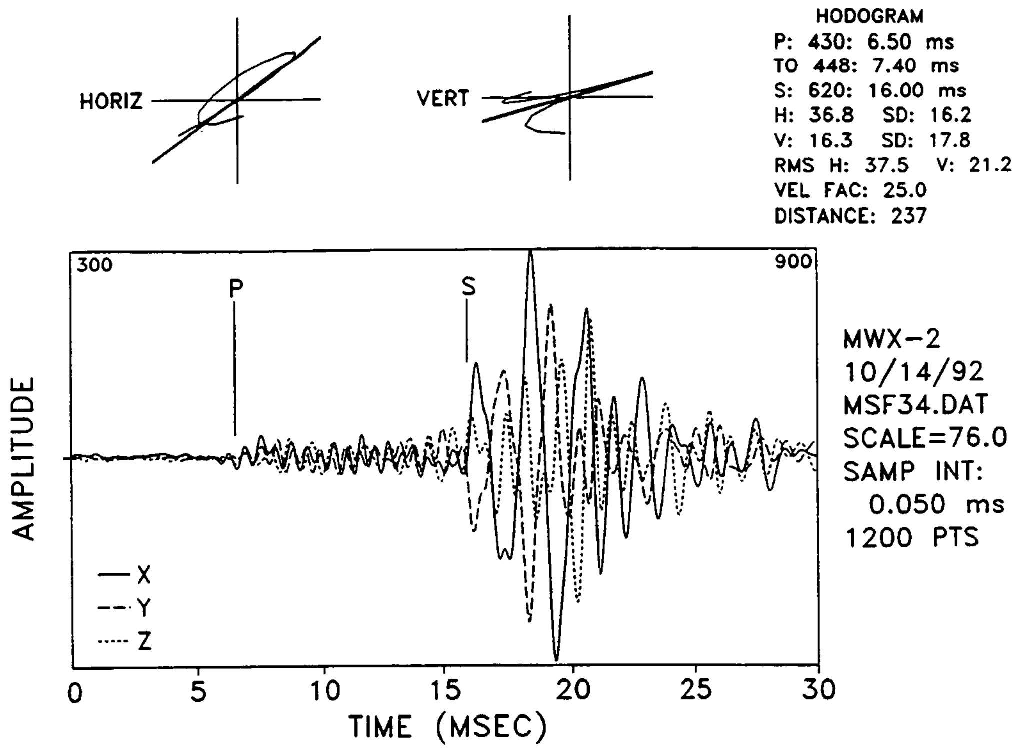

Figure 40 Overlay of Traces and Hodograms for Event No. 34, Filtered

filtered data set. The orientation of this signal is 37° north of the x axis (east-west), with a p-s separation of 9.5 msec for a distance of 238 ft.

Figure 41 shows the three unfiltered traces from Event No. 4, a small signal that was detected during pumping when the background noise level was at its highest. The overlay of the unfiltered data is shown in Figure 42, where the first arrival of the signal is not as clear as in previous examples, nor are the hodograms as well polarized. The filtered results are shown in Figure 43 and 44, where it can be seen that the signals are much more difficult to process when noise levels are high or signal strength is low, or both. First arrivals of both the p and s waves are difficult to determine and polarizations have large uncertainties, in this case yielding standard deviations of 24° and 30° for the horizontal and vertical planes, respectively.

The plots shown in Figures 35 through 44 are examples of the results taken from the 67 processed events. Table 6 gives the usable information from every event in which both p and s wave arrivals could be determined. Figures 33 and 34 were derived from the data in this table. Plots of all the other analyzable microseisms are given in Appendix 3.

4.4.3 Spectral Content of the Microseisms

Spectra of both the noise and the microseisms were obtained for various events to determine if there was any characteristic frequency of the microseisms or other factor that may be important for microseismic monitoring at this site. Figure 45 shows the spectral response from 0 to 2,000 Hz for the filtered x channel (east-west) data for Event No. 34 (shown previously in Figures 38 through 40). The noise spectrum is taken from the ambient background just prior to the event. Noise levels during pumping are elevated, but the microseism signal level is still 20 to 40 db greater, and both the noise and the microseism exhibit broadband frequency response. The same is true of the y-channel response, shown in Figure 46, and the z-channel response, shown in Figure 47, although the energy content of the z channel appears to drop off above about 1,500 Hz.

Figures 48 through 50 show the x, y and z channels for the filtered data of Event No. 25, where all three channels exhibit a flat, broadband response out to 2,000 Hz. Again, the microseism signal is 20 to 30 db above the ambient noise level. These results show that microseismic monitoring at this site, and probably any other location, will require a seismic receiver that is capable of acquiring signal information over a broad frequency range.

4.4.4 Conclusions of Seismic Suitability Assessment

The primary conclusion of the seismic suitability assessment is that the M-Site No. 1 represents a favorable site for conducting hydraulic fracture diagnostic and fracture modeling experiments. Technical reasons for this assessment are:

1. Both of the current wellbores (MWX-2 and MWX-3) are acceptable for seismic monitoring experiments. Noise conditions were low, and signals were clearly observed in both wellbores.

2. Even with ongoing production activities in two nearby wellbores (MWX-1 and SHCT-1), the background noise level at the site was extremely low.

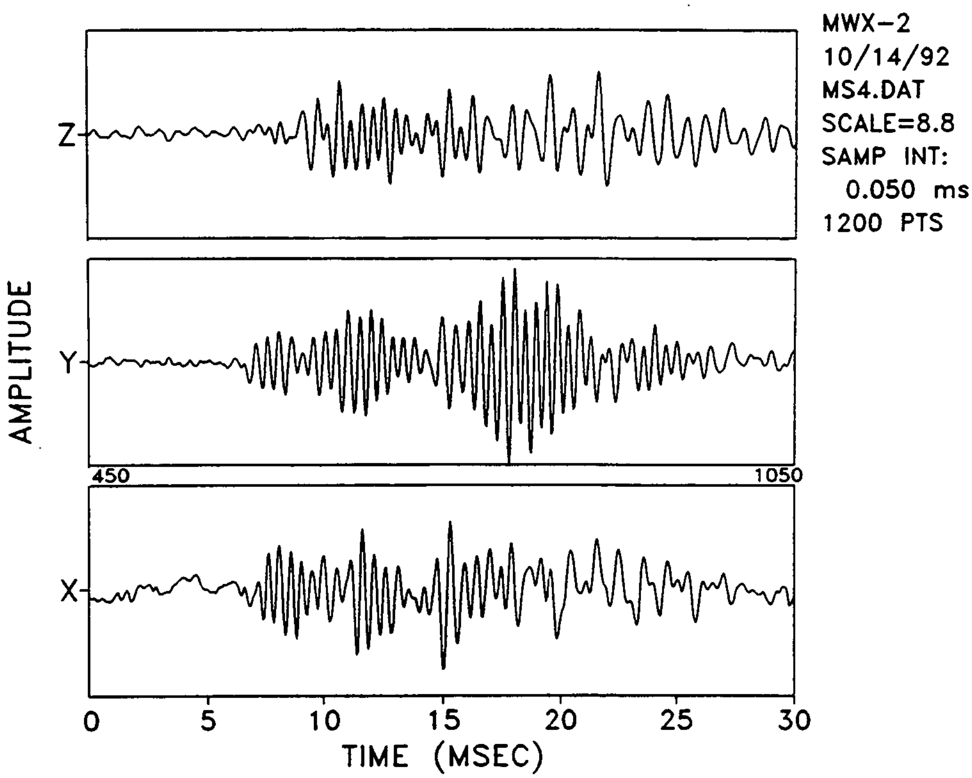

Figure 41 All Traces for Event No. 4, Unfiltered

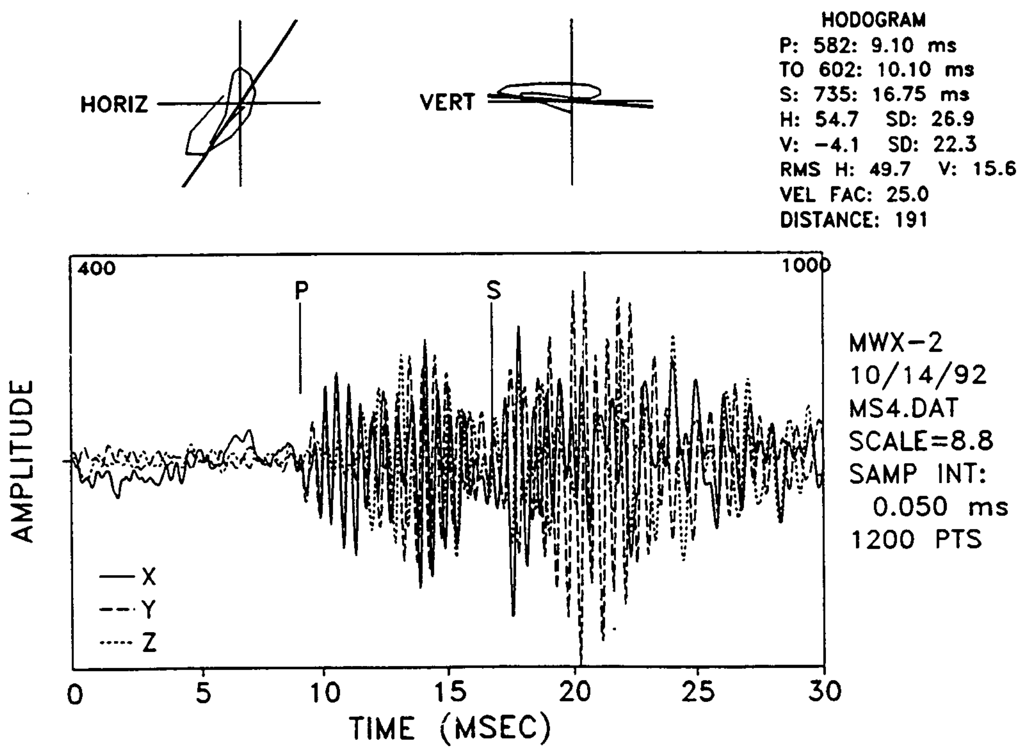

Figure 42 Overlay of Traces and Hodograms for Event No. 4, Unfiltered

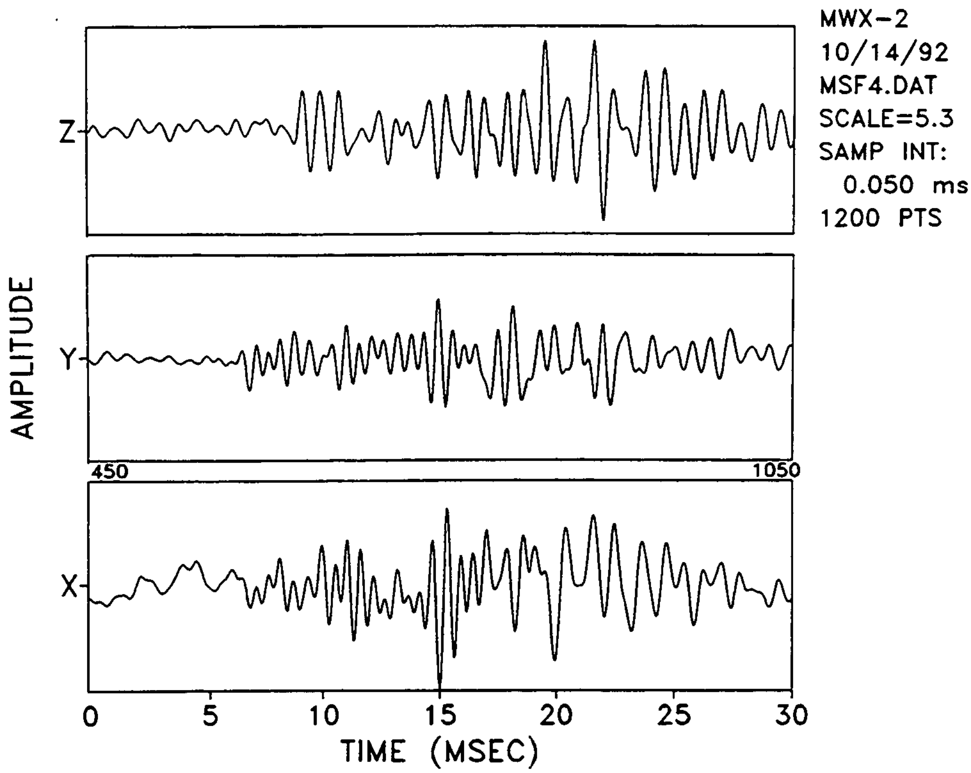

Figure 43 All Traces for Event No. 4, Filtered

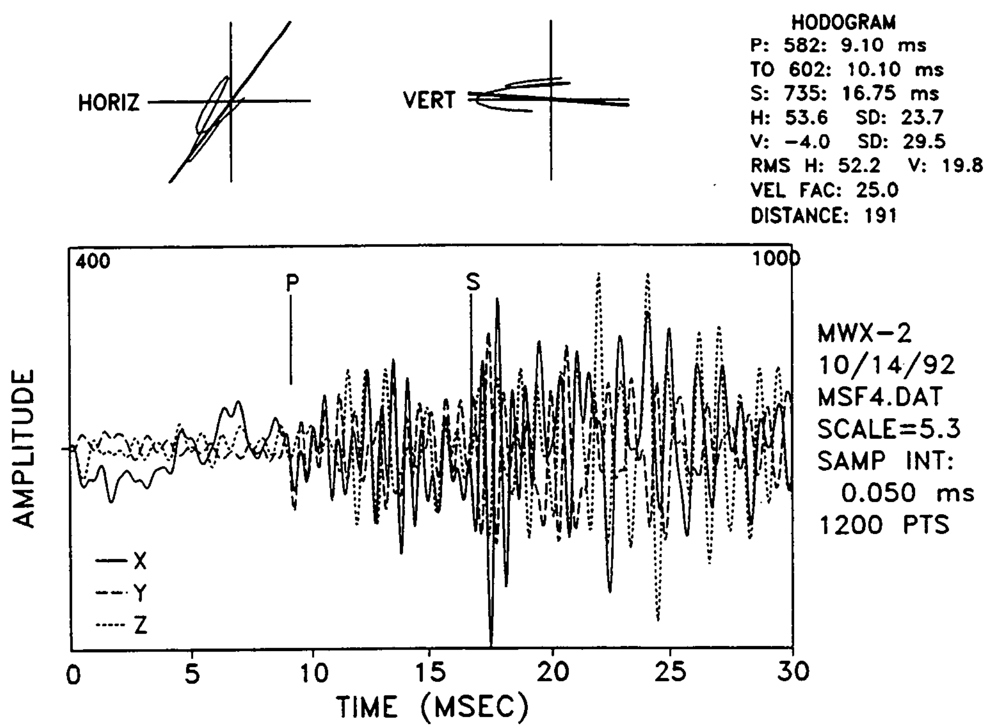

Figure 44 Overlay of Traces and Hodograms for Event No. 4, Filtered

Table 6 Microseismic Distance and Orientation Results

Event No.	Azimuth, deg.	Azimuth St. Dev., deg.	Inclination, deg.	Inclination St. Dev., deg.	$t_p - t_s$, msec	Distance, ft
1	-78	16	27	24	9.7	244
2	67	11	-12	18	7.2	181
4	54	24	-4	30	7.6	191
6	74	18	3	20	8.0	201
9	61	41	-30	34	6.7	169
11	41	38	8	19	7.5	188
12	-27	21	16	18	13.2	331
14	88	15	-14	26	7.5	188
15	65	22	-1	16	7.7	193
16	61	16	-12	21	8.7	218
17	55	27	-16	37	9.6	240
19	48	39	-21	32	7.4	186
20	75	22	-4	14	7.7	194
21	63	13	-7	24	7.5	188
22	68	34	-15	32	10.5	263
24	66	37	1	49	8.1	203
25	80	20	-15	14	9.5	238
28	67	38	9	22	7.1	178
29	-88	31	17	21	7.0	175
30	-83	14	16	31	11.5	288
32	58	29	1	14	7.9	198
33	66	14	-8	8	8.8	221
34	37	16	16	18	9.5	238
36	43	6	-80	59	10.2	256
38	80	7	-9	7	10.5	263
40	20	16	11	24	10.4	260
41	75	40	-15	28	9.2	231
42	73	19	-14	27	10.8	271
43	77	16	-12	8	7.6	190
44	77	37	-50	27	7.4	186
45	21	27	-10	23	11.6	290
46	51	35	-10	21	6.7	169
47	64	21	-11	17	9.0	225
48	4	14	16	14	16.8	421
49	-30	14	16	18	10.2	256
50	83	17	-1	17	12.5	313
51	77	20	-17	19	6.5	163
52	-88	18	41	21	11.4	285
53	57	11	-2	30	9.1	229
55	54	11	-3	9	7.7	194
56	46	29	-4	20	7.4	185
57	89	5	-9	4	11.7	294
61	59	11	1	9	7.5	188
62	66	32	-2	35	8.2	206
63	-85	9	18	18	10.9	273
65	-89	25	27	31	7.5	188
67	70	9	3	18	10.0	250

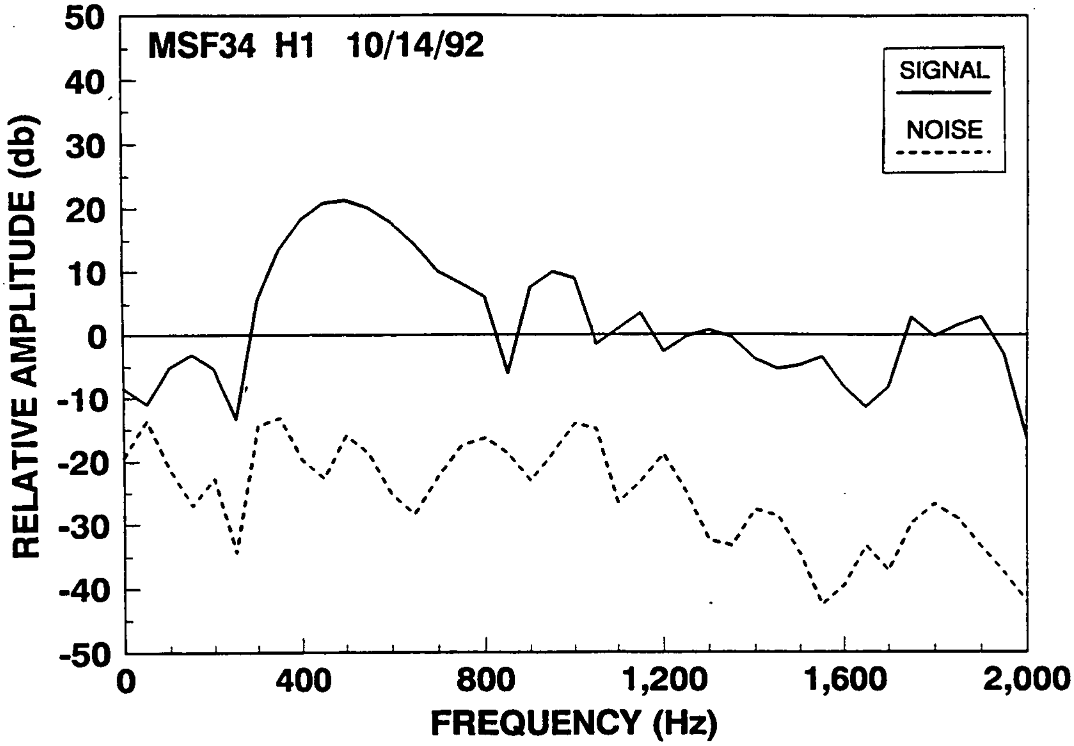

Figure 45 Noise and Signal Spectra, Event No. 34, X Channel

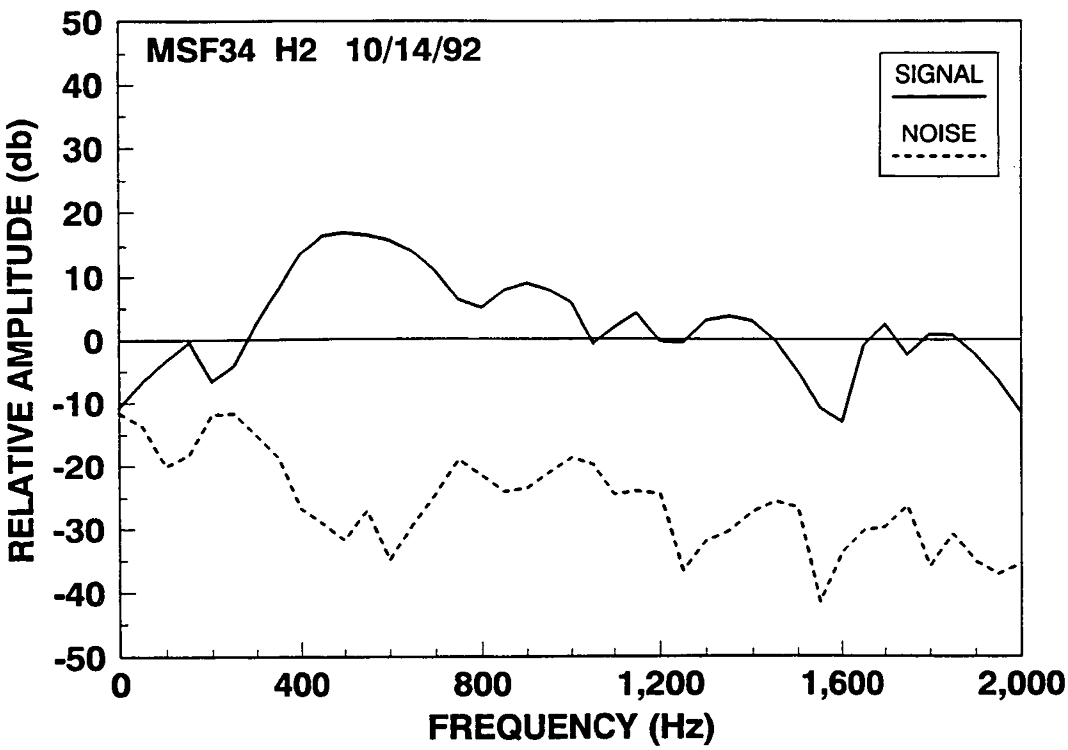

Figure 46 Noise and Signal Spectra, Event No. 34, Y Channel

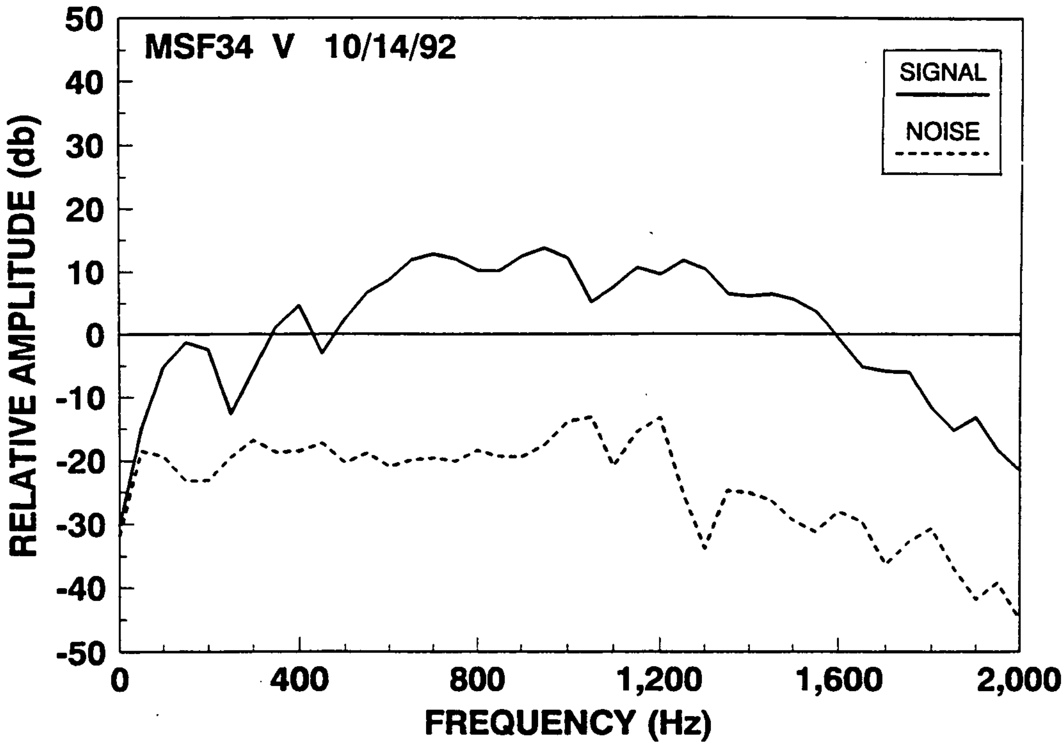

Figure 47 Noise and Signal Spectra, Event No. 34, Z Channel

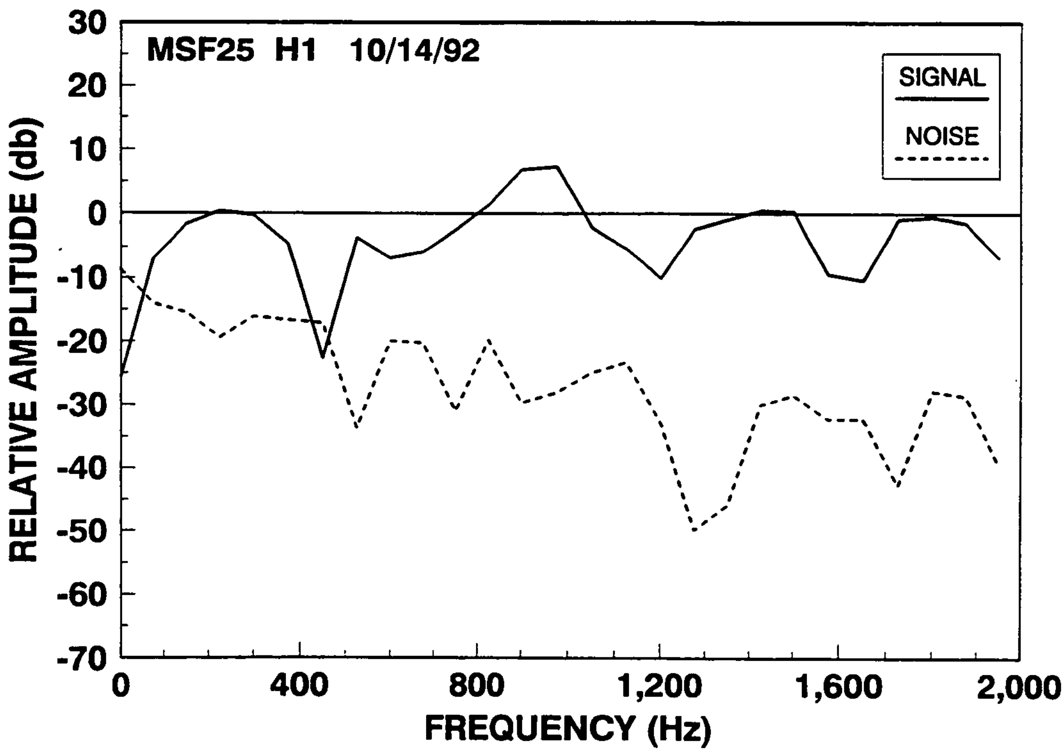

Figure 48 Noise and Signal Spectra, Event No. 25, X Channel

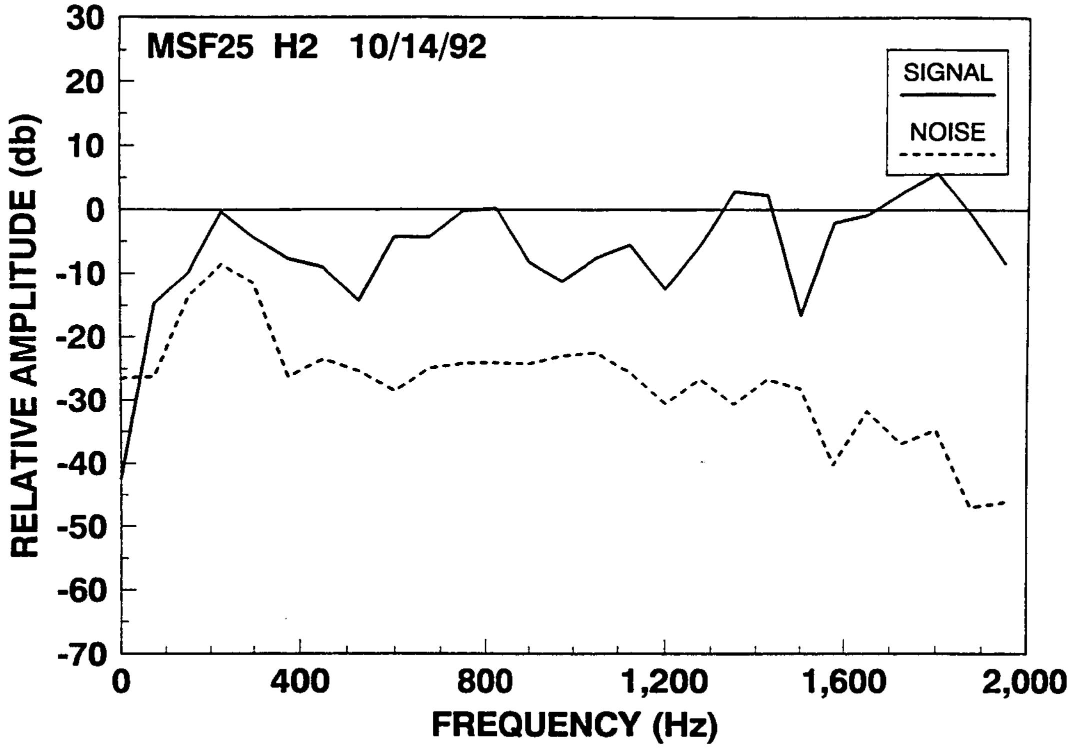

Figure 49 Noise and Signal Spectra, Event No. 25, Y Channel

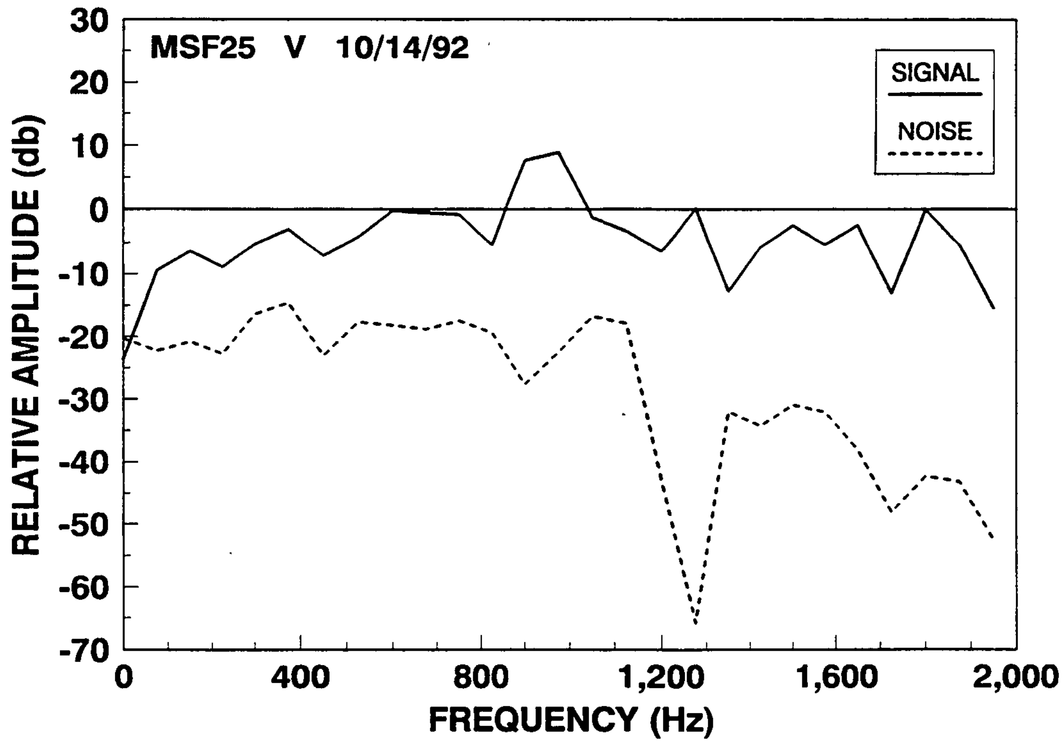

Figure 50 Noise and Signal Spectra, Event No. 25, Z Channel

3. Over 1,000 microseismic signals were generated during the hydraulic-fracture injections. Thus, large numbers of signals are available for mapping the hydraulic fracture.

4. Many microseisms have clear first arrivals with high signal-to-noise ratios. This is the most important characteristic for determining distance to an event since triangulation techniques will be used for distance estimates.

5. Many microseisms had highly polarized p-wave arrivals, indicating that the orientation of the events can be determined. Coupled with the distance estimate, this experiment demonstrates that seismic signals can be located.

6. Many microseisms had both p- and s-waves that were well defined, demonstrating that event distance can also be determined from p-s separations, assuming that the velocity structure is known.

7. A rough map of the fracture could be made with a limited number of signals and the orientation of the fracture agrees with the orientation of the stress field at this site.

The results of this site suitability assessment have implications for any additional work done at this site or other sites. Recommendations for future monitoring are:

- Record continuously on a wide-band-width, wide-dynamic-range audio-digital recorder such as the Sony used in these tests.
- Develop a high-sample rate, real-time event detector.
- Use a gyro or other means for an accurate, ground-truth orientation of the receiver(s).
- Take special precautions to assure a good quality clamp of the receiver(s).
- Consider multi-station receiver arrays for improved range and azimuth measurements.
- Develop techniques to automate the processing as much as possible. With so many microseisms, only a small fraction of them can be processed individually by an analyst.

5.0 Overall Conclusions

Assessments of mechanical wellbore conditions, background seismic noise, seismic signal attenuation, remote seismic signal detection, stress contrast and hydraulic fracture pressure response have clearly shown that the MWX site is suitable for future fracture diagnostics experimentation to be conducted by GRI and DOE. The GRI contractor team consisting of CER, Resources Engineering Systems and Sandia National Laboratories recommend that GRI and DOE pursue the establishment of a subsurface laboratory for fracture diagnostics and modeling research at the MWX site.

With the acceptance of this conclusion, M-Site No. 1 planning can progress. It is anticipated that the 1993 operations and experiments will include:

- Design and construction of data acquisition systems capable of acquiring, storing and distributing pressure and seismic data during injection experiments.

- Installation of additional site infrastructure (power, cabling, control trailers) to facilitate the implementation of the experiments.

- Design and drilling of a monitor well capable of housing accelerometer and inclinometer instrumentation for future comprehensive fracture mapping experiments.

- Acquisition of additional core and log data during the drilling of the monitor well to develop a complete reservoir description.

- Acquisition of additional stress test data in the MWX wells in and around the sandstone units that will be the focus of the fracture experimentation.

- Execution of several mini-frac injections in the MWX wells while acquiring bottomhole pressure data and remotely monitoring seismic data. These experiments will be designed to test the infrastructure and data acquisition systems, as well as collect data for fracture diagnostics and fracture modeling. These experiments are considered to be an intermediate step taken before conducting more comprehensive experimentation using monitor well instrumentation.

Planning beyond 1993 is tentative and will be confirmed after evaluating the project's initial phase.

6.0 References

Cleary, M.P., D.E. Johnson, H.H. Kogsboll, K.A. Owens, K.F. Perry, C.J. de Pater, A. Stachel, H. Schmidt, and M. Tambini, 1993: "Field Implementation of Proppant Slugs to Avoid Premature Screen-Out of Hydraulic Fractures with Adequate Proppant Concentration," SPE No. 25892 to be presented at the 1993 Low Permeability Reservoir Symposium, Denver, April.

Crockett, A.R. and N.M. Okusu, 1986: "A Complete Integrated Model for Design and Real-Time Analysis of Hydraulic Fracture Operations," SPE No. 15069 presented at the 56th California Regional Meeting, Oakland, April.

Warpinski, N.R., 1990: *Multiwell Experiment Final Report, IV. The Fluvial Interval of the Mesaverde Formation*, Sandia Report SAND 89-2612/Part A, Chapter 6: "In Situ Stress," p. 6.19, prepared for the U.S. Department of Energy under Contract No. DE-AC04-76DP00789.

Appendix 1

BIBLIOGRAPHY OF REPORTS AND TECHNICAL PAPERS RESULTING FROM MWX RESEARCH

The Multiwell Experiment—A Field Laboratory in Tight Gas Sandstone Reservoirs

David A. Northrop, SPE, Sandia Natl. Laboratories, and
Karl-Heinz Frohne, SPE, U.S. DOE

Summary. The U.S. DOE's Multiwell Experiment (MWX) was a field laboratory aimed at improved characterization and gas production from low-permeability reservoirs typified by the Mesaverde Group in western Colorado. A broad spectrum of activities was conducted over 8 years at a site containing three closely spaced (<225 ft [<68 m]), deep (7,550 to 8,350 ft [2300 to 2550 m]) wells. The results yielded insights and contributions into the technology of gas production from this resource.

Introduction

New and improved technology is required to enhance natural gas production from the extensive low-permeability sandstone reservoirs of the U.S. This large potential resource has more than 600 Tcf [17 Gm^3] of technically recoverable gas.[1] More specific to this study, a resource analysis of the Mesaverde Group's tight sandstones in the Piceance basin estimated 420 Tcf [11.9 Gm^3] gas in place, with 68 Tcf [1.9 Gm^3] identified as technically recoverable.[2]

Government-sponsored tight gas research efforts to stimulate production from these reservoirs began in the mid-1960's. The initial focus was on the development of stimulation technology with the use of nuclear explosives to induce fracturing. Results showed that substantial further development and public support were necessary.[3] Efforts then focused on massive-hydraulic-fracturing (MHF) tests, cost-shared with industry in several western basins. Field tests were conducted in the Piceance (Colorado),[4] Uinta (Utah),[5] and Greater Green River (Wyoming) basins, and consisted of coring, special logging, and productivity testing followed by large hydraulic stimulations. Results from tests conducted through 1979 were disappointing and did not improve technology or consistently enhance production.

Review and analysis of this pool of reservoir and fracturing information indicated that tight gas reservoir parameters varied widely within the three basins. Well production performance following the cost-shared MHF's was unpredictable. The basic shortcomings were that these tests failed to separate reservoir behavior from stimulation effectiveness and did not provide sufficient data to define the critical factors affecting gas production.

As a result, the U.S. DOE developed and operated the MWX, a research-oriented field laboratory, during 1981–88. The principal objective was to obtain sufficient information on the geologic and technical aspects of gas production from the widespread Mesaverde Group to unlock its tight gas resource.

A key feature of the MWX was three wells spaced 110 to 215 ft [34 to 66 m] apart (**Fig. 1**). Drilling and configuration for the three wells are described in Refs. 6 through 8, and general project overviews detailing objectives, plans, and activities are in Refs. 9 through 13. Detailed core, log, and well-test data from such close well spacings and direct geologic study of nearby surface outcrops of the Mesaverde provided detailed reservoir characterizations. Interference and tracer tests, as well as the use of fracture diagnostics in offset wells, provided additional uncommon information on stimulation and production behavior. Another key feature was the synergism resulting from a broad spectrum of supporting activities: geophysical surveys, sedimentological studies, core and log analyses, well testing, in-situ stress determination, stimulation experiments with fracture diagnostics, and reservoir performance analyses.

This paper highlights some of the insights on natural gas production from low-permeability sandstones and the technological contributions gained from the MWX. Employees at Sandia Natl. Laboratories and CER Corp. were the principal investigators at the MWX, with the DOE providing research management. Many other independent researchers added to the information pool with studies of MWX core, logs, and other experimental data. This paper summarizes the results from this unique project.

Description

The MWX's focus was the Mesaverde formation of northwest Colorado. This thick sequence was deposited during the Late Cretaceous over a broad region of the western U.S., and contemporaneous formations are found in the Green River, Wind River, Uinta, and San Juan basins. The MWX field laboratory is in the Rulison field in the east-central portion of the Piceance basin. The site is in Section 34, T6S, R94W in Garfield County and is 7 miles [11 km] southwest of Rifle, just south of the Colorado River (Fig. 1). Here, the Mesaverde formation lies at 4,000 to 8,250 ft [1220 to 2520 m] between the overlying Wasatch formation and the underlying Mancos shale.

Three wells were drilled: MWX-1 to 8,350 ft [2550 m], MWX-2 to 8,300 ft [2530 m], and MWX-3 to 7,565 ft [2305 m]. More than 4,100 ft [1250 m] of 4-in. [10-cm] core—approximately 30% of it oriented—was cut with >99% recovery.[14-18] Numerous logging programs containing both standard and experimental logs were conducted. The three wells are exceptionally straight, with relative separations of 110 to 215 ft [34 to 66 m] at depth (Fig. 1). Significant gas shows were encountered throughout the section in all three wells and mud weights as high as 15 lbm/gal [1800 kg/m^3] were required to maintain well control. **Fig. 2** shows gamma ray logs from the three wells over the entire Mesaverde at the MWX site; the various tested zones are identified.

Activities at the MWX site were conducted from Aug. 1981 to Dec. 1987. Natural productivity tests were conducted in the Corcoran/Cozzette marine sandstones (Aug. 1982 to July 1983).[19] Complete stimulation experiments were conducted in the lenticular sands of the overlying (nonmarine) paludal (July 1983 to Aug. 1984), coastal (through June 1986), and fluvial (through Dec. 1988) intervals.[20-22] Each experiment consisted of detailed interval characterization, prefracture well tests, stress tests, stimulation-related tests (e.g., step-rate, flowback, and minifracture), a propped stimulation with fracture diagnostics, and postfracture well tests. The well testing included production, drawdown, buildup, pulse, and nitrogen-

June 22, 1993

To: Carol Patterson DOE/OSTI

From: Norm Warpinski, SANDIA NATL LABS, 6114

Re: Multi-Site Project Seismic Verification Experiment and Assessment of Site Suitability

Within this report is an SPE paper by Northrop and Frohne, "The Multiwell Experiment - A Field Laboratory in Tight Gas Sandstone Reservoirs." The SPE number for this paper is SPE18286. This paper was written under DOE funding and a copyright exemption is given by SPE for all government-funded papers. Thus this paper belongs to DOE.

I called SPE to confirm this and spoke to Carol Paschetag who checked the files. She confirmed that SPE does not hold a copyrig and this paper is open information. She also stated that the copyright note was either inadvertent or placed there because it was in a JPT (Journal of Petroleum Technology) magazine. Regardless, Carol says it is open information and DOE can do what it wants.

Norm R. Warpinski

Norm Warpinski

(505) 844-3640

The Multiwell Experiment—A Field Laboratory in Tight Gas Sandstone Reservoirs

David A. Northrop, SPE, Sandia Natl. Laboratories, and
Karl-Heinz Frohne, SPE, U.S. DOE

Summary. The U.S. DOE's Multiwell Experiment (MWX) was a field laboratory aimed at improved characterization and gas production from low-permeability reservoirs typified by the Mesaverde Group in western Colorado. A broad spectrum of activities was conducted over 8 years at a site containing three closely spaced (<225 ft [<68 m]), deep (7,550 to 8,350 ft [2300 to 2550 m]) wells. The results yielded insights and contributions into the technology of gas production from this resource.

Introduction

New and improved technology is required to enhance natural gas production from the extensive low-permeability sandstone reservoirs of the U.S. This large potential resource has more than 600 Tcf [17 Gm^3] of technically recoverable gas.[1] More specific to this study, a resource analysis of the Mesaverde Group's tight sandstones in the Piceance basin estimated 420 Tcf [11.9 Gm^3] gas in place, with 68 Tcf [1.9 Gm^3] identified as technically recoverable.[2]

Government-sponsored tight gas research efforts to stimulate production from these reservoirs began in the mid-1960's. The initial focus was on the development of stimulation technology with the use of nuclear explosives to induce fracturing. Results showed that substantial further development and public support were necessary.[3] Efforts then focused on massive-hydraulic-fracturing (MHF) tests, cost-shared with industry in several western basins. Field tests were conducted in the Piceance (Colorado),[4] Uinta (Utah),[5] and Greater Green River (Wyoming) basins, and consisted of coring, special logging, and productivity testing followed by large hydraulic stimulations. Results from tests conducted through 1979 were disappointing and did not improve technology or consistently enhance production.

Review and analysis of this pool of reservoir and fracturing information indicated that tight gas reservoir parameters varied widely within the three basins. Well production performance following the cost-shared MHF's was unpredictable. The basic shortcomings were that these tests failed to separate reservoir behavior from stimulation effectiveness and did not provide sufficient data to define the critical factors affecting gas production.

As a result, the U.S. DOE developed and operated the MWX, a research-oriented field laboratory, during 1981-88. The principal objective was to obtain sufficient information on the geologic and technical aspects of gas production from the widespread Mesaverde Group to unlock its tight gas resource.

A key feature of the MWX was three wells spaced 110 to 215 ft [34 to 66 m] apart (**Fig. 1**). Drilling and configuration for the three wells are described in Refs. 6 through 8, and general project overviews detailing objectives, plans, and activities are in Refs. 9 through 13. Detailed core, log, and well-test data from such close well spacings and direct geologic study of nearby surface outcrops of the Mesaverde provided detailed reservoir characterizations. Interference and tracer tests, as well as the use of fracture diagnostics in offset wells, provided additional uncommon information on stimulation and production behavior. Another key feature was the synergism resulting from a broad spectrum of supporting activities: geophysical surveys, sedimentological studies, core and log analyses, well testing, in-situ stress determination, stimulation experiments with fracture diagnostics, and reservoir performance analyses.

This paper highlights some of the insights on natural gas production from low-permeability sandstones and the technological contributions gained from the MWX. Employees at Sandia Natl. Laboratories and CER Corp. were the principal investigators at the MWX, with the DOE providing research management. Many other independent researchers added to the information pool with studies of MWX core, logs, and other experimental data. This paper summarizes the results from this unique project.

Description

The MWX's focus was the Mesaverde formation of northwest Colorado. This thick sequence was deposited during the Late Cretaceous over a broad region of the western U.S., and contemporaneous formations are found in the Green River, Wind River, Uinta, and San Juan basins. The MWX field laboratory is in the Rulison field in the east-central portion of the Piceance basin. The site is in Section 34, T6S, R94W in Garfield County and is 7 miles [11 km] southwest of Rifle, just south of the Colorado River (Fig. 1). Here, the Mesaverde formation lies at 4,000 to 8,250 ft [1220 to 2520 m] between the overlying Wasatch formation and the underlying Mancos shale.

Three wells were drilled: MWX-1 to 8,350 ft [2550 m], MWX-2 to 8,300 ft [2530 m], and MWX-3 to 7,565 ft [2305 m]. More than 4,100 ft [1250 m] of 4-in. [10-cm] core—approximately 30% of it oriented—was cut with >99% recovery.[14-18] Numerous logging programs containing both standard and experimental logs were conducted. The three wells are exceptionally straight, with relative separations of 110 to 215 ft [34 to 66 m] at depth (Fig. 1). Significant gas shows were encountered throughout the section in all three wells and mud weights as high as 15 lbm/gal [1800 kg/m^3] were required to maintain well control. **Fig. 2** shows gamma ray logs from the three wells over the entire Mesaverde at the MWX site; the various tested zones are identified.

Activities at the MWX site were conducted from Aug. 1981 to Dec. 1987. Natural productivity tests were conducted in the Corcoran/Cozzette marine sandstones (Aug. 1982 to July 1983).[19] Complete stimulation experiments were conducted in the lenticular sands of the overlying (nonmarine) paludal (July 1983 to Aug. 1984), coastal (through June 1986), and fluvial (through Dec. 1988) intervals.[20-22] Each experiment consisted of detailed interval characterization, prefracture well tests, stress tests, stimulation-related tests (e.g., step-rate, flowback, and minifracture), a propped stimulation with fracture diagnostics, and postfracture well tests. The well testing included production, drawdown, buildup, pulse, and nitrogen-injection tests. Most often tests were conducted in a three-well interference configuration with downhole shut-off tools and quartz pressure tranducers in all three wells. Several different well-test and simulation analysis techniques were used. A fully transient, 3D, naturally fractured, reservoir model and a stimulation-pressure history-match procedure provided the most valuable results.

Tables 1 and 2 summarize fracture, core, reservoir, and gas production data for the different intervals studied.

Insights

Insights into the characteristics of the reservoirs and their gas-production behavior at the MWX site are described under several topics,[23] as follows.

Depositional Environment. Historically, the Mesaverde Group has been subdivided by depositional environment into the marine Iles and the nonmarine Williams Fork formations. The different morphologies of the relatively continuous, blanket marine rocks and the discontinuous, lenticular, nonmarine rocks were recognized in early studies. However, there was no subdivision of the nonmarine rocks before the MWX.

One of the first MWX studies was a detailed examination of Mesaverde sedimentology.[24] This study was aided by the fact that the Mesaverde is exposed in outcrop at Rifle Gap in the Grand Hogback, about 11 miles [18 km] northeast of the MWX site. The sandstones stand out clearly in the outcrop, and sedimentological studies[25-27] showed that the Mesaverde could be divided into five distinct intervals according to their depositional environments. Other works provide detail on the mineralogy[28-30] and general geology[31-39] of the MWX and surrounding area.

1. The lowest interval (7,450 to 8,250 ft [2270 to 2520 m]), the marine, is composed of widespread shoreline-to-marine blanket sandstones and marine shales. The interval contains the Corcoran, Cozzette, and Rollins sandstones, which are interspersed with tongues of the Mancos shale.

2. The paludal interval (6,600 to 7,450 ft [2010 to 2270 m]) lies above the Rollins sandstone and was formed in a lower delta-plain environment. It is made up of lenticular distributary channel and splay sandstones interbedded with mudstones, siltstones, and abundant coal deposits.

3. The coastal interval (6,000 to 6,600 ft [1830 to 2010 m]) is characterized by distributary channel sandstones that were deposited in an upper delta-plain environment. The lack of coal is the primary difference between this interval and the paludal.

4. The fluvial interval (4,400 to 6,000 ft [1340 to 1830 m]) consists of irregularly shaped, multistory, composite sandstones that were deposited by broad meandering-stream systems.

5. The uppermost interval (4,000 to 4,400 ft [1220 to 1340 m]), the paralic, is a zone of returned-marine influence with more widespread, uniform sandstones. (This interval is believed to be water-saturated at the MWX site and has received little attention.)

One result of different depositional environments is widely different reservoir morphologies. The marine deposits are essentially continuous, blanket-like formations that are often traceable over much of the basin; as such, there is no preferred direction or trend in reservoir shape. The distributary channels of the delta-plain environment in the paludal and coastal intervals are relatively narrow, with estimated widths of 200 to 500 ft [60 to 150 m][33,34]; they have a distinct trend depending on the geography of the ancient river system. The fluvial sandstones are an intermediate case. They are significantly wider (1,000 to 2,500 ft [300 to 750 m]) than the channels and are a multilayered combination of many sinuous, point-bar units that have undergone several episodes of erosion and deposition. The nonmarine deposits can also contain overbank or splay deposits that give rise to fan-like, wedge-shaped deposits that are distinctly different from the other reservoir morphologies. Vertical seismic profiles,[40,41] testing and application of an experimental well-to-well borehole-tomography technique,[42-45] and a deep 3D seismic survey[45,46] were also conducted at the MWX site.

The energies and dynamics of the different depositional processes created different reservoir properties and distributions.[47] Properties in marine environments tend to be relatively uniform vertically and can be correlated laterally. In contrast, nonmarine reservoirs have a high degree of variability, both vertically and horizontally.

Natural Fractures. A major result of the MWX was the demonstration of the importance of natural fractures in gas production from Mesaverde reservoirs. The principal evidence for the existence of natural fractures is twofold.

1. Many natural fractures were observed in core. The 4,100 ft [1250 m] of core (much of it slabbed) was studied carefully for natural fractures, and fracture types, frequencies, widths, and other characteristics were determined.[18]

2. In all the intervals examined, the overall reservoir permeabilities determined by well tests and production are one to three orders of magnitude higher than the permeabilities of the matrix rock measured in core under restored conditions.[48,49]

Other studies[50-52] describe the macroscopic fracture networks across the Piceance basin.

A model was specially developed for the natural fracture system that exists at MWX,[48] but it is not considered unique to this area. We believe this model also applies to other low-permeability, flat-lying reservoir rocks with a history of high pore pressures and relatively low differential horizontal stresses. The principal features of the model follow.

1. Fractures are unidirectional and subparallel with infrequent, low-angle, echelon intersections.

2. Fractures occur in a wide spectrum of lengths, widths, and spacings.

3. Fractures and their interconnections are often narrow and/or mineralized, resulting in a stress-sensitive, easily damaged system.

4. Fractures terminate vertically at lithologic changes, both at the reservoir boundaries and at discontinuities within the reservoir.

The model was derived from a variety of evidence, including extensive core-based reservoir-characterization research[53-57] and special precision core-analysis[58-61] and mechanical-properties measurements.[62] Effective nonmarine-reservoir permeabilities range from 0.012 to 0.05 md in the intervals tested, yet pressure interference was rarely observed in the nearby observation wells. Model analysis indicates that a highly anisotropic reservoir, with its primary natural fracture network oriented parallel to the induced hydraulic fracture, will best match the test observations.[48,49,63] Other related studies concerned model development[49,64] and overviews of MWX modeling.[65,66]

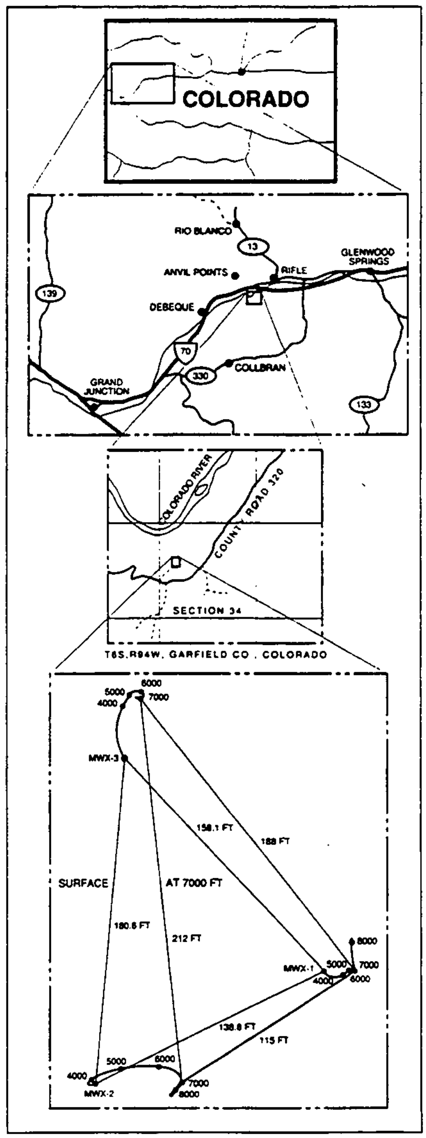

Fig. 1—Location of the MWX site and layout of the three MWX wells at the surface and at 7,000 ft.

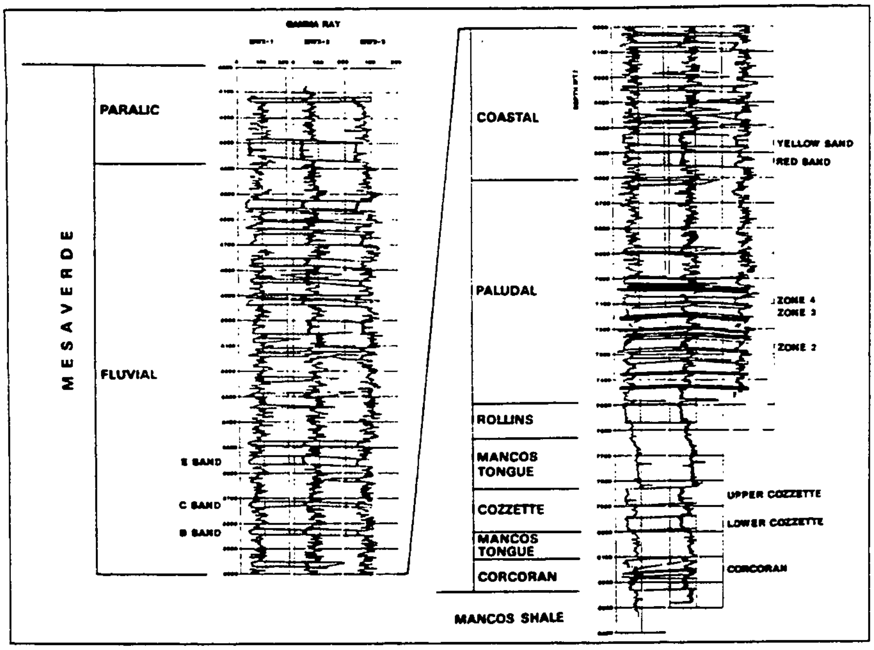

Fig. 2—Gamma ray logs of the three MWX wells through the Mesaverde Group showing the reservoirs tested.

In addition, nitrogen-injection tests showed that fracture interconnections, although poor, do exist. Also, the reservoirs are stress sensitive.[58] Production can be essentially shut off by reducing the reservoir pressure; then the in-situ stress effectively squeezes the fractures shut. Conversely, high-pressure injection of gas results in a dramatically increased reservoir permeability caused by the fractures' opening. Observations indicate a strong directionality for the fractures: of 62 fractures that occur in oriented MWX core, 51 strike west-northwest. Finally, outcrop studies provide an excellent picture of this unidirectional pattern, which is aligned parallel to the present maximum horizontal compressive stress.

Fractures occur principally in the sandstones and siltstones, and they terminate at mudstone or shale contacts of a reservoir boundary and at lithologic discontinuities within the reservoirs. In outcrop, <10% of all fractures extend the full thickness of a reservoir and half extend <40% of the full thickness. Thus, the average fracture spacing in heterogeneous sandstones is always significantly less than would be suggested by the one-to-one rule of thumb for fracture spacing and overall bed thickness.[47]

In-Situ Stresses. Detailed characterization of the stresses occurring over almost 4,000 ft [1200 m] of the Mesaverde was a unique result from MWX. Primary data sources were 63 small-volume hydraulic-fracture tests conducted to measure the minimum in-situ stresses[67-69] and the anelastic-strain recovery (ASR)[70-76] on selected oriented core. Supplemental data were provided by limited differential-strain-curve analysis on oriented core,[68] step-rate and pump-in/flowback tests associated with stimulations,[19-22] openhole log (televiewer and caliper) measurements of wellbore eccentricity and breakouts,[19-22] and seismic mapping of the geometry and orientation of the hydraulic fractures.[77-83]

Stress data obtained in sandstone, siltstone, mudstone, shale, and coal intervals by small-volume hydraulic-fracture stress tests show the effect of lithology on the minimum in-situ stress. The minimum horizontal-stress difference between the sandstones and the abutting rock is often >1,000 psi [>7 MPa]. Nonreservoir rocks are generally near lithostatic stress (~1 psi/ft [~23 kPa/m]). This large contrast is an important parameter in designing hydraulic-fracture treatments for these reservoirs because it implies a strong tendency for fracture containment and that high pressures would be required to fracture nonreservoir rock.

Analysis of the ASR data provides estimates of the relative magnitudes of the two horizontal stresses.[68] In sandstones, the horizontal-stress differences are typically

TABLE 1—SUMMARY OF FRACTURE, CORE, AND RESERVOIR DATA FOR THE DIFFERENT RESERVOIRS STUDIED

Depositional environment	Marine	Paludal	Coastal	Fluvial	
Average reservoir width	Several miles	200 to 500 ft	200 to 500 ft	1,000 to 2,500 ft	
Reservoir heterogeneity	Low	Moderate	Moderate	High	
Reservoir examined	Corcoran and Cozzette	Zones 3 and 4	Red and Yellow Sands	Sand B	Sand E
Approximate depth, ft	7,850 to 8,200	7,100	6,500	5,850	5,500
Core,* ft					
Examined	221	229	457	115	86
In pay	119	75	263	57	61
Oriented	221	87	277	17	14
Natural fractures in core					
Number observed	10	4	9	11	19
Number oriented	8	0	3	1	7
Strike					
West-northwest	3	—	3	1	4
North-northwest	4	—	—	—	2
Other	1 (north)	—	—	—	1 (northeast)
Width, mm	0.25 to 4.0	<0.25 to >1.0	<0.25 to 1.5	<0.25 to 1.5	<0.25 to >2.0
Well-test data (reservoir)					
Reservoir pressure, psi	6,300**	5,350	4,360 to 4,400	3,450	~3,200
Rate, Mcf/D†	550**	250	60	25	70
Interference?	Yes**	No	No	No	Yes
Core analysis data (matrix)					
Porosity, %	6 to 8	8 to 10	6 to 7	6 to 8	6 to 8
Permeability, μd‡	0.5 to 1.0	1.0 to 2.0	0.1 to 0.5	0.1 to 2.0	0.1 to 2.0
Water saturation, %	30 to 40	20 to 30	30 to 40	30 to 40	40 to 50

*Core in vicinity of selected reservoirs used in detailed examination; may include core from more than one well.
**Well-test data for the Upper Cozzette.
†After 10 days of production.
‡At reservoir pressure and water saturation.

about 600 to 800 psi [4.1 to 5.5 MPa]. The horizontal stresses in the mudstones or shales, however, are essentially isotropic, and on the average, slightly below the overburden value.

In sandstone and siltstone layers, where the horizontal stresses are anisotropic, the different measurement techniques show a fairly consistent maximum-horizontal-stress orientation of N85°E to N115°E.[68-77] The data suggest a clockwise rotation of the maximum-horizontal-stress direction with depth, which has been interpreted to result from the stresses associated with the large topographic relief superimposed on the regional stress field of the basin.[84]

TABLE 2—GAS PRODUCTION SUMMARY

Depositional Environment	Reservoir	Perforated Net Pay (ft)	Production (Mcf/D)* Prefracture	Postfracture	Test Activity
Fluvial	Sand E	30	70	240	Stimulation experiment
	Sand C	22	50	—	Unpropped minifractures
	Sand B	17	25	35	Stimulation experiment
Coastal	Red and Yellow Sands	66	60	90	Stimulation experiment
Paludal	Zones 3 and 4	4	250	170, 400**	Stimulation experiment
	Zone 2	28	160	—	Single well test
Marine	Upper Cozzette	37	550	—	Interference test
	Lower Cozzette	14	>150	—	Single well test
	Corcoran	65	>450	—	Single well test

*Generally after 10 days of production.
**Upon re-entry after 20-month shut-in.

Hydraulic Fracturing. The combination of the effects of depositional environment, natural fractures, and in-situ stresses places constraints on the effectiveness of hydraulic fracturing as a means of stimulating these reservoirs. Results of stimulation tests at the MWX site are shown in Table 2. Treatment designs were supported by laboratory tests of rock/fluid interactions and other parameters,[85-90] and the resulting fracture geometry was monitored in real time by downhole seismic instrumentation.[77-83]

At the MWX site, the current stress state and the paleostress state that created the unidirectional fracture system have the same orientation. This means that a hydraulic fracture will parallel the natural fractures and thus intersect relatively few of the more conductive paths. As such, the hydraulic fracture contacts mostly microdarcy-to-submicrodarcy rock, and the few fractures that it intersects can be damaged, leading to an overall postfracture reduction in gas production. (The feasibility of altering the stress state so that a hydraulic fracture would propagate perpendicular to the fracture system was shown at this site.[91])

In nonmarine intervals, the limited size of the reservoir affects the efficiency of hydraulic fracturing. For a single reservoir, the intersection of the hydraulic-fracture plane relative to the reservoir direction and size is important. This intersection is controlled by both the reservoir size and the relative angle between the maximum principal horizontal stress (fracture plane) and the reservoir width.

An important result of different in-situ stresses in different lithologies is that a hydraulic fracture will not easily break out of a low-stress sandstone, traverse the high-stress confining rocks, and intersect another sandstone. Thus the intersection, propping, and drainage of a large number of remote reservoirs (i.e., those not connected to the wellbore) will not be feasible in the presence of large stress contrasts.

During all the fracturing tests, very high treating pressures were observed; these were considerably higher than would be expected from simple analysis of fracturing.[92] The high pressures may be caused by high stresses in the confining lithologies, backstresses, multiple fracturing, or the presence of thin, high-stress stringers in the reservoir. Whatever their cause, these high pressures can result in many deleterious effects, such as shorter and wider fractures that have less effective drainage and damage to the narrow natural fracture by the fracturing fluids. The high pumping pressures may have opened the intersecting natural fractures and forced fracture fluid and its additives into them. Evidence for opening the fracture system is found in the observation of significantly increased leakoff coefficients above a threshold pressure of 850 to 1,050 psi [5.9 to 7.2 MPa] at this site above closure.[93]

Gas Production. Table 2 summarizes gas production from individual Mesaverde reservoirs as measured during MWX testing, and **Table 3** gives the Mesaverde gas-in-place estimates at the MWX site from these test results. A correlation clearly exists between depositional environment and production.[47] Marine reservoirs have the highest production potential, and the coastal and paludal reservoirs have the same basic limited, lenticular morphologies. The paludal, however, has better potential than the coastal because of improved reservoir properties, much higher pore pressures, and adjacent coal seams and organic-rich sediments. Fluvial sandstones have average natural production, but offer the potential of better stimulation improvement ratios because of their greater average reservoir widths.

Natural fractures control the overall reservoir permeability in all zones tested. The anisotropic, unidirectional fracture system, however, limited the effectiveness of hydraulic fracturing at this site, as discussed previously, and prevented pressure interference from being observed in most well tests.

In general, breakdowns followed by extended cleanup times and well-test periods were required for all the Mesaverde reservoirs, as illustrated by marine productivity tests.[19-22,94] In each case, the well would not flow following perforation. After breakdown of the perforations with modest amounts (1.0 to 1.5 bbl/perforation [0.16 to 0.24 m^3/perforation]) of 3% KCl water with ball sealers, however, the well began to unload and produce gas. After initially flowing 75, 200, and 300 Mcf/D [2100, 5700, and 8500 std m^3/d], respectively, overall productivity of the Corcoran and Lower and Upper Cozzette sandstones continued to increase during the weeks of well testing. Final production rates from the three zones were 150, 400, and 750 Mcf/D [4200, 11 300, and 21 200 std m^3/d], respectively, and might have increased further with time. These rates are excellent for naturally fractured tight sandstones with submicrodarcy matrix permeability. The point is that if only the initial data or short well tests had been used, they would have provided an inaccurate measure of the true productive potential of the reservoir.

While the KCl breakdowns with extended cleanup were successful in early tests, it became evident that the lenticular reservoirs above the marine interval were very water-sensitive. This was particularly true in the coastal and fluvial zones, where the low gas flow rates and pressures were insufficient to clean up the natural fractures and wellbore. Various ways were tried to achieve the necessary perforation breakdowns without the addition of water.[95] Nitrogen gas was injected at high rates to break down the sands, but it became clear that not all perforations were being treated equally. A propellant-based dynamic-fracturing method was also attempted, but experimental problems prevented a conclusive assessment. A new and simple approach attempted in the last breakdown at the test site gave excellent results. The zone was perforated while the casing was pressurized with nitrogen gas to around 3,000 psi [20.6 MPa] above the in-situ formation stress. When all perforations were fired simultaneously, the high pressures of the dynamic treatment apparently cleaned all perforations; excellent communication was immediately established with the formation.

The sensitivity of these naturally fractured reservoirs to stimulation fluids is well illustrated in the stimulation experiment conducted in Zones 3 and 4 of the paludal interval.[92,96,97] Prefracture production was 250 Mcf/D [7100 std m^3/d]. After step-rate and pump-in/flowback tests with KCl water, two minifractures (totaling 45,000 gal [170 m^3] of 30 and 60 lbm/1,000 gal [3.6 and 7.2 kg/m^3] of linear gel), and relatively good cleanup (~90% fluid recovery), sustainable production was only 200 Mcf/D [5700 std m^3/d]. Then a propped-hydraulic-fracture treatment was conducted with 65,000 gal [250 m^3] of 25 to 40 lbm/1,000 gal [3.0 to 4.8 kg/m^3] of crosslinked gel

TABLE 3—GAS IN PLACE

Interval	Reservoir	Each Reservoir* (Bcf/mile)	Total Interval** (Bcf/section)
Fluvial	Sand E	1.9	54.7
	Sand C	1.4	
	Sand B	0.6	
Coastal	Yellow Sand	0.5	31.2
	Red Sand	1.1	
Paludal	Zones 3 and 4	0.6	35.0 (+23)†
	Zone 2	0.7	
Marine	Upper Cozzette	15.2‡	35.2 (+3)†
	Lower Cozzette	10.9‡	
	Corcoran	7.9‡	
Total			156.1 (+26)†

*From measured properties and individual reservoir widths.
**From measured properties and sandstone fraction of the interval.
†Estimated contribution of gas from coal seams.
‡Assumed mile width for blanket marine reservoirs.

and 193,000 lbm [88 000 kg] of sand proppant. Several problems arose during the lengthy cleanup, however, and total recovery of fracture fluid was <80%. Postfracture well testing showed a maximum sustainable production of only 170 Mcf/D [4800 std m^3/d]. There were indications that the zone was continuing to improve slowly with time, but such long cleanup times will be a problem for operators.

After 20 months of shut-in beneath a bridge plug while other operations were conducted uphole, this paludal zone was reentered and tested; it averaged 320 Mcf/D [9100 std m^3/d] over 7 weeks.[92,97] No liquids were produced initially, but after 5 days of flowing, water production began and increased rapidly to about 35 B/D [5.6 m^3/d]. Re-entry results of the paludal zone show that the damage after the fracture was reversible and was probably caused by water and gel blockage of the natural fractures. Over the long shut-in, the gel may have degraded further, and imbibition of the water into the matrix rock probably cleared the natural fractures of most water. When production was resumed, gas flow through the natural fractures was no longer blocked, and flow rates increased significantly and were sufficient to sweep produced water from the well.

Contributions to Technology

MWX's contributions to the fields of geology, reservoir, and production technology and practice are listed below.

1. Between late 1981 and 1983, more than 4,100 ft [1250 m] of Mesaverde formation core was recovered during drilling of the three test wells. Much of this very-low-permeability core was sent through one service laboratory for conventional and special reservoir-property analyses. When this service contract started, state-of-the-art permeability-measurement capability was limited to a 10-to-100-μd range (i.e., very low permeabilities were commonly expressed as <0.01 md). The large amount of MWX core catalyzed development of more precise measurement apparatus and techniques and brought about the capability to measure permeabilities $\ll 1$ μd routinely. This represents more than two orders of magnitude of increased precision.

2. The same availability of core, the extensive MWX stress-measurement program (by hydraulic breakdown), and geologic investigations supported development of the ASR technique[70-72] to measure stress orientations (e.g., hydraulic-fracture azimuth) in oriented core. This approach has been accepted as an alternative to direct in-situ field measurement of stress and is now offered to industry by service organizations. Viscoelastic models applied to ASR data also provide estimates of the in-situ stress magnitudes.[74]

3. The need for precise, research-grade interpretation of the extensive geophysical log suites run on the three MWX wells advanced the state of the art for tight-sands log analysis. Special crossplot and other interpretation techniques were developed specifically for tight-sands application and were then refined during the analysis of the complete MWX suites.[98-103] The result was a computerized tight-sands log-analysis system, which is now available to the industry.

4. A detailed geologic/reservoir model of the Mesaverde formation was derived by MWX researchers from standard and directionally oriented core, surface outcrops of the formation, research-grade log suites, regional natural fracture studies, and extensive well-test data. Two key features are the significance of different depositional environments[27,47] and the predominant role of natural fractures in Mesaverde production.[47,48] Studies of stratigraphy, sedimentology, and paleodeposition patterns from detailed examination of core structure and fossil evidence were used to reconstruct depositional environments. Direct inspection of outcrops (at Rifle Gap close to the test site and at Cameo at the opposite end of the Piceance basin) combined with log/core correlations and well-test information defined natural fracture patterns and the mechanics of gas flow from the reservoir matrix to the wellbore. Thus, the geologic model of the Mesaverde, although based primarily on information derived from the MWX site, can be extrapolated and applied by operators across the basin.

5. A methodology was developed to estimate the width of a nonmarine reservoir from single-well data.[33,34] The key is first determining the specific depositional environment. Empirical relationships derived from similar outcrops and/or contemporary environments are then used to relate reservoir height (measured in the wellbore) to reservoir width. This procedure usually provides a minimum width because the well may not have penetrated the greatest thickness or the deposit may have been partially eroded by a subsequent fluvial episode.

6. Vertical containment of hydraulic fractures in the target formation is very important to stimulation efficiency. It is known that fracture-height growth is primarily controlled by the in-situ stress in the pay zone relative to stresses in the strata above and below the perforated interval and that these stresses must be measured to optimize treatment design. The extensive series of small-hydraulic-fracture tests conducted to profile geologic stresses at the MWX site resulted in developing and demonstrating a reliable stress-measurement technique.[67-69] The method uses a downhole shut-in device combined with a quartz pressure gauge to record the instantaneous shut-in pressure in a 2-ft [0.6-m] interval after injection of small volumes of fluid. The stress-determination technique is now commonly accepted by the industry as a basic requirement for good fracture-treatment design.

7. A dual leakoff phenomenon was identified during hydraulic-fracture treatments in these formations.[93] In these cases, a significantly increased (50 times) leakoff occurred above a threshold pressure (850 to 1,050 psi [5.9 to 7.2 MPa] at this site), above the formation closure pressure. This increased leakoff results in rapid fluid loss and is a probable cause of early screenouts. It was shown that the use of fine (100-mesh) sand, along with increased pad volumes and careful fracture design and execution, reduces this leakoff to manageable levels.[93]

8. The five complete stimulation experiments executed in the fully characterized MWX reservoirs provided much information on fracturing performance in the lenticular Mesaverde sandstones.[20-22,92,104,105] Stimulation effectiveness was evaluated with a combination of state-of-the-art fracture design and execution under controlled conditions, fracture diagnostic instrumentation, core-based laboratory studies of the interaction of fracture fluids and proppants with the formation, and pre- and postfracture production performance testing. This systems approach to analyzing the experiments demonstrated that fracture fluid compatibility with the stimulated formation, and the possible effects of formation damage, plays a large part in the performance of hydraulic fracturing in tight naturally fractured sandstones.

9. The cutting of more than 4,100 ft [1250 m] of core at one site presented an opportunity to evaluate the performance of coring hardware. When polycrystalline-diamond-compact (PDC) coring bits came into limited

usage, the MWX core program provided the test bed for the new technology in the Rocky Mountain oil and gas province. Repeated head-to-head runs of conventional diamond and PDC core bits clearly demonstrated the effectiveness of the new design in the hard, interbedded, sand/silt/shale sequences common to the Mesaverde.[6-8]

10. The overall scope and variety of tight-sandstone research at the site, regional geologic studies, and the supporting laboratory research generated much new information on tight gas sands. This information is entering the literature, as illustrated by this paper's (by no means all-inclusive) references. Finally, a comprehensive technical data base, which contains the detailed engineering, scientific, and geological data resulting from the research, is available.[19-22]

Conclusion

In-depth studies of a sequence of low-permeability gas reservoirs in the Mesaverde formation were conducted during the DOE's MWX. The synergism of the various disciplines working jointly at this field laboratory resulted in an unprecedented study of such reservoirs. The insights and contributions from the MWX project have enhanced the ability of gas-producing industries to recover gas from this large resource.

Acknowledgments

We thank Norman Warpinski, John Lorenz, Allan Sattler, and Paul Branagan, who were principal investigators at the MWX. This paper merely highlights many excellent studies that resulted from the skilled efforts and hard work of many people at Sandia Natl. Laboratories, CER Corp., and elsewhere who have participated in the MWX. This work was sponsored by the U.S. DOE Western Gas Sands Subprogram under Contract No. DE-AC04-76DP00789.

References

1. *Unconventional Gas Sources—Volume V: Tight Gas Reservoirs, Part I*, Natl. Petroleum Council (Dec. 1980).
2. Johnson, R.C. *et al.*: "An Assessment of Gas in Low-Permeability Sandstones of the Upper Cretaceous Mesaverde Group, Piceance Basin, Colorado," open-file report No. 87-357, U.S. Geological Survey, Denver (1987) 1-21.
3. Luetkehans, G.R. and Toman, J.: "Status Report on the Three Nuclear Experiments for Stimulation of Tight Gas Sands," *Proc.*, Symposium on Stimulation of Low Permeability Reservoirs, Golden, CO, Feb. 16-17, 1976.
4. Fitch, J.L., Medlin, W.L., and Strubhar, M.K.: "Demonstration of Massive Hydraulic Fracturing, Piceance Basin, Rio Blanco County, Colorado," *Proc.*, Fifth Annual DOE Symposium on Enhanced Oil and Gas Recovery, Tulsa, OK (Aug. 22-24, 1979) M-1/1-20.
5. Merrill, R.G.: "Progress Report and Review of Natural Buttes Unit—Massive Hydraulic Fracturing Project," *Proc.*, Fourth Annual DOE Symposium on Enhanced Oil and Gas Recovery, Tulsa, OK (Aug. 29-31, 1978) F-3/1-14.
6. "Multiwell Experiment MWX-1 As-Built Report," CER Corp. report SAND82-7201, Sandia Natl. Laboratories, Albuquerque (July 1982).
7. "Multiwell Experiment MWX-2 As-Built Report," CER Corp. report SAND82-7100, Sandia Natl. Laboratories, Albuquerque (Feb. 1984).
8. "Multiwell Experiment MWX-3 As-Built Report," CER Corp. report SAND84-7132, Sandia Natl. Laboratories, Albuquerque (Feb. 1984).
9. Atkinson, C.H. *et al.*: "The Department of Energy's Western Gas Sands Project Multiwell Experiment," paper SPE 9891 presented at the 1981 SPE/DOE Symposium on Low Permeability Gas Reservoirs, Denver, May 27-29.
10. Northrop, D.A. and Sattler, A.R.: "The Multiwell Experiment: A Field Laboratory for Tight Gas Sands Research," *Proc.*, 17th Intersociety Energy Conversion Engineering Conference, Los Angeles (Aug. 8-13, 1982) paper 829175, 1027-34.
11. Crawley, A.B., Northrop, D.A., and Sattler, A.R.: "The Department of Energy's Western Gas Sands Project Multiwell Experiment Update," paper SPE 11183 presented at the 1982 SPE Annual Technical Conference and Exhibition, New Orleans, Sept. 26-29.
12. Northrop, D.A., Sattler, A.R., and Westhusing, J.K.: "Multiwell Experiment: A Field Laboratory for Tight Gas Sands," paper SPE 11646 presented at the 1983 SPE/DOE Symposium on Low Permeability Gas Reservoirs, Denver, March 14-16.
13. Northrop, D.A. *et al.*: "Current Status of the Multiwell Experiment," paper SPE 12868 presented at the 1984 SPE Unconventional Gas Recovery Symposium, Pittsburgh, May 13-15.
14. Sattler, A.R.: "The Multiwell Experiment Core Program: Part I," paper SPE 11763 presented at the 1983 SPE/DOE Symposium on Low Permeability Gas Reservoirs, Denver, March 14-16.
15. Sattler, A.R.: "The Multiwell Experiment Core Program: Part II," paper SPE 12854 presented at the 1984 SPE Unconventional Gas Recovery Symposium, Pittsburgh, May 13-15.
16. Sattler, A.R.: "Core Analysis in a Low Permeability Sandstone Reservoir: Results from the Multiwell Experiment," report SAND89-0710, Sandia Natl. Laboratories, Albuquerque (April 1989).
17. Sattler, A.R., Heckes, A.A., and Clark, J.A.: "Pressure-Core Measurements in Tight Sandstone Lenses During the Multiwell Experiment," *SPEFE* (Sept. 1988) 645-50.
18. Finley, S.J. and Lorenz, J.C.: "Characterization of Natural Fractures in Mesaverde Core From the Multiwell Experiment," report SAND88-1800, Sandia Natl. Laboratories, Albuquerque (Sept. 1988).
19. "Multiwell Experiment Final Report: I. The Marine Interval of the Mesaverde Formation," Multiwell Experiment Project Groups, Sandia Natl. Laboratories and CER Corp. report SAND87-0327, Sandia Natl. Laboratories, Albuquerque (April 1987).
20. "Multiwell Experiment Final Report: II. The Paludal Interval of the Mesaverde Formation," Multiwell Experiment Project Groups, Sandia Natl. Laboratories and CER Corp. report SAND88-1008, Sandia Natl. Laboratories, Albuquerque (May 1988).
21. "Multiwell Experiment Final Report: III. The Coastal Interval of the Mesaverde Formation," Multiwell Experiment Project Groups, Sandia Natl. Laboratories and CER Corp. report SAND88-3284, Sandia Natl. Laboratories, Albuquerque (March 1989).
22. "Multiwell Experiment Final Report: IV. The Fluvial Interval of the Mesaverde Formation," Sandia Natl. Laboratories and CER Corp. report SAND89-2612, Sandia Natl. Laboratories, Albuquerque (Jan. 1990) Parts A and B.
23. Northrop, D.A.: "Insights Into Natural Gas Production From Low-Permeability Reservoirs," paper SPE 17706 presented at the 1988 SPE Gas Technology Symposium, Dallas, June 13-15.
24. Lorenz, J.C.: "Sedimentology of the Mesaverde Formation at Rifle Gap, Colorado and Implications for Gas Bearing Intervals in the Sub-Surface," report SAND82-0604, Sandia Natl. Laboratories, Albuquerque (March 1982).
25. Lorenz, J.C. and Rutledge, A.K.: "Late Cretaceous Group Outcrops at Rifle Gap, Piceance Creek Basin, Northwestern Colorado," Geological Soc. of America Centennial Field Guide, GSA Rocky Mountain Section (1987).
26. Lorenz, J.C.: "Reservoir Sedimentology in Mesaverde Rocks at the Multiwell Experiment Site," report SAND83-1078, Sandia Natl. Laboratories, Albuquerque (June 1983).
27. Lorenz, J.C.: "Reservoir Sedimentology of Mesaverde Rocks at the Multiwell Experiment Site and East Central Piceance Creek Basin," report SAND87-0040, Sandia Natl. Laboratories, Albuquerque (Jan. 1987).
28. Heinze, D.M.: "Mineralogy and Petrology Aspects of the Mesaverde Formation at Rifle Gap, Colorado, Specific to the Sedimentology and Gas Bearing Intervals in the Subsurface," report SAND83-0287, Sandia Natl. Laboratories, Albuquerque (March 1983).
29. Heinze, D.M.: "Clay Identification and Amount Measured by Laboratory Techniques Compared to Well Log Responses: Application to Tight Gas Sands and Shales," report SAND85-0312, Sandia Natl. Laboratories, Albuquerque (March 1985).
30. Eatough, M.O.: "Mineralogic and Petrologic Overview of Core Samples From the U.S. DOE's Western Gas Sands Project Multiwell Experiment, Piceance Basin, Colorado," paper SPE 11764 presented at the 1983 SPE/DOE Symposium on Low Permeability Gas Reservoirs, Denver, March 14-16.
31. Lorenz, J.C.: "Lateral Variability in the Corcoran and Cozzette Suites of Blanket Sandstones, Piceance Creek Basin, Northwestern Colorado," paper SPE 11608 presented at the 1983 SPE/DOE Symposium on Low Permeability Gas Reservoirs, Denver, March 14-16.
32. Peterson, R.E. and Kohout, J.: "An Approximation of Continuity of Lenticular Mesaverde Sandstone Lenses Utilizing Close-Well Correlations, Piceance Basin, Northwestern Colorado," paper SPE 11610 presented at the 1983 SPE/DOE Symposium on Low Permeability Gas Reservoirs, Denver, March 14-16.
33. Lorenz, J.C.: "Predictions of Size and Orientations of Lenticular Reservoirs in the Mesaverde Group, Northwestern Colorado," paper SPE 13851 presented at the 1985 SPE/DOE Symposium on Low Permeability Gas Reservoirs, Denver, May 19-22.

34. Lorenz, J.C. *et al.*: "Determination of Widths of Meander-Belt Sandstone Reservoirs from Vertical Downhole Data, Mesaverde Group, Piceance Creek Basin, Colorado," *AAPG Bulletin* (May 1985) **69**, No. 5, 710–21.
35. Pitman, J.K. and Spencer, C.W.: "Petrology of Selected Sandstones in the MWX Wells (Northwest Colorado) and its Relationship to Borehole Geophysical Log Analysis and Reservoir Quality," open-file report No. 84-757, U.S. Geological Survey, Denver (1984) 33–66.
36. Lorenz, J.C.: "Tectonic and Stress Histories of the Piceance Creek Basin and the MWX Site, from 75 Million Years Ago to the Present," report SAND84-2603, Sandia Natl. Laboratories, Albuquerque (March 1985).
37. Peterson, R.E.: "Geological and Production Characteristics of the Nonmarine Part of the Mesaverde Group, Rulison Field Area, Piceance Basin, Colorado," paper SPE 12835 presented at the 1984 SPE Unconventional Gas Recovery Symposium, Pittsburgh, May 13–15.
38. "Geologic Studies in Support of the U.S. DOE's Multiwell Experiment, Garfield County, Colorado," C.W. Spencer and C.W. Keighin (eds.), open-file report No. 84-757, U.S. Geological Survey, Denver (1984) 1–134.
39. Lorenz, J.C. and Rutledge, A.K.: "Facies Relationships and Reservoir Potential of the Ohio Creek Interval Across the Piceance Basin," report SAND84-2610, Sandia Natl. Laboratories, Albuquerque (Jan. 1985).
40. Lee, M.W.: "Vertical Seismic Profiles at the Multiwell Experiment Site, Garfield County, Colorado," open-file report No. 84-168, U.S. Geological Survey, Denver (1983) 1–54.
41. Lee, M.W.: "Delineation of Lenticular-Type Sand Bodies by the Vertical Seismic Profiling Method," open-file report No. 84-265, U.S. Geological Survey, Denver (1984) 1–88.
42. Albright, J.N., Terry, D.A., and Bradley, C.R.: "Pattern Recognition and Tomography Using Crosswell Acoustic Data," paper SPE 13854 presented at the 1985 SPE/DOE Symposium on Low Permeability Gas Reservoirs, Denver, May 19–22.
43. Johnson, P.A. and Albright, J.N.: "In-Situ Physical Properties Using Crosswell Acoustic Data," paper SPE 13881 presented at the 1985 SPE/DOE Symposium on Low Permeability Gas Reservoirs, Denver, May 19–22.
44. Albright, J.N. *et al.*: "The Crosswell Acoustic Surveying Project," report LA-11157-MS, Los Alamos Natl. Laboratory (March 1988).
45. Searls, C.A. *et al.*: "A Coordinated Seismic Study of the Multiwell Experiment Site," paper SPE 11613 presented at the 1983 SPE/DOE Symposium on Low Permeability Gas Reservoirs, Denver, March 14-16.
46. Searls, C.A.: "The Multiwell Experiment Geophysics Program," final report SAND85-1013, Sandia Natl. Laboratories, Albuquerque (Sept. 1985).
47. Lorenz, J.C. and Finley, S.J.: "Differences in Fracture Characteristics and Related Production: Mesaverde Formation, Northwestern Colorado," *SPEFE* (March 1989) 11–16.
48. Lorenz, J.C. *et al.*: "Fracture Characteristics and Reservoir Behavior of Stress-Sensitive Fracture Systems in Flat-Lying Lenticular Formations," *JPT* (June 1989) 615–22; *Trans.*, AIME, **287.**
49. Branagan, P.T., Cipolla, C., and Lee, S.J.: "Designing and Evaluating Hydraulic Fracture Treatments in Naturally Fractured Reservoirs," paper SPE 16434 presented at the 1987 SPE/DOE Symposium on Low Permeability Reservoirs, Denver, May 18–19.
50. Verbeek, E.R. and Grout, M.A.: "Fracture History of the Northern Piceance Creek Basin, Northwestern Colorado," *Proc.*, 16th Oil Shale Symposium, J.H. Gary (ed.), Colorado School of Mines Press, Golden (1983) 26–44.
51. Grout, M.A. and Verbeek, E.R.: "Fracture History of the Plateau and Adjacent Colorado River Valleys, Southern Piceance Basin: Implications for Predicting Joint Patterns at Depth," open-file report No. 85-744, U.S. Geological Survey, Denver (1985) 1–17.
52. Verbeek, E.R. and Grout, M.A.: "Fracture Studies in Cretaceous and Paleocene Strata In and Around The Piceance Basin—Preliminary Results and Their Bearing on a Fracture-Controlled Natural Gas Reservoir at the MWX Site," open-file report No. 84-156, U.S. Geological Survey, Denver (1984) 1-30.
53. Ward, J.S. and Morrow, N.R.: "Capillary Pressures and Gas Relative Permeabilities of Low-Permeability Sandstone," *SPEFE* (Sept. 1987) 345–56.
54. Morrow, N.R., Brower, K.R., and Kilmer, N.H.: "Relationship of Core Structure to Fluid Behavior in Low Permeability Gas Sands," final report, DOE/BC 10216-13, New Mexico Inst. of Mining & Technology, Socorro, NM (Sept. 1984).
55. Wei, K.K., Morrow, N.R., and Brower, K.R.: "Effect of Fluid, Confining Pressure, and Temperature on Absolute Permeabilities of Low-Permeability Sandstones," *SPEFE* (Aug. 1986) 413–23.
56. Ward, J. and Morrow, N.R.: "Multiwell Special Core Analysis," final report PRRC 84-25, New Mexico Petroleum Recovery Research Center, Socorro, NM (Oct. 1984).
57. Brower, K.R. and Morrow, N.R.: "Fluid Flow in Cracks as Related to Low-Permeability Gas Sands," *SPEJ* (April 1985) 191–201.
58. Randolph, P.L., Soeder, D.J., and Chowdiah, P.: "Effects of Water and Stress Upon Permeabilities to Gas of Paludal and Coastal Sands," topical report, DOE/MC/20342-1838, Inst. of Gas Technology, Chicago (Feb. 1985).
59. Randolph, P.L., Soeder, D.J., and Chowdiah, P.: "Porosity and Permeability of Tight Sands," paper SPE 12836 presented at the 1984 SPE Unconventional Gas Recovery Symposium, Pittsburgh, May 13–15.
60. Soeder, D.J. and Randolph, P.L.: "Porosity, Permeability, and Pore Structure of the Tight Mesaverde Sandstone, Piceance Basin, Colorado," *SPEFE* (June 1987) 129–36; *Trans.*, AIME, **283.**
61. Randolph, P.L.: "Porosity and Permeability of Mesaverde Sandstone Core From the U.S. DOE Multiwell Experiment, Garfield County, Colorado," paper SPE 11765 presented at the 1983 SPE/DOE Symposium on Low Permeability Gas Reservoirs, Denver, March 14–16.
62. Senseny, P.E.: "Laboratory Measurements of Mechanical Properties of Sandstones and Shales," paper SPE 11762 presented at the 1983 SPE/DOE Symposium on Low Permeability Gas Reservoirs, Denver, March 14–16.
63. Duda, J.R.: "Reservoir Characterization and Modeling Analysis of the Coastal Yellow Zone at the Multiwell Experiment," technical note, DOE/METC-87/4072, U.S. DOE Morgantown Energy Technology Center (Sept. 1986).
64. Palmer, I.D. and Craig, H.R.: "Modeling of Asymmetrical Vertical Growth in Elongated Hydraulic Fractures and Application to First MWX Stimulation," paper SPE 12879 presented at the 1984 SPE Unconventional Gas Recovery Symposium, Pittsburgh, May 13–15.
65. Horton, A.I.: "Status of Multiwell Experiment Reservoir Modeling Analysis," technical note, DOE/METC-85/ 4007, U.S. DOE Morgantown Energy Technology Center (Feb. 1985) **I.**
66. Horton, A.I.: "Multiwell Experiment: Reservoir Modeling Analysis," technical note, DOE/METC-85/4050, U.S. DOE Morgantown Energy Technology Center (May 1985) **II.**
67. Warpinski, N.R., Branagan, P., and Wilmer, R.: "In-Situ Stress Measurements at U.S. DOE's Multiwell Experiment Site, Mesaverde Group, Rifle, Colorado," *JPT* (March 1985) 527–36.
68. Warpinski, N.R. and Teufel, L.W.: "In-Situ Stresses in Low-Permeability, Nonmarine Rocks," *JPT* (April 1989) 405–14; *Trans.*, AIME, **287.**
69. Warpinski, N.R.: "Investigation of the Accuracy and Reliability of the In Situ Stress Measurements Using Hydraulic Fracturing in Perforated Cased Holes," *Proc.*, 24th U.S. Natl. Symposium on Rock Mechanics, College Station, TX (June 20–22, 1983) 773–86.
70. Teufel, L.W.: "Determination of In-Situ Stress From Anelastic Strain Recovery Measurements of Oriented Core," paper SPE 11649 presented at the 1983 SPE/DOE Symposium on Low Permeability Gas Reservoirs, Denver, March 14–16.
71. Teufel, L.W.: "Prediction of Hydraulic Fracture Azimuth from Anelastic Strain Recovery Measurements of Oriented Core," *Proc.*, 23rd U.S. Natl. Rock Mechanics Symposium, Berkeley (Aug. 25-27, 1982) 238–46.
72. Teufel, L.W. and Warpinski, N.R.: "Determination of In Situ Stress from Anelastic Strain Recovery Experiments of Oriented Core: Comparison to Hydraulic Stress Measurements in the Rollins Sandstone, Piceance Basin, Colorado," *Proc.*, 25th U.S. Symposium on Rock Mechanics, Northwestern U., Evanston, IL (June 25-27, 1984) 176–85.
73. Warpinski, N.R.: "Elastic and Viscoelastic Model of the Stress History of Sedimentary Rocks," report SAND86-0238, Sandia Natl. Laboratories, Albuquerque (April 1986).
74. Warpinski, N.R. and Teufel, L.W.: "A Viscoelastic Constitutive Model for Determining In-Situ Stress Magnitudes From Anelastic Strain Recovery of Core," *SPEPE* (Aug. 1989) 272–80; *Trans.*, AIME, **287.**
75. Blanton, T.L.: "Discussion of A Viscoelastic Constitutive Model for Determining In-Situ Stress Magnitudes From Anelastic Strain Recovery of Core," *SPEPE* (Aug. 1989) 281–86; *Trans.*, AIME, **287.**
76. Warpinski, N.R. and Teufel, L.W.: "Authors' Reply to Discussion of A Viscoelastic Constitutive Model for Determining

In-Situ Stress Magnitudes From Anelastic Strain Recovery of Core," *SPEPE* (Aug. 1989) 287-89; *Trans.*, AIME, **287**.
77. **Teufel, L.W.** *et al.*: "Determination of Hydraulic Fracture Azimuth by Geophysical, Geological, and Oriented Core Methods at the Multiwell Experiment Site, Rifle, Colorado," paper SPE 13226 presented at the 1984 SPE Annual Technical Conference and Exhibition, Houston, Sept. 16-19.
78. Thorne, B.J. and Morris, H.E.: "Advances in Borehole Seismic Fracture Diagnostics," *SPEFE* (Dec. 1988) 711-15.
79. Engi, D.: "A Numerical Signal Processing Technique for Borehole Fracture Diagnostics," report SAND86-1865, Sandia Natl. Laboratories, Albuquerque (Jan. 1984).
80. Thorne, B.J. and Morris, H.E.: "An Assessment of Borehole Seismic Fracture Diagnostics," paper SPE 18193 presented at the 1988 SPE Annual Technical Conference and Exhibition, Houston, Oct. 2-5.
81. Thorne, B.J. and Morris, H.E.: "Passive Seismic Monitoring of Hydraulic Fracture Experiments at the Multiwell Experiment Site," report SAND88-1284, Sandia Natl. Laboratories, Albuquerque (June 1988).
82. Hart, C.M., Engi, D., and Morris, H.E.: "A Comprehensive Fracture-Diagnostics Instrumentation Fielding Program," paper SPE 11810 presented at the 1983 SPE/DOE Symposium on Low Permeability Gas Reservoirs, Denver, March 14-16.
83. Hart, C.M. *et al.*: "Fracture Diagnostics Results for the First Multiwell Experiment's Paludal Zone Stimulation," *SPEFE* (Sept. 1987) 320-26; *Trans.*, AIME, **283**.
84. Clark, J.A.: "The Prediction of Hydraulic Fracture Azimuth Through Geological, Core, and Analytical Studies," paper SPE 11611 presented at the 1983 SPE/DOE Symposium on Low Permeability Gas Reservoirs, Denver, March 14-16.
85. Gall, B.L. and Raible, C.J.: "Molecular Size Studies of Degraded Fracturing Fluid Polymers," paper SPE 13566 presented at the 1985 SPE Intl. Symposium on Oilfield and Geothermal Chemistry, Phoenix, April 9-11.
86. Sattler, A.R., Raible, C.J., and Gall, B.L.: "Integration of Laboratory and Field Data for Insight on the Multiwell Experiment Paludal Stimulation," paper SPE 13891 presented at the 1985 SPE/DOE Symposium on Low Permeability Gas Reservoirs, Denver, May 19-22.
87. Raible, C.J. and Gall, B.L.: "Laboratory Formation Damage Studies of Western Tight Gas Sands," paper SPE 13903 presented at the 1985 SPE/DOE Symposium on Low Permeability Gas Reservoirs, Denver, May 19-22.
88. Sattler, A.R. *et al.*: "Laboratory Studies for the Design and Analysis of Hydraulic Fracture Stimulations in Lenticular, Tight Gas Reservoirs," paper SPE 15245 presented at the 1986 SPE Unconventional Gas Technology Symposium, Louisville, KY, May 18-21.
89. Gall, B.L. *et al.*: "Permeability Damage to Natural Fractures Caused by Fracturing-Fluid Polymers," paper SPE 17542 presented at the 1988 SPE Rocky Mountain Regional Meeting, Casper, WY, May 11-13.
90. Sattler, A.R. *et al.*: "Stimulation-Fluid Systems for Naturally Fractured Tight Gas Sandstones: A General Case Study from Multiwell Experiment Stimulations," paper SPE 17717 presented at the 1988 SPE Gas Technology Symposium, Dallas, June 13-15.
91. Warpinski, N.R. and Branagan, P.T.: "Altered-Stress Fracturing," *JPT* (Sept. 1989) 990-97.
92. Warpinski, N.R. *et al.*: "Fracturing and Testing Case Study of Paludal, Tight, Lenticular Gas Sands," *SPEFE* (Dec. 1987) 535-45.
93. Warpinski, N.R.: "Dual Leakoff Behavior in Hydraulic Fracturing of Tight, Lenticular Gas Sands," paper SPE 18259 presented at the 1988 SPE Annual Technical Conference and Exhibition, Houston, Oct. 2-5.
94. Branagan, P.T., Cotner, G., and Lee, S.J.: "Interference Testing of the Naturally Fractured Cozzette Sandstone: A Case Study at the DOE MWX Site," paper SPE 12869 presented at the 1984 SPE Unconventional Gas Recovery Symposium, Pittsburgh, May 13-15.
95. Branagan, P.T. and Wilmer, R.: "Breakdown Procedures Designed to Minimize Naturally Fractured Reservoir Damage," paper SPE 17716 presented at the 1988 Gas Technology Symposium, Dallas, June 13-15.
96. Branagan, P.T. *et al.*: "Comprehensive Well Testing and Modeling of Pre and Post Fracture Well Performance of the MWX Lenticular Tight Gas Sands," paper SPE 13867 presented at the 1985 SPE/DOE Symposium on Low Permeability Gas Reservoirs, Denver, May 19-22.
97. Branagan, P.T. *et al.*: "Case History of Hydraulic Fracture Performance in the Naturally Fractured Paludal Zone: The Transitory Effects of Damage," paper SPE 16397 presented at the 1987 SPE/DOE Symposium on Low Permeability Gas Reservoirs, Denver, May 18-19.
98. Kukal, G.C. *et al.*: "Critical Problems Hindering Accurate Log Interpretation of Tight Gas Sand Reservoirs," paper SPE 11620 presented at the 1983 SPE/DOE Symposium on Low Permeability Gas Reservoirs, Denver, March 14-16.
99. Kukal, G.C.: "Log Analysis in Low Permeability Sand Sequences—Correcting for Variable Unflushed Gas Saturation," paper F presented at the 24th SPWLA Annual Logging Symposium, Calgary, June 27-30, 1983.
100. Kukal, G.C.: "A Systematic Approach for the Effective Log Analysis of Tight Gas Sands," paper SPE 12851 presented at the 1984 SPE Unconventional Gas Recovery Symposium, Pittsburgh, May 13-15.
101. Kukal, G.C. and Simons, K.E.: "Log Analysis Techniques for Quantifying the Permeability of Sub-Millidarcy Sandstone Reservoirs," paper SPE 13880 presented at the 1985 SPE/DOE Symposium on Low Permeability Gas Reservoirs, Denver, May 19-22.
102. Kukal, G.C. and Hill, R.E.: "Improved Shaly Sand Analysis in Heavy Drilling Muds: A Simple Technique for Using the Photoelectric Measurement," paper U presented at the 26th SPWLA Annual Logging Symposium, Dallas, June 17-20, 1985.
103. Kukal, G.C. and Hill, R.E.: "Log Analysis of Clay Volume: An Evaluation of Techniques and Assumptions Used in an Upper Cretaceous Sand Sequence," paper RR presented at the 1986 SPWLA Annual Logging Symposium, Houston, June 9-13.
104. Branagan, P.T. *et al.*: "Prefracturing Interference Testing of a Naturally Fractured, Tight Fluvial Reservoir," paper SPE 17724 presented at the 1988 SPE Gas Technology Symposium, Dallas, June 13-15.
105. Warpinski, N.R. *et al.*: "A Case Study of a Stimulation Experiment in a Fluvial, Tight, Sandstone Gas Reservoir," paper SPE 18258 presented at the 1988 SPE Annual Technical Conference and Exhibition, Houston, Oct. 2-5.

Authors


Northrop | Frohne

David A. Northrop, supervisor of the Geotechnology Research Div. at Sandia Natl. Laboratories in Albuquerque, NM, manages Sandia's programs in enhanced oil and gas recovery. Northrop, who was responsible for the technical direction of the MWX project, holds BS, MS, and PhD degrees in chemistry from the U. of Chicago. Karl-Heinz Frohne is a project manager at the U.S. DOE in Morgantown, WV. His primary research interest is improvement of gas recovery from western tight reservoirs. He holds a BS degree from the U. of Pittsburgh and an MS degree from West Virginia U., both in petroleum engineering.

SI Metric Conversion Factors

bbl	×	1.589 873	E−01	=	m³
ft	×	3.048*	E−01	=	m
ft³	×	2.831 685	E−02	=	m³
gal	×	3.785 412	E−03	=	m³
in.	×	2.54*	E+00	=	cm
lbm	×	4.535 924	E−01	=	kg
md	×	9.869 233	E−04	=	μm²
miles	×	1.609 344*	E+00	=	km
psi	×	6.894 757	E+00	=	kPa

*Conversion factor is exact.

Provenance

Original SPE manuscript, **Insights and Contributions From the Multiwell Experiment: A Field Laboratory in Tight Gas Sandstone Reservoirs,** received for review Oct. 2, 1988. Paper accepted for publication Feb. 27, 1990. Revised manuscript received Nov. 3, 1989. Paper (SPE 18286) first presented at the 1988 SPE Annual Technical Conference and Exhibition held in Houston, Oct. 2-5.

JPT

APPENDIX 2

STRESS PROFILES FOR THE UPPER MESAVERDE, MWX-2 AND MWX-3

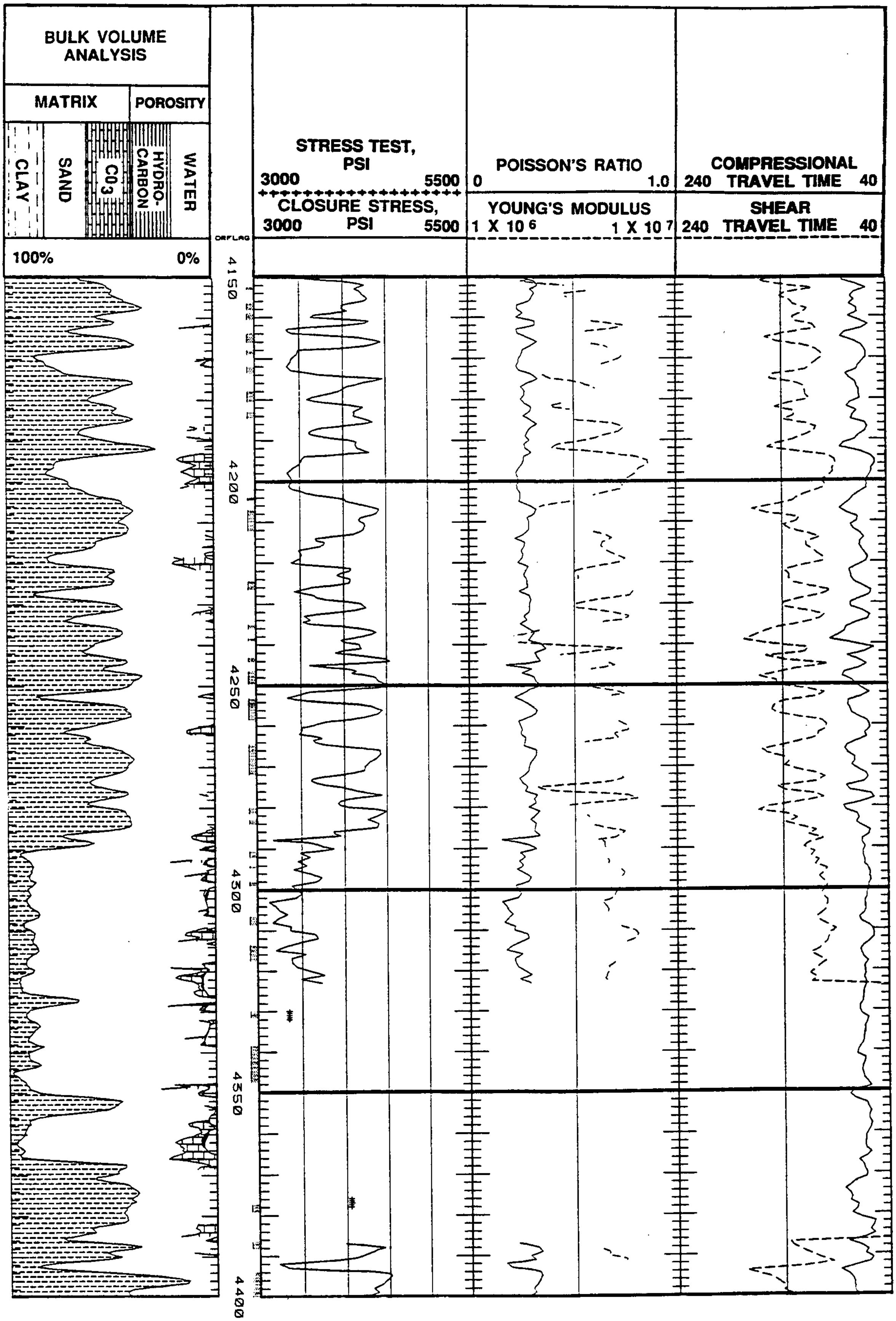

In-Situ Stress Log, Upper Mesaverde Interval, MWX-2

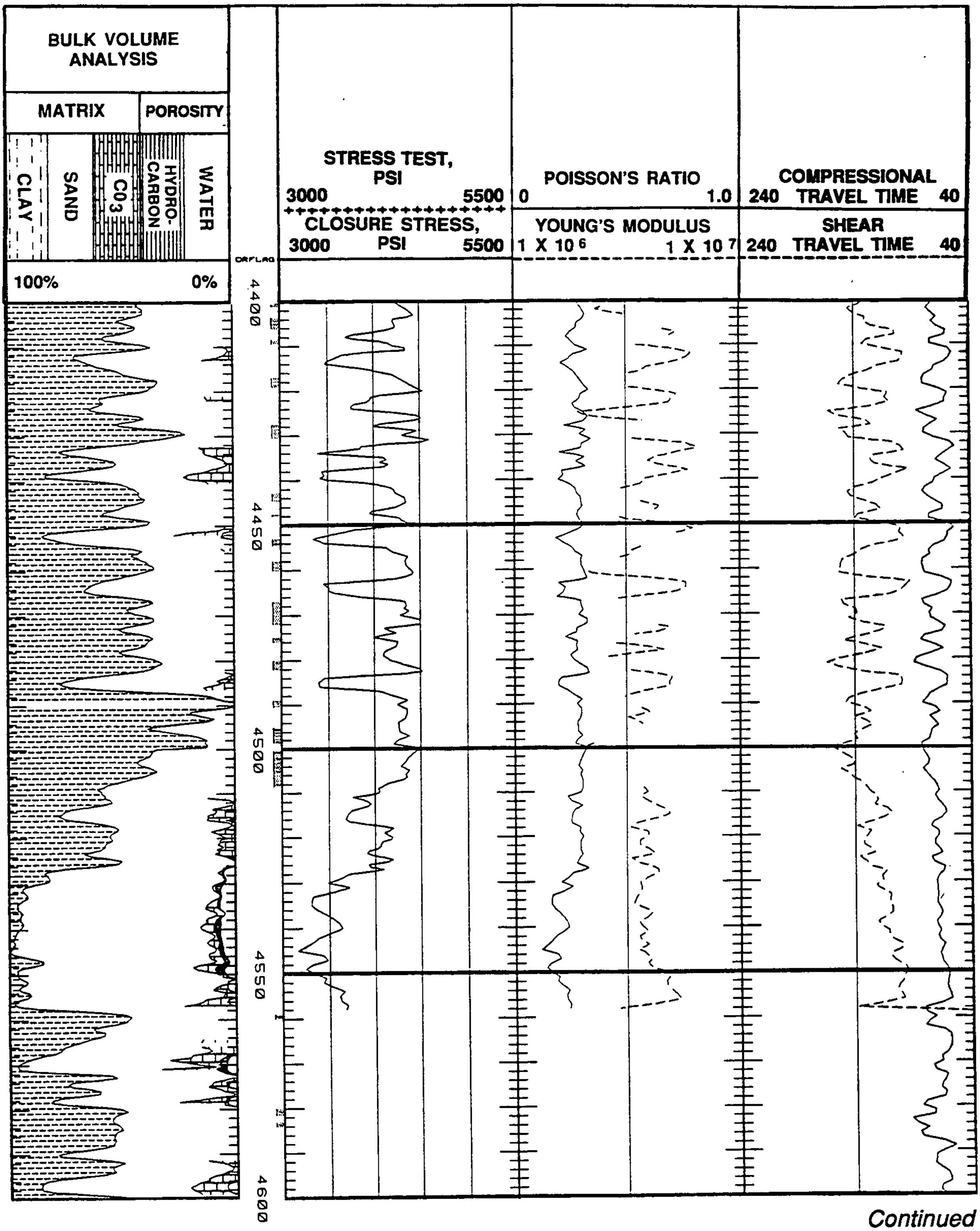
BULK VOLUME ANALYSIS
MATRIX
POROSITY
CLAY
SAND
C03
HYDRO-CARBON
WATER
100%
0%
STRESS TEST, PSI
3000
5500
CLOSURE STRESS, PSI
3000
5500
POISSON'S RATIO
0
1.0
YOUNG'S MODULUS
1 X 10 6
1 X 10 7
COMPRESSIONAL TRAVEL TIME
240
40
SHEAR TRAVEL TIME
240
40
4400
4450
4500
4550
4600

Continued

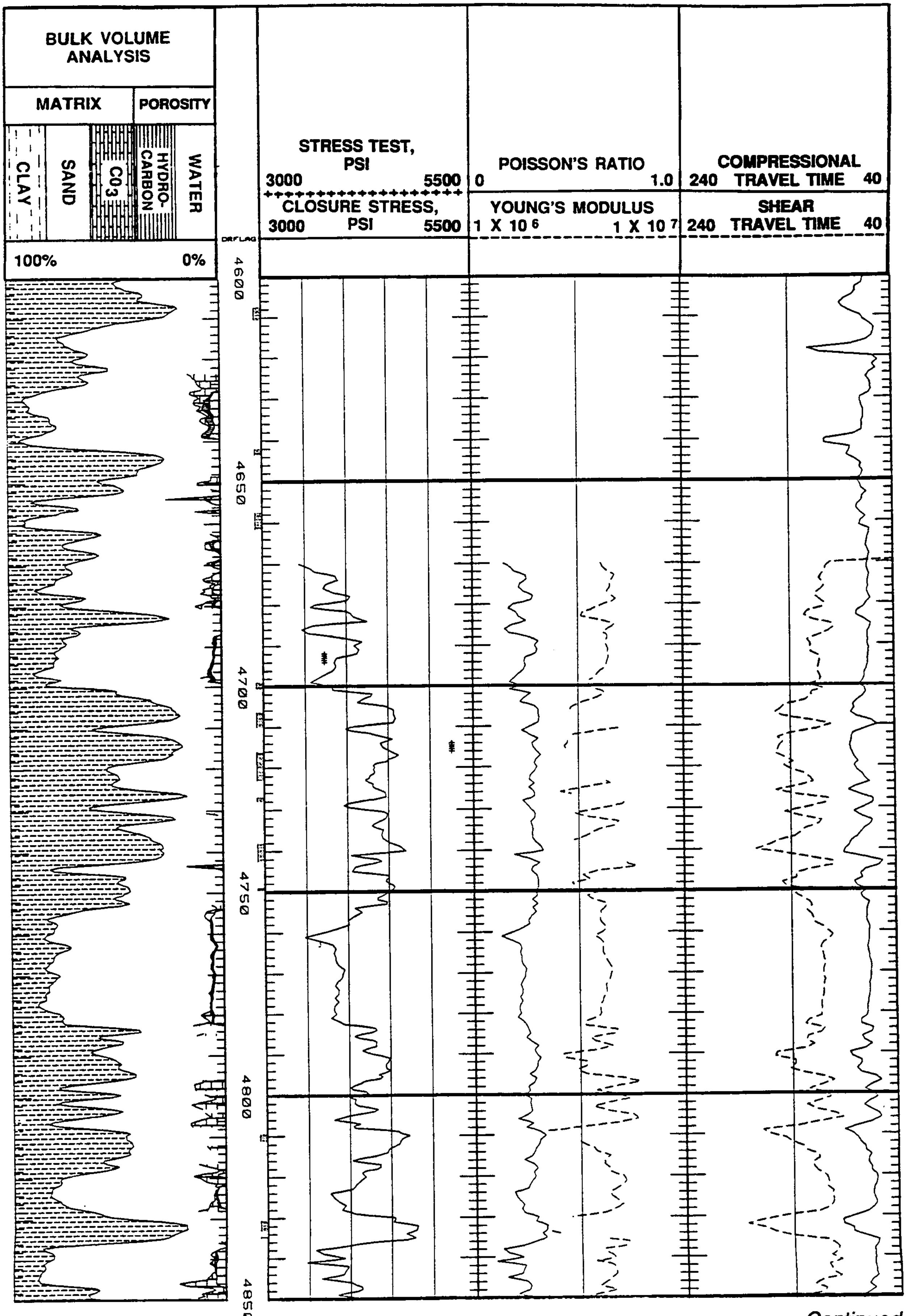
BULK VOLUME ANALYSIS
MATRIX
POROSITY
CLAY
SAND
C03
HYDRO-CARBON
WATER
100%
0%
STRESS TEST, PSI
3000
5500
CLOSURE STRESS, PSI
3000
5500
POISSON'S RATIO
0
1.0
YOUNG'S MODULUS
1 X 10 6
1 X 10 7
COMPRESSIONAL TRAVEL TIME
240
40
SHEAR TRAVEL TIME
240
40
4600
4650
4700
4750
4800
4850

Continued

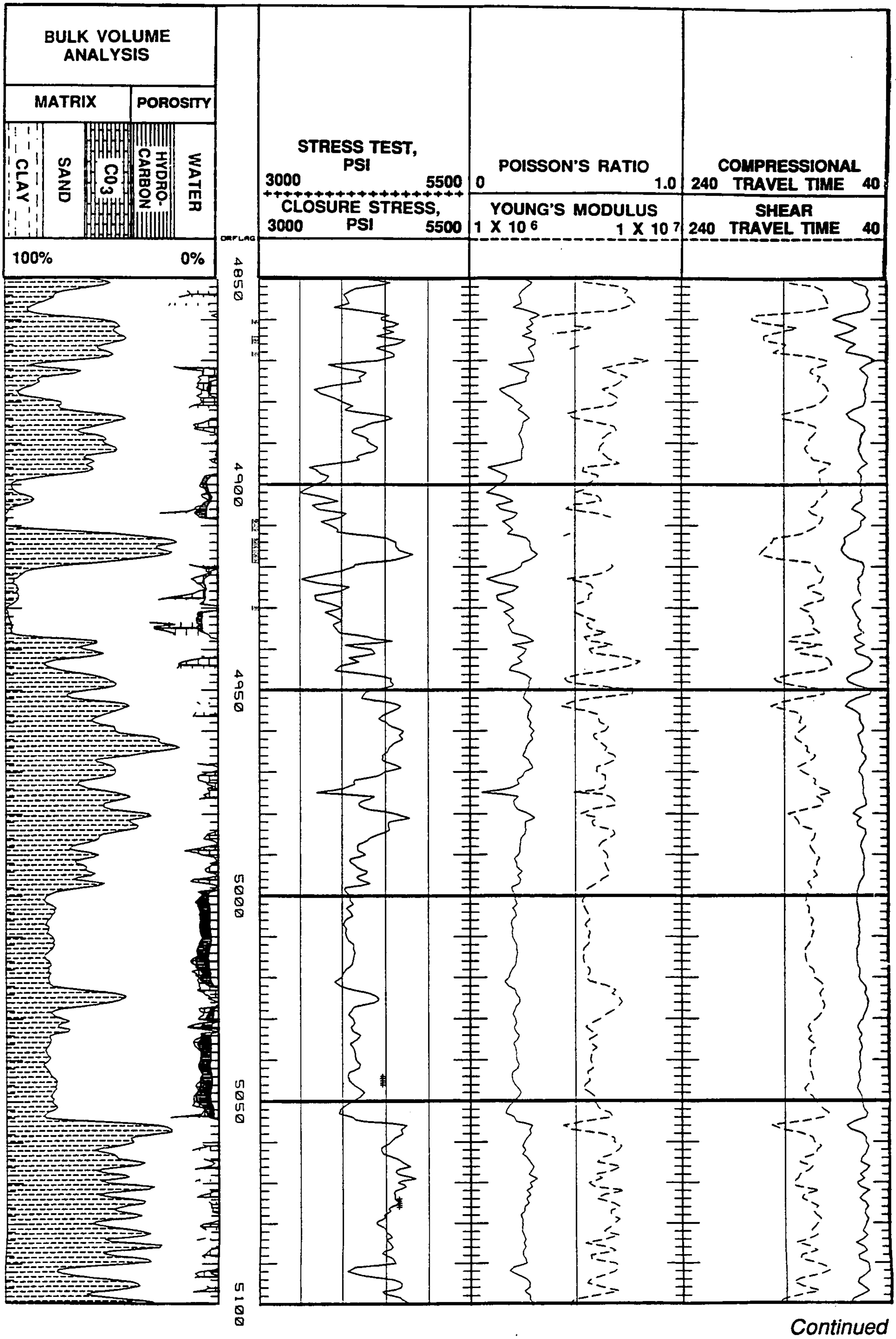

BULK VOLUME ANALYSIS
MATRIX
POROSITY
CLAY
SAND
CO3
HYDRO-CARBON
WATER
100%
0%
STRESS TEST, PSI
3000
5500
CLOSURE STRESS, PSI
3000
5500
POISSON'S RATIO
0
1.0
YOUNG'S MODULUS
1 X 10 6
1 X 10 7
COMPRESSIONAL TRAVEL TIME
240
40
SHEAR TRAVEL TIME
240
40
4850
4900
4950
5000
5050
5100

Continued

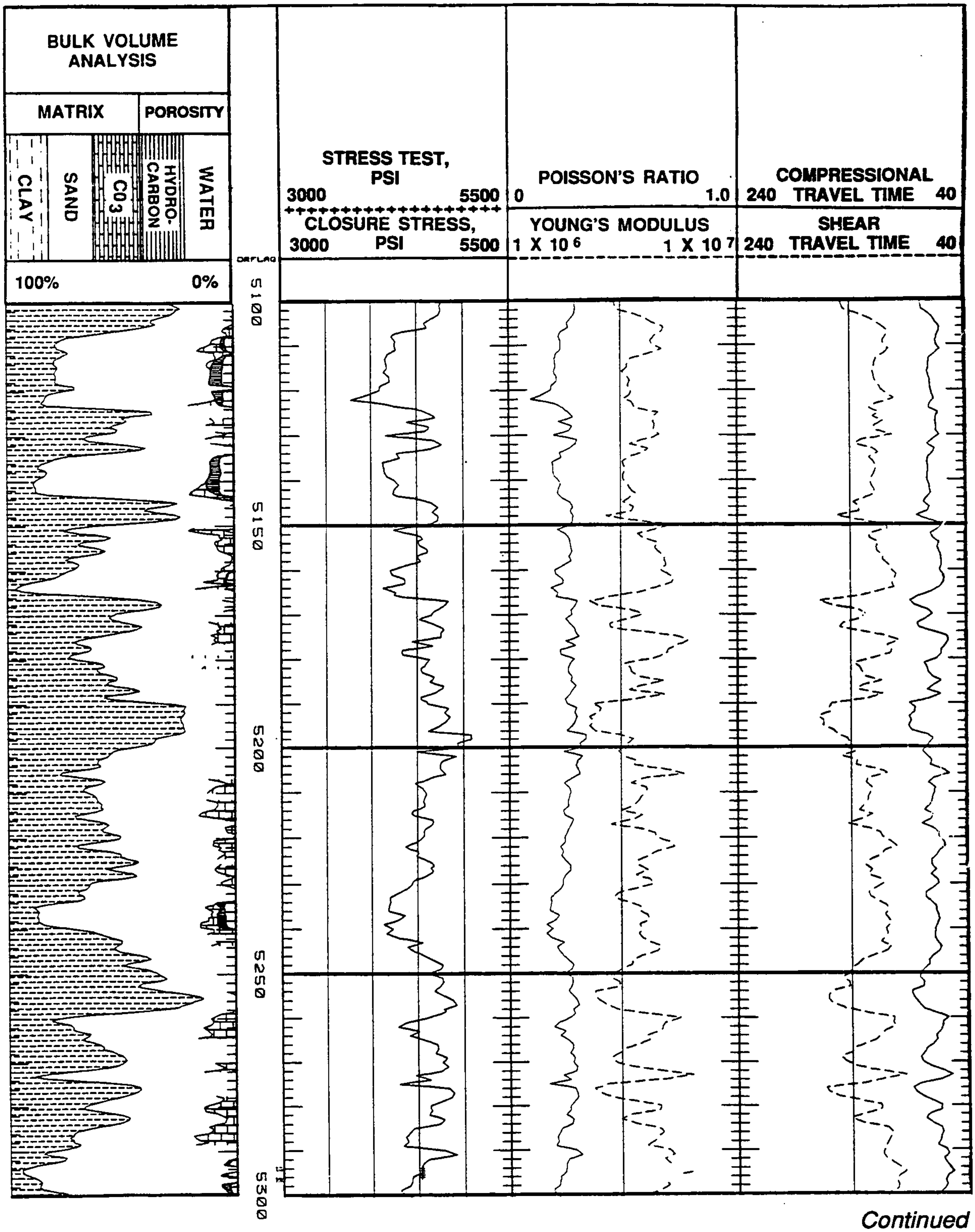
BULK VOLUME ANALYSIS
MATRIX
POROSITY
CLAY
SAND
CO3
HYDRO-CARBON
WATER
100%
0%
STRESS TEST, PSI
3000
5500
CLOSURE STRESS, PSI
3000
5500
POISSON'S RATIO
0
1.0
YOUNG'S MODULUS
1 X 10 6
1 X 10 7
COMPRESSIONAL TRAVEL TIME
240
40
SHEAR TRAVEL TIME
240
40
5100
5150
5200
5250
5300

Continued

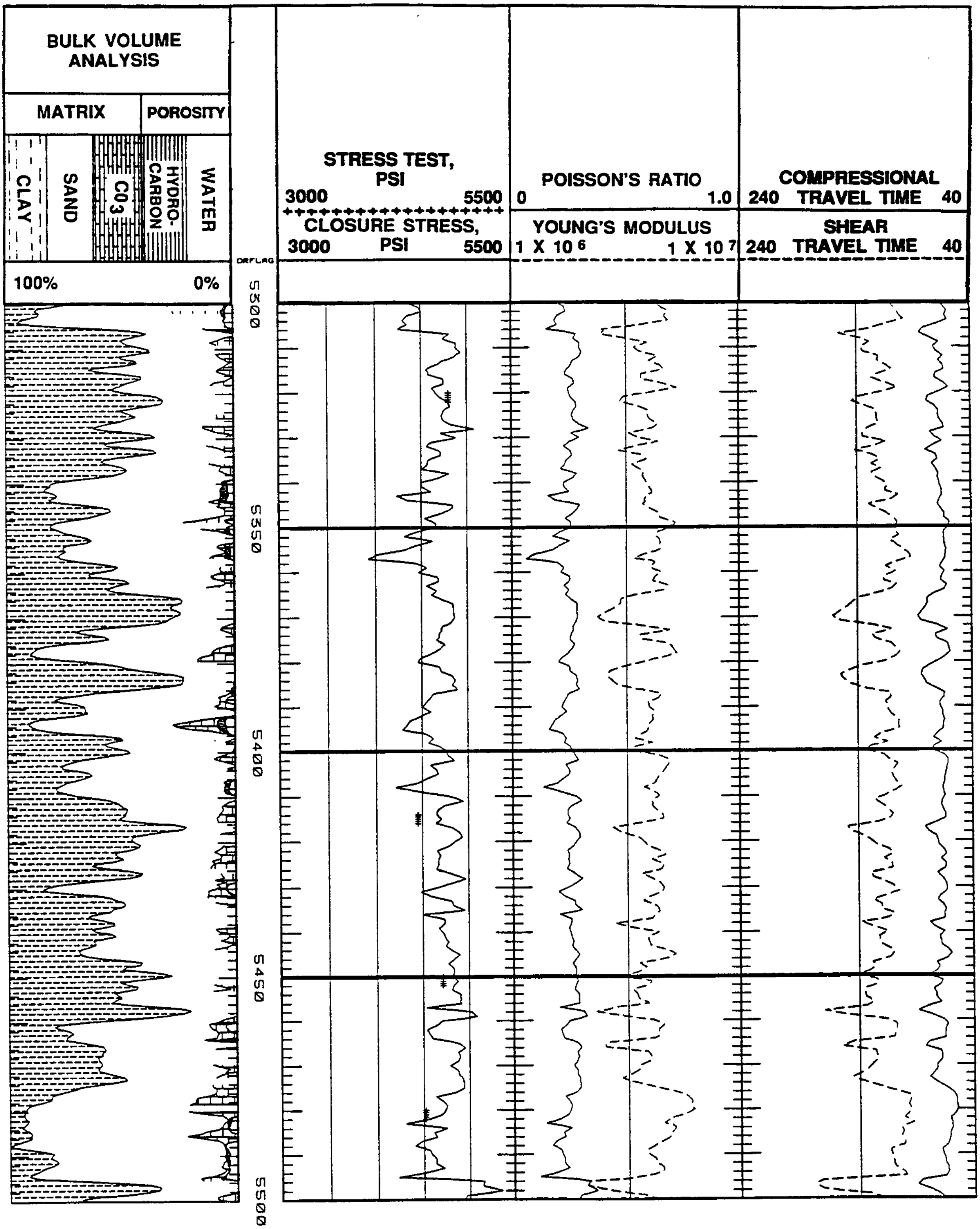
BULK VOLUME ANALYSIS
MATRIX
POROSITY
CLAY
SAND
CO_3
HYDRO-CARBON
WATER
100%
0%
DRFLAG
STRESS TEST, PSI
3000
5500
CLOSURE STRESS, PSI
3000
5500
POISSON'S RATIO
0
1.0
YOUNG'S MODULUS
1 X 10 6
1 X 10 7
COMPRESSIONAL TRAVEL TIME
240
40
SHEAR TRAVEL TIME
240
40
5300
5350
5400
5450
5500

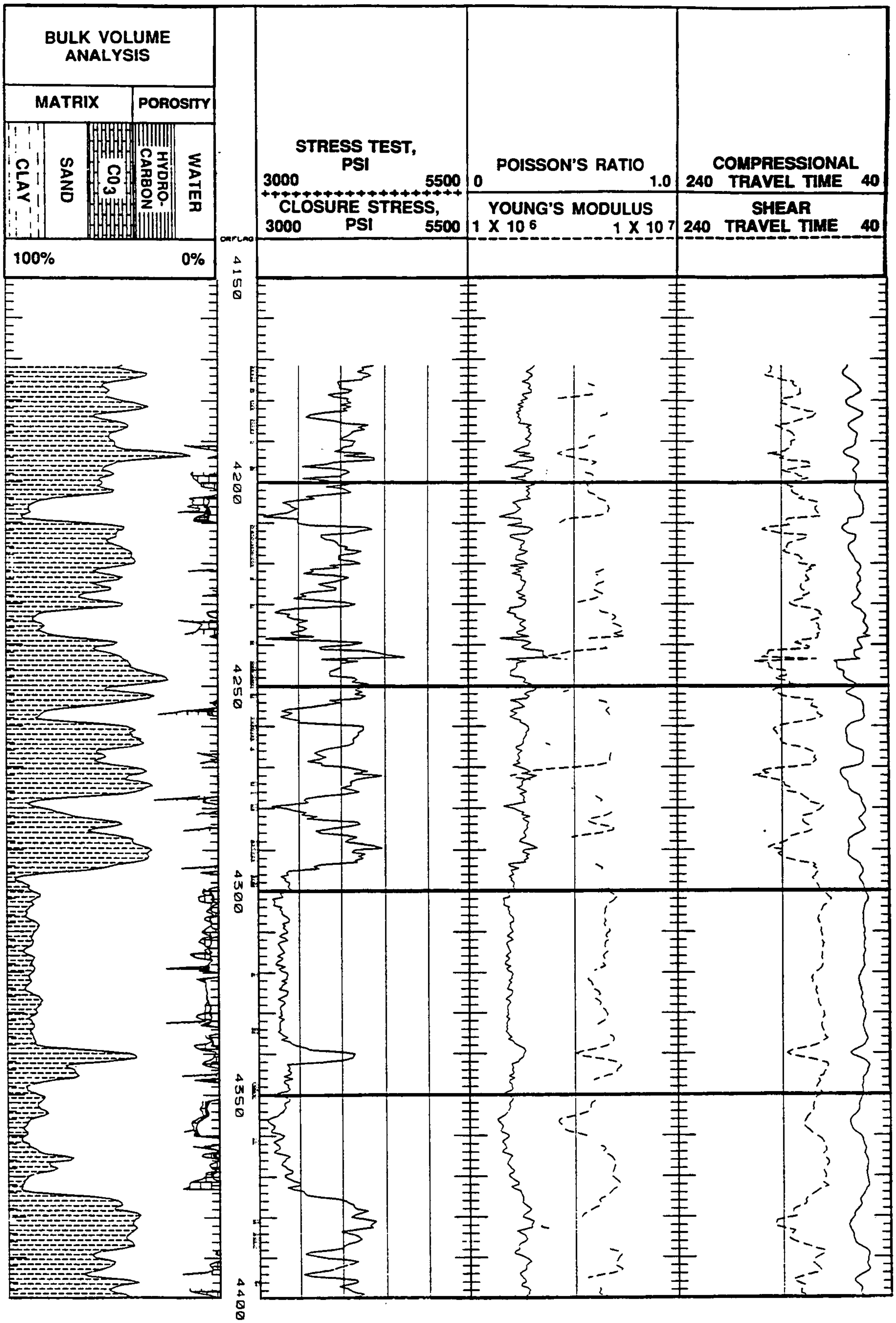

In-Situ Stress Log, Upper Mesaverde Interval, MWX-3

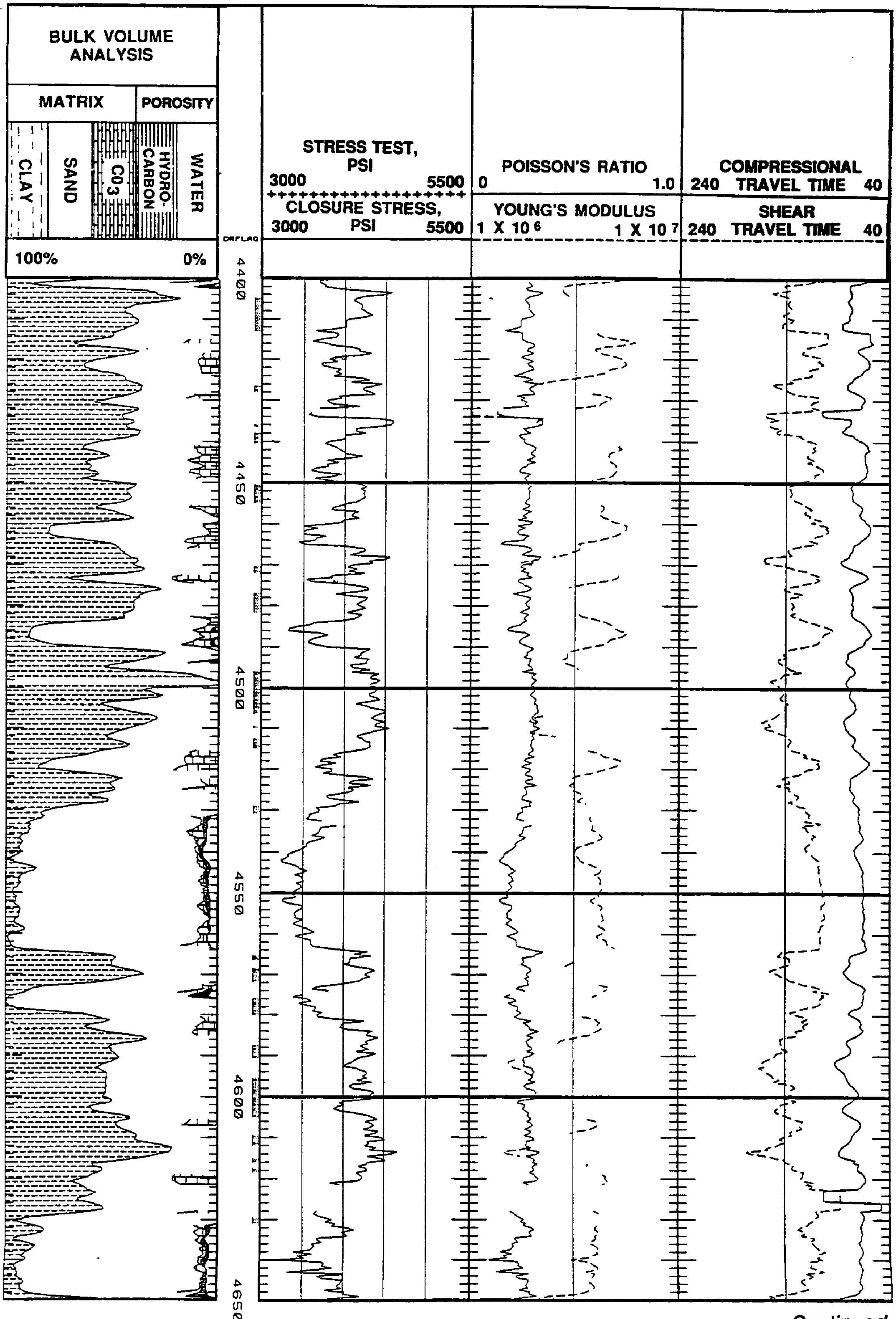
BULK VOLUME ANALYSIS
MATRIX
POROSITY
CLAY
SAND
CO3
HYDRO-CARBON
WATER
100%
0%
STRESS TEST, PSI
3000
5500
CLOSURE STRESS, PSI
3000
5500
POISSON'S RATIO
0
1.0
YOUNG'S MODULUS
1 X 10 6
1 X 10 7
COMPRESSIONAL TRAVEL TIME
240
40
SHEAR TRAVEL TIME
240
40
4400
4450
4500
4550
4600
4650

Continued

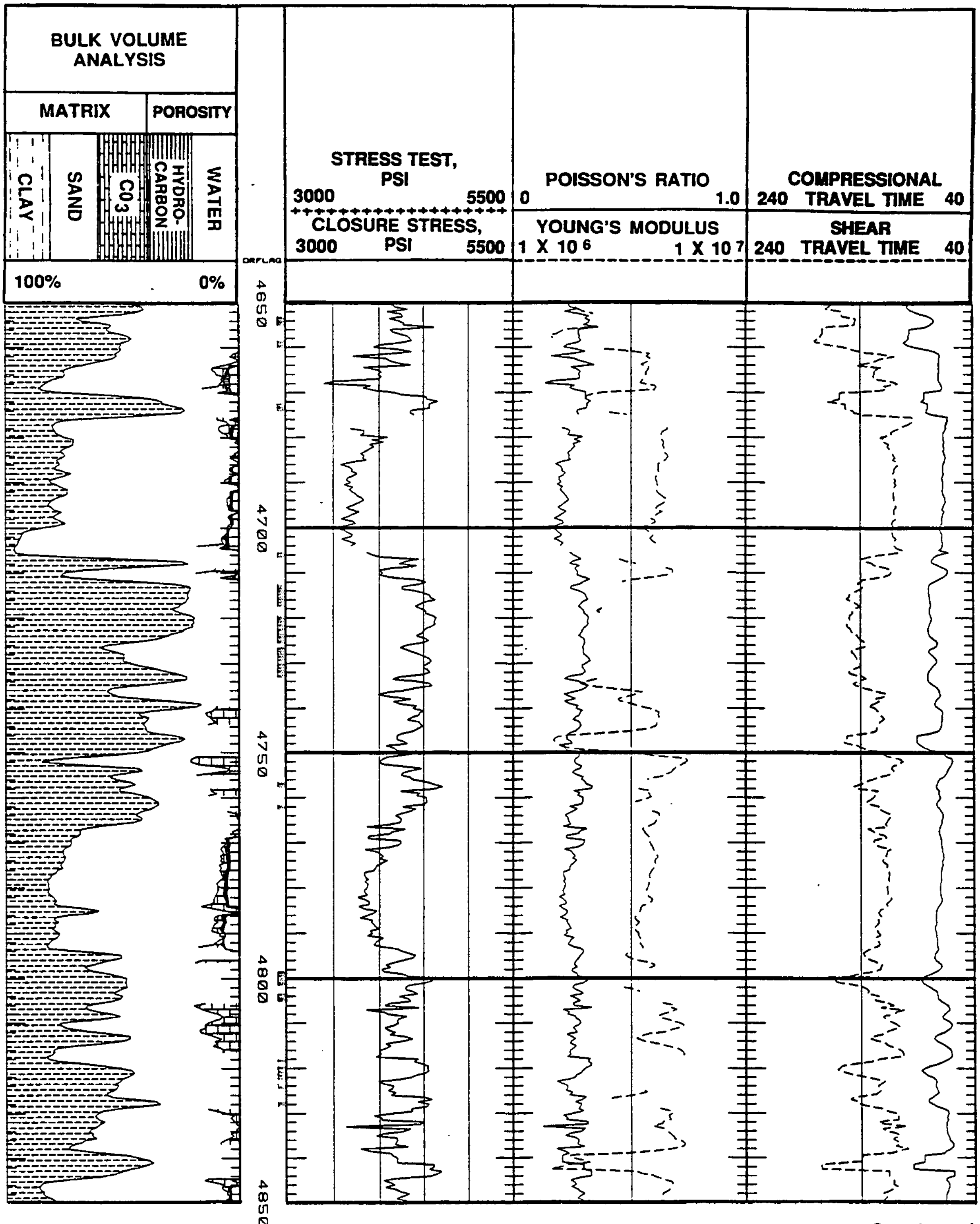
BULK VOLUME ANALYSIS
MATRIX
POROSITY
CLAY
SAND
CO3
HYDRO-CARBON
WATER
100%
0%
DRFLAG
4650
4700
4750
4800
4850
STRESS TEST, PSI
3000
5500
CLOSURE STRESS, PSI
3000
5500
POISSON'S RATIO
0
1.0
YOUNG'S MODULUS
1 X 10 6
1 X 10 7
COMPRESSIONAL TRAVEL TIME
240
40
SHEAR TRAVEL TIME
240
40

Continued

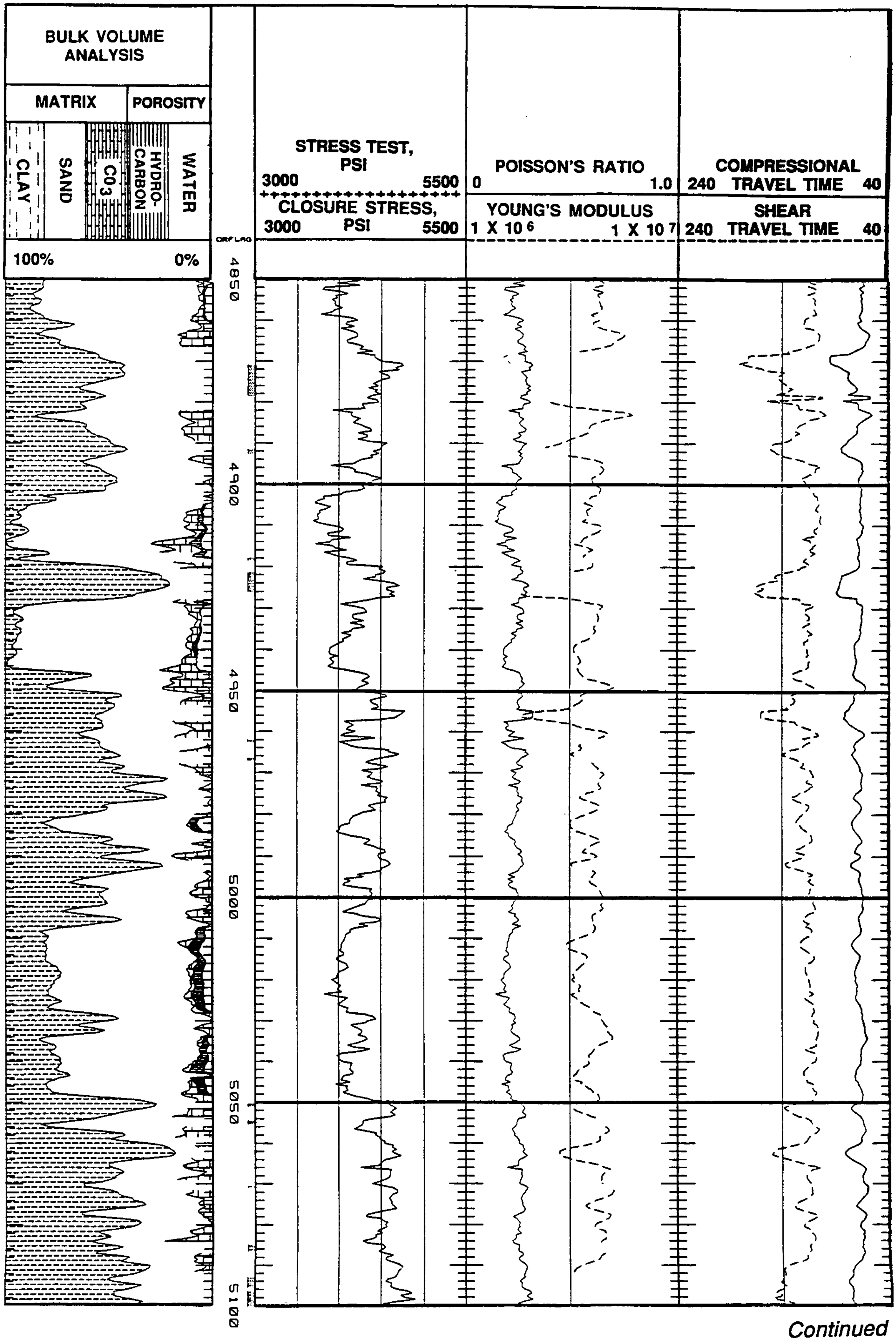
BULK VOLUME ANALYSIS
MATRIX
POROSITY
CLAY
SAND
CO3
HYDRO-CARBON
WATER
100%
0%
STRESS TEST, PSI
3000
5500
CLOSURE STRESS, PSI
3000
5500
POISSON'S RATIO
0
1.0
YOUNG'S MODULUS
1 X 10 6
1 X 10 7
COMPRESSIONAL TRAVEL TIME
240
40
SHEAR TRAVEL TIME
240
40
4850
4900
4950
5000
5050
5100

Continued

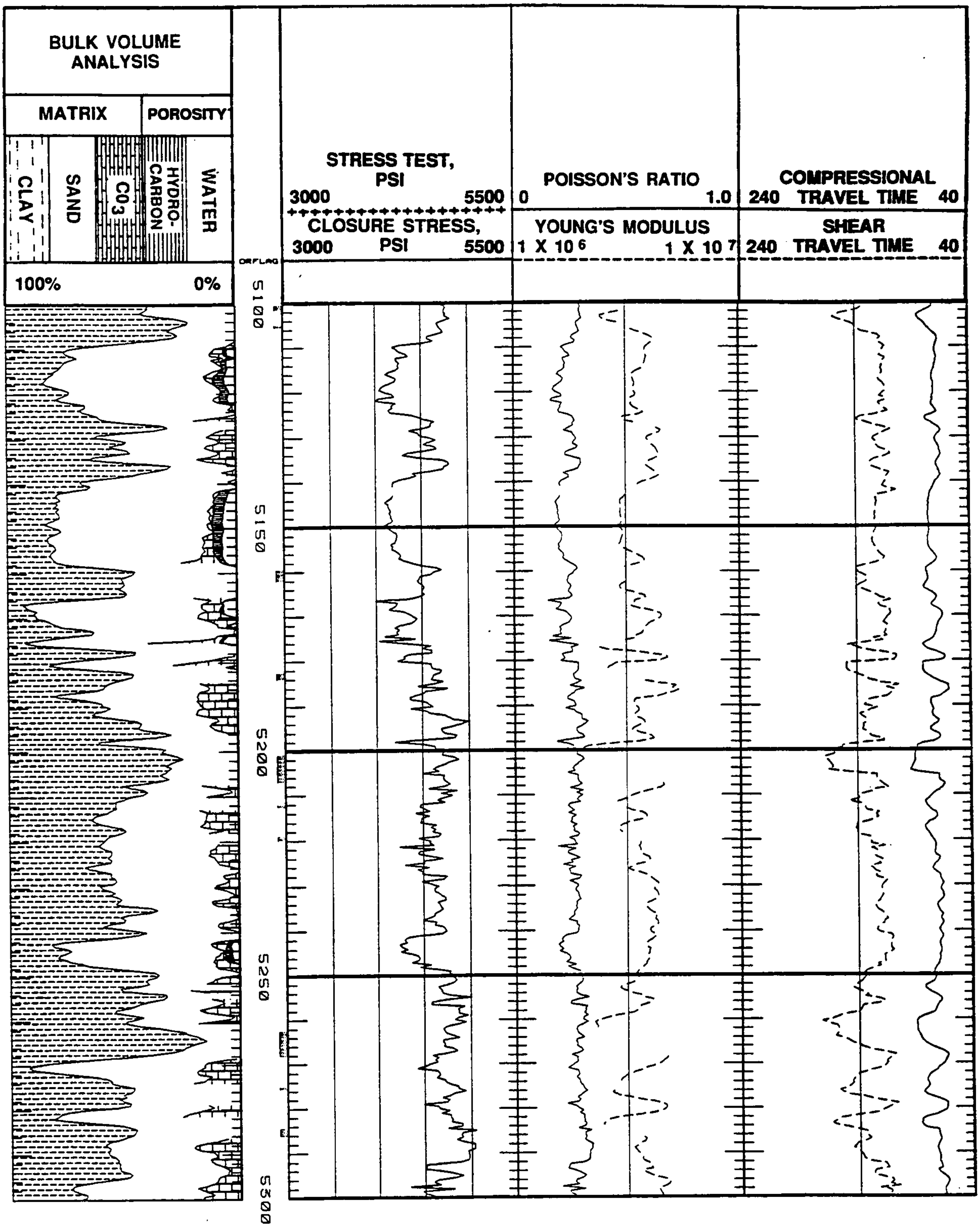
BULK VOLUME ANALYSIS
MATRIX
POROSITY
CLAY
SAND
C03
HYDRO-CARBON
WATER
100%
0%
STRESS TEST, PSI
3000
5500
CLOSURE STRESS, PSI
3000
5500
POISSON'S RATIO
0
1.0
YOUNG'S MODULUS
1 X 10 6
1 X 10 7
COMPRESSIONAL TRAVEL TIME
240
40
SHEAR TRAVEL TIME
240
40
5100
5150
5200
5250
5300

Appendix 3

PLOTS OF ANALYZABLE MICROSEISMS RESULTING FROM MINI-FRAC MONITORING

Appendix 3
Analyzable Microseisms

Figures A1 through A46 show overlaid traces and polarization plots of the filtered data from all of the analyzable microseisms. Polarization data are straightforward in all cases, but p- and s-wave arrivals may have been determined from the unfiltered data or from some combination of techniques that is not readily apparent from these figures. Many of these events are very high quality, while others have large uncertainty. With such a limited data set, all were used in developing the seismic maps.

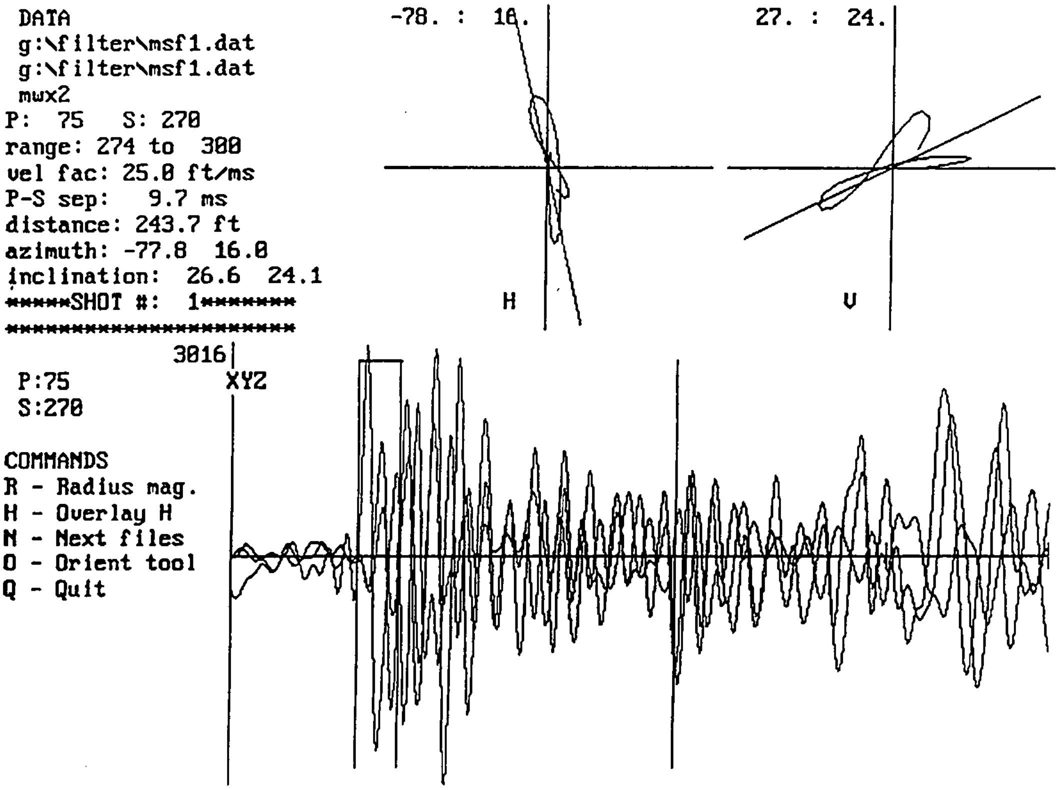

Figure A1 Event 1

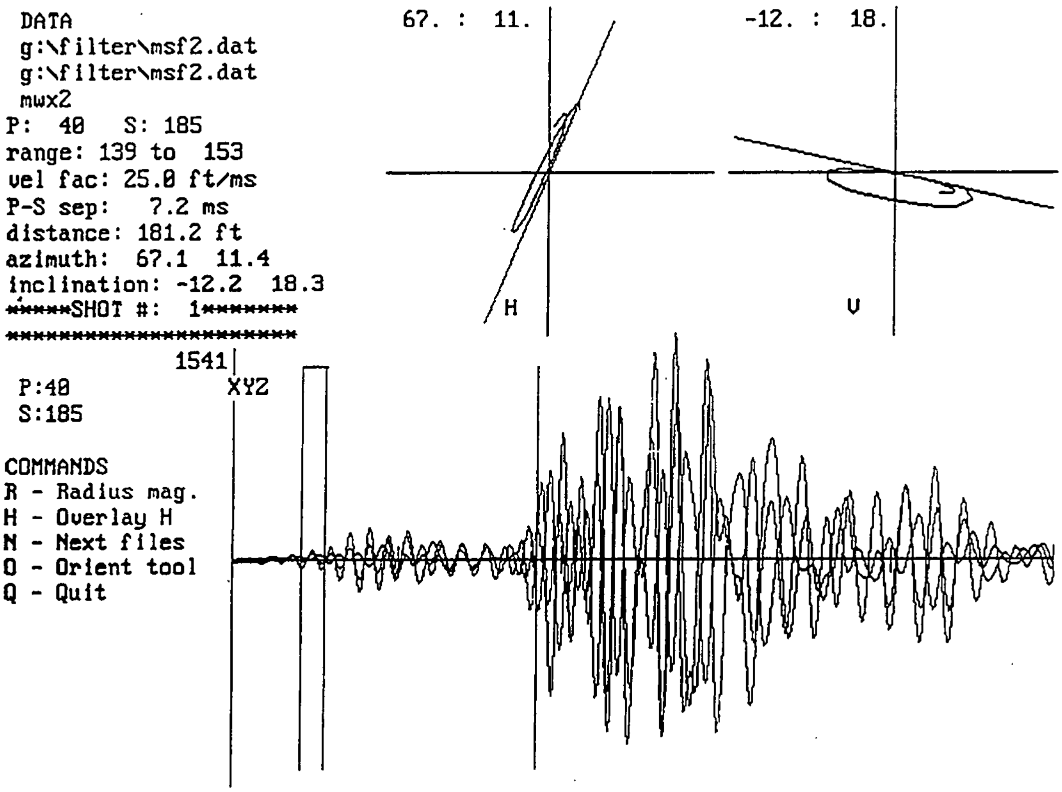

Figure A2 Event 2

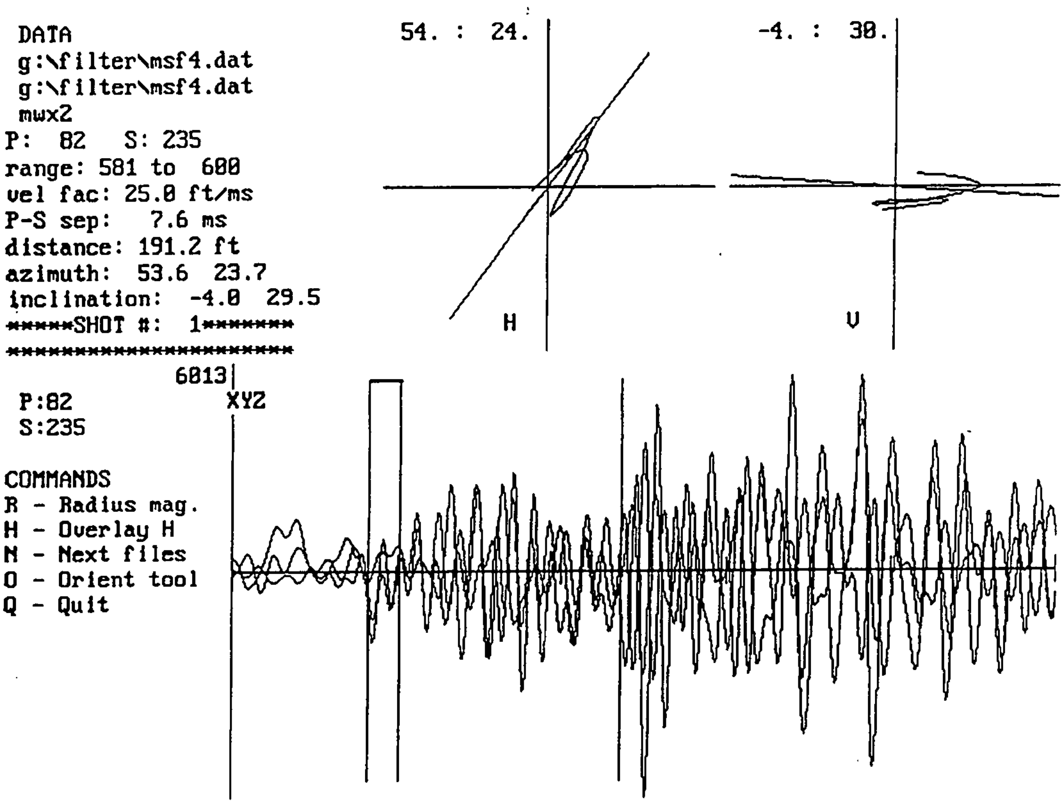

Figure A3 Event 4

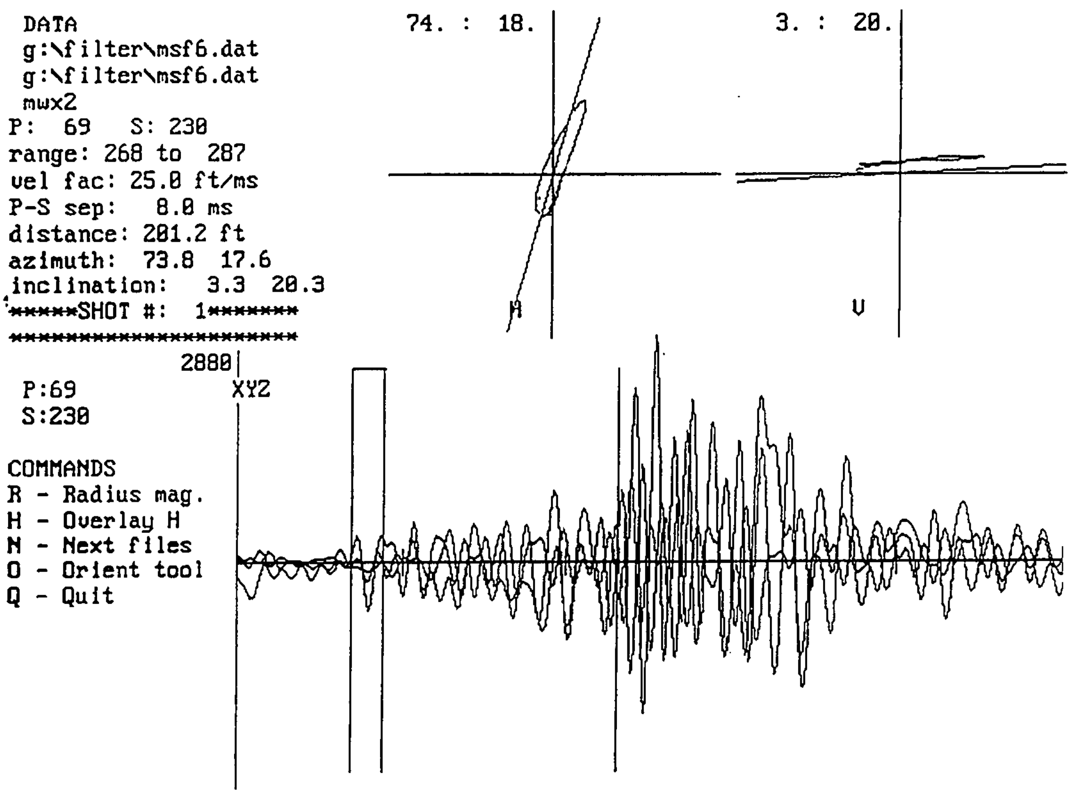

Figure A4 Event 6

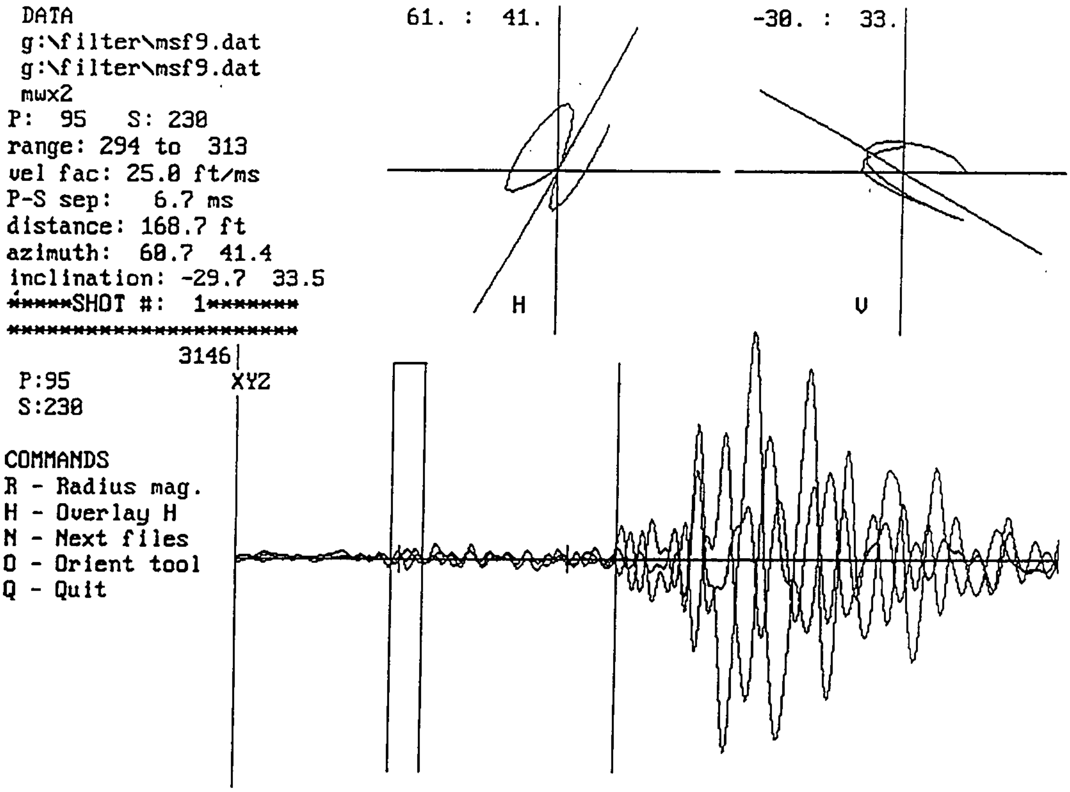

Figure A5 Event 9

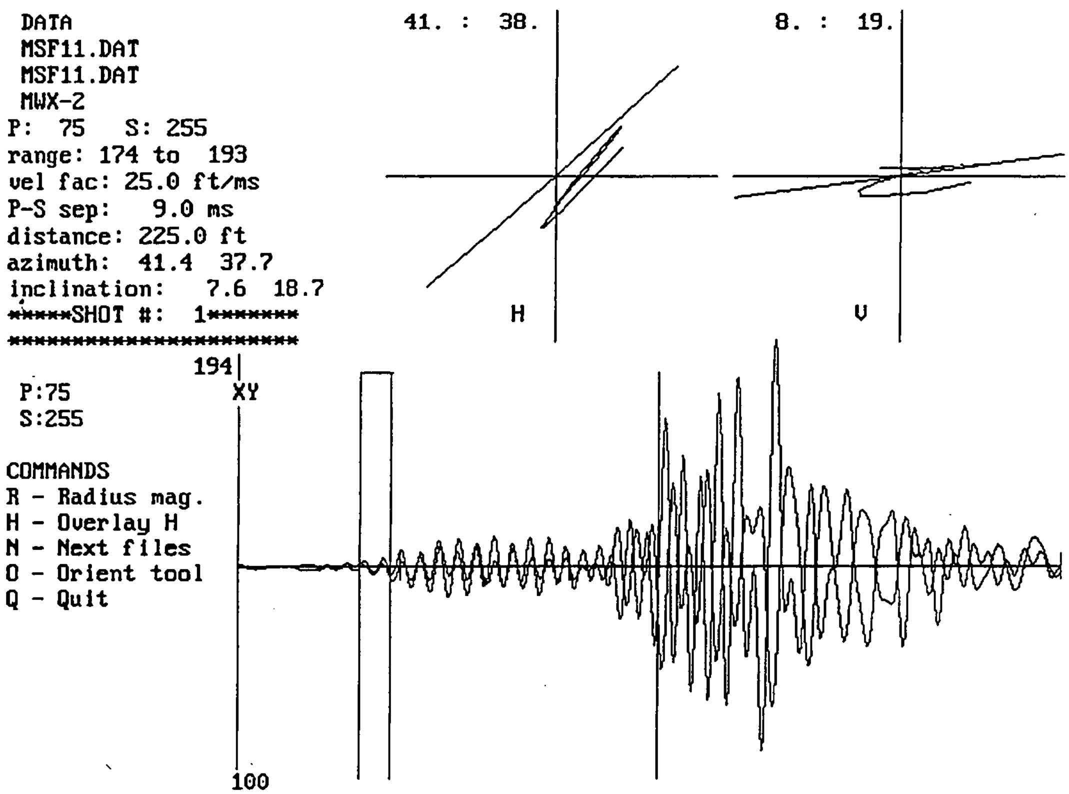

Figure A6 Event 11

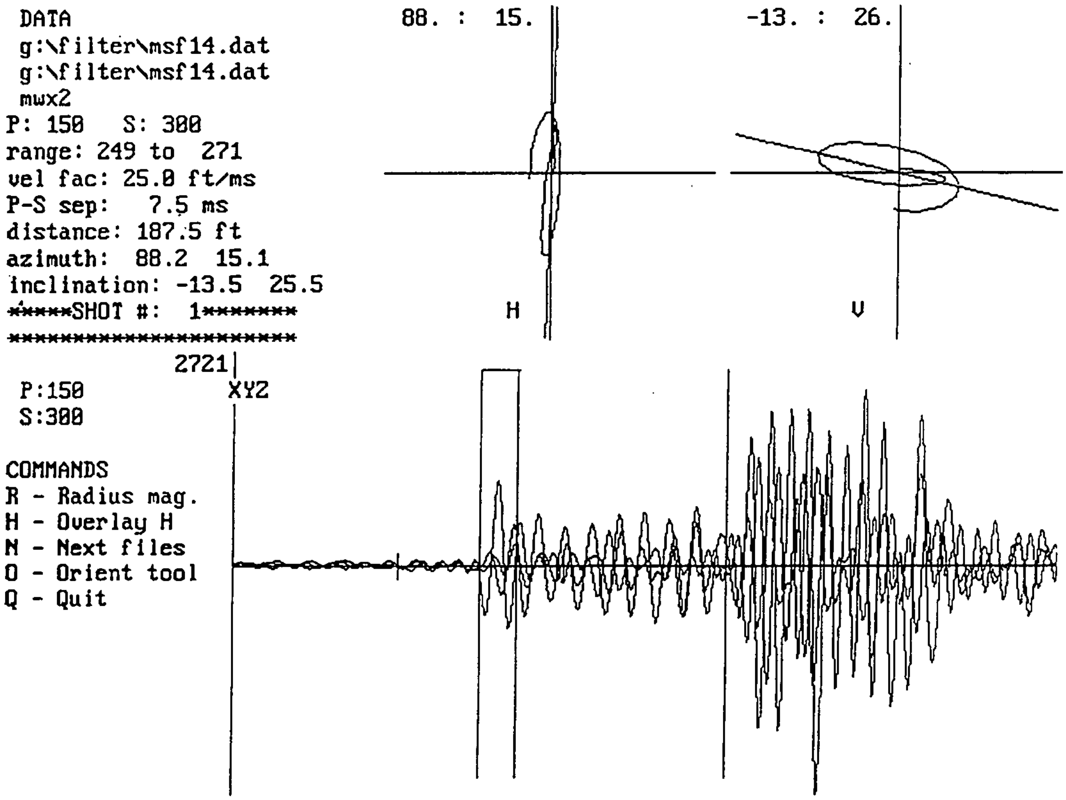

Figure A7 Event 14

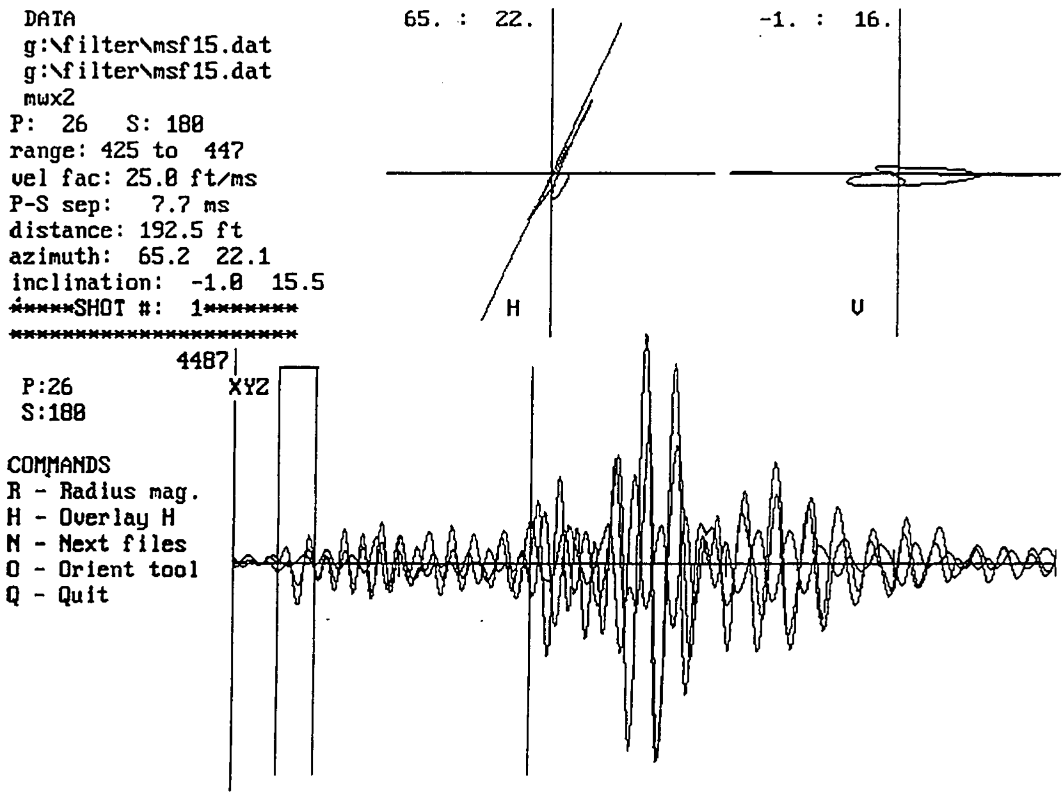

Figure A8 Event 15

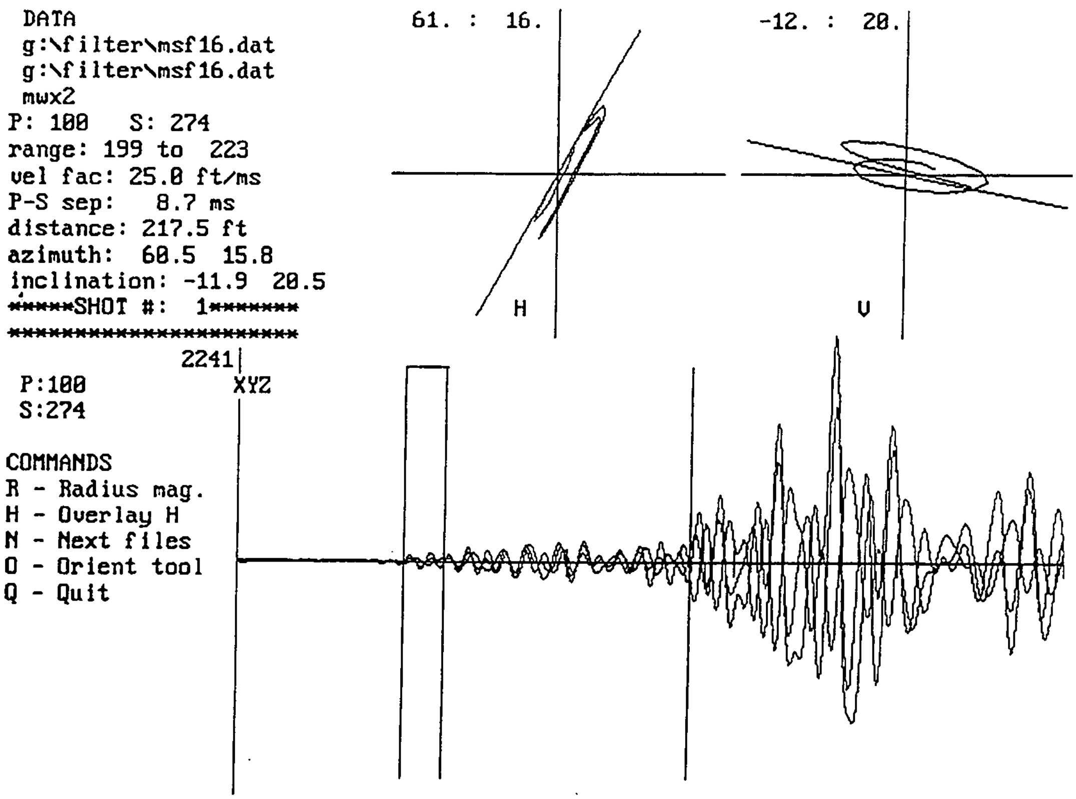

Figure A9 Event 16

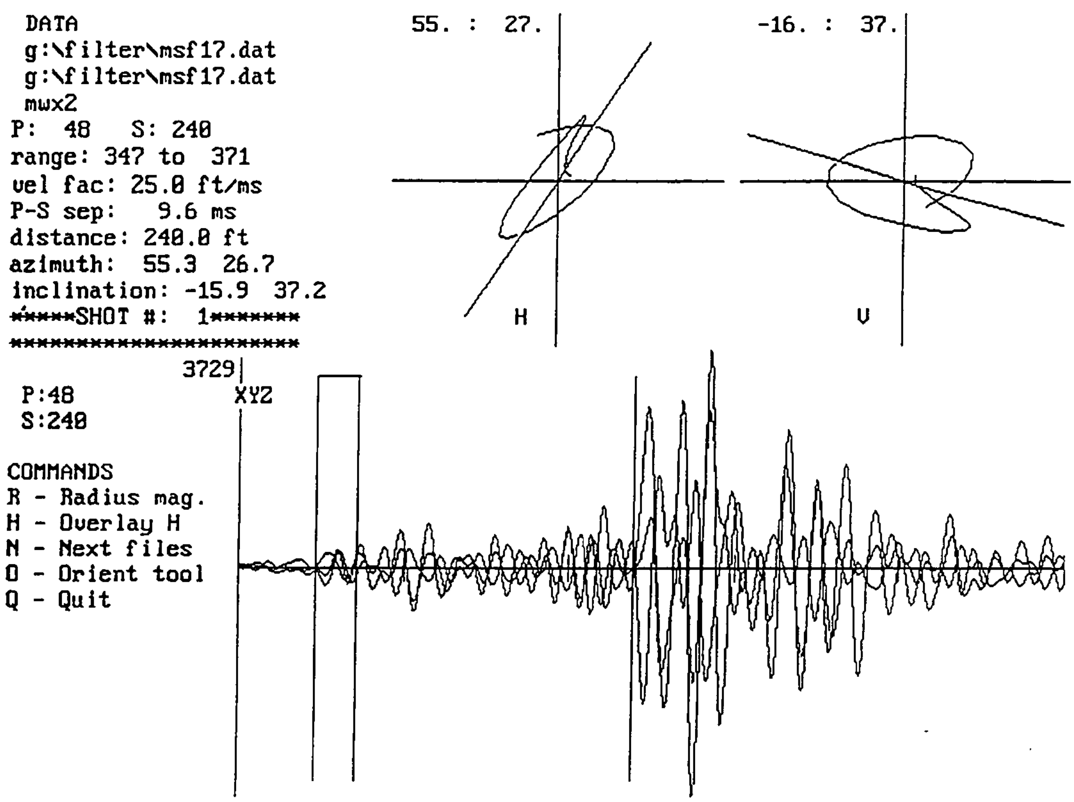

Figure A10 Event 17

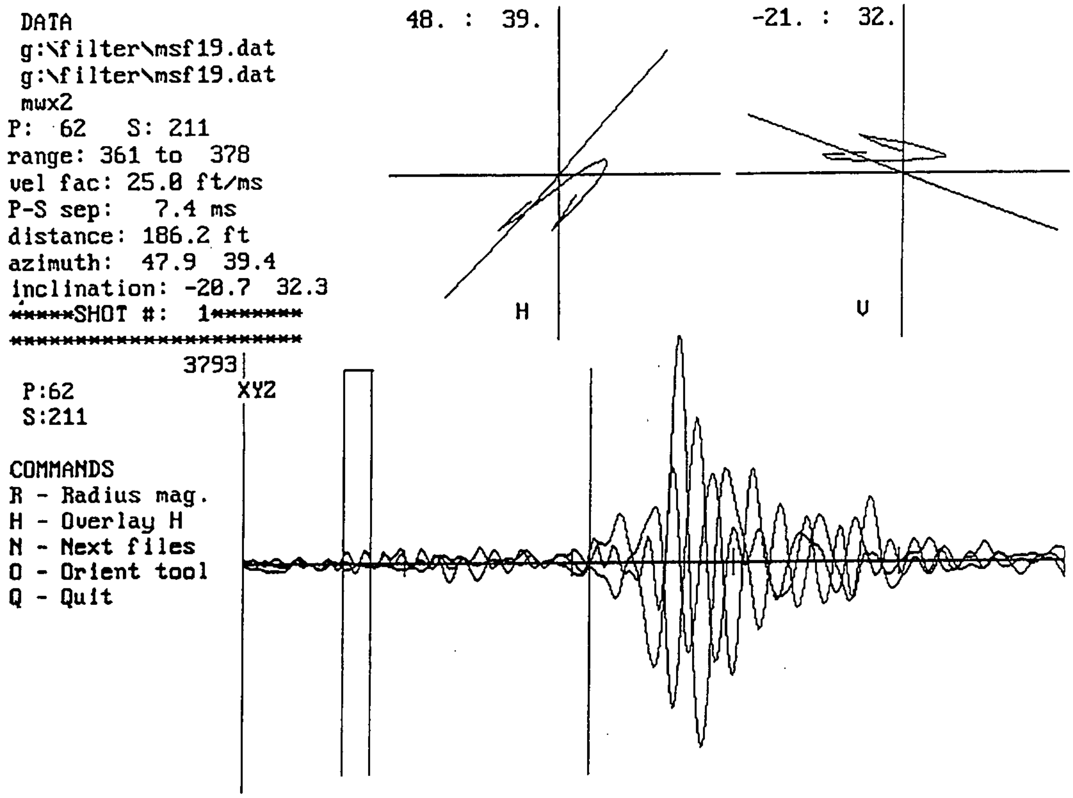

Figure A11 Event 19

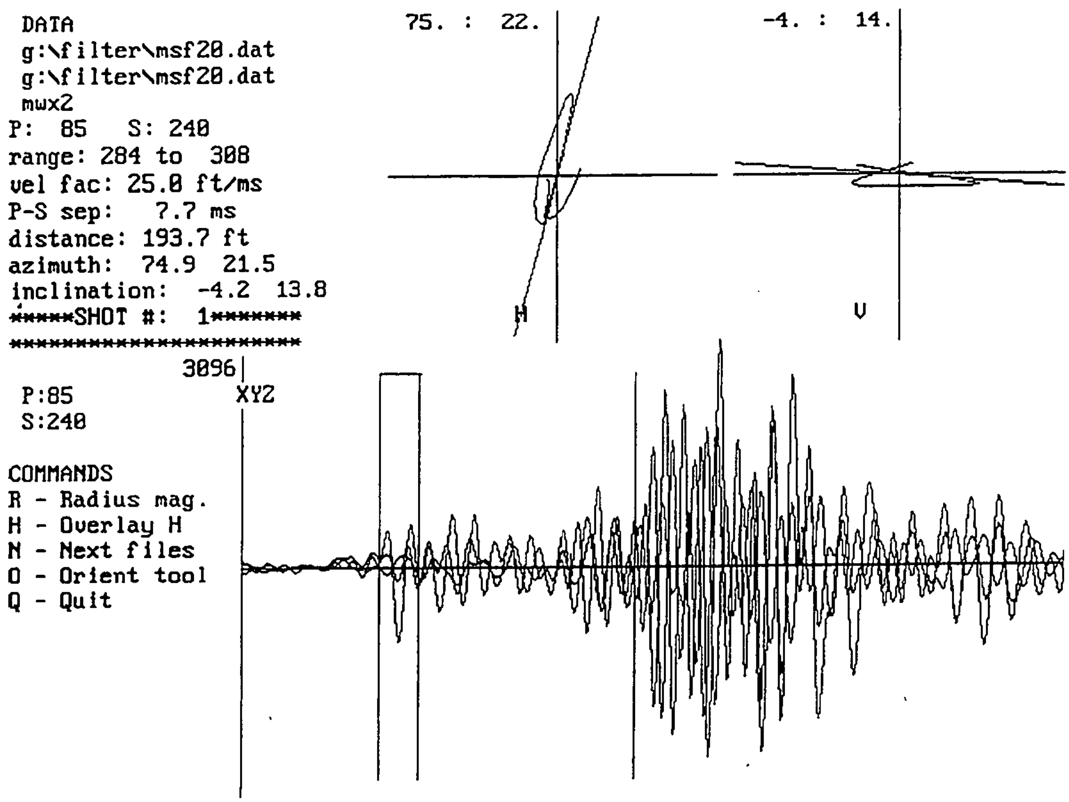

Figure A12 Event 20

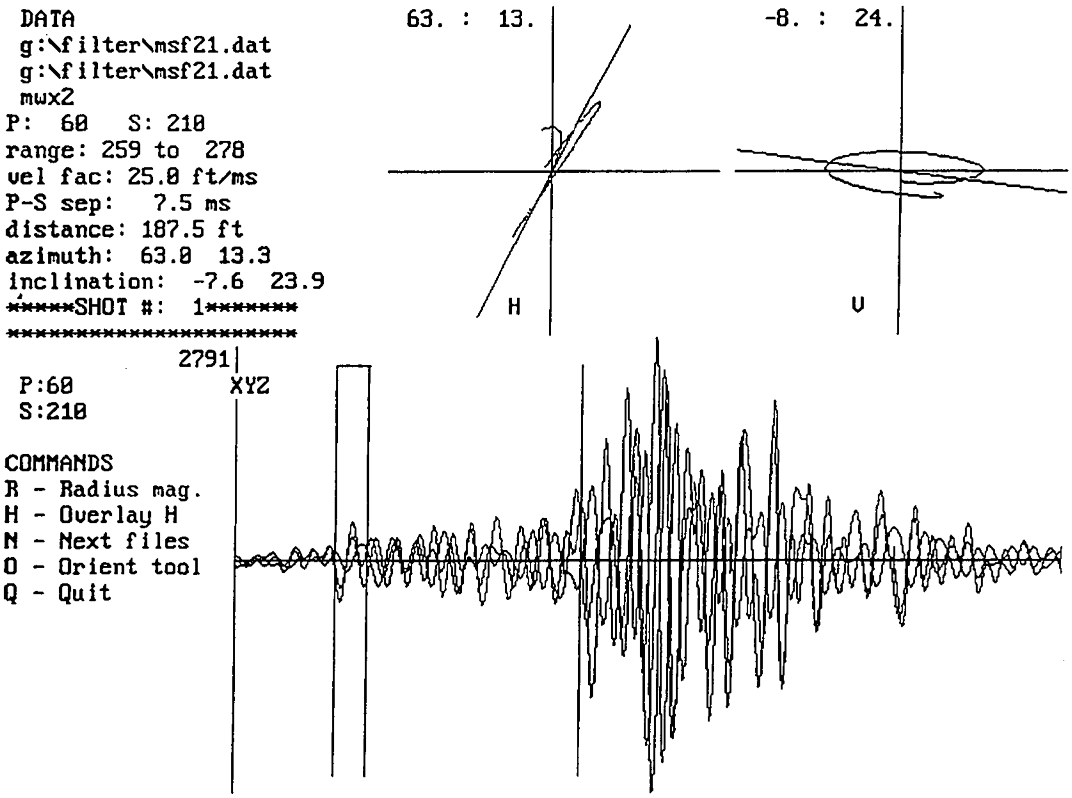

Figure A13 Event 21

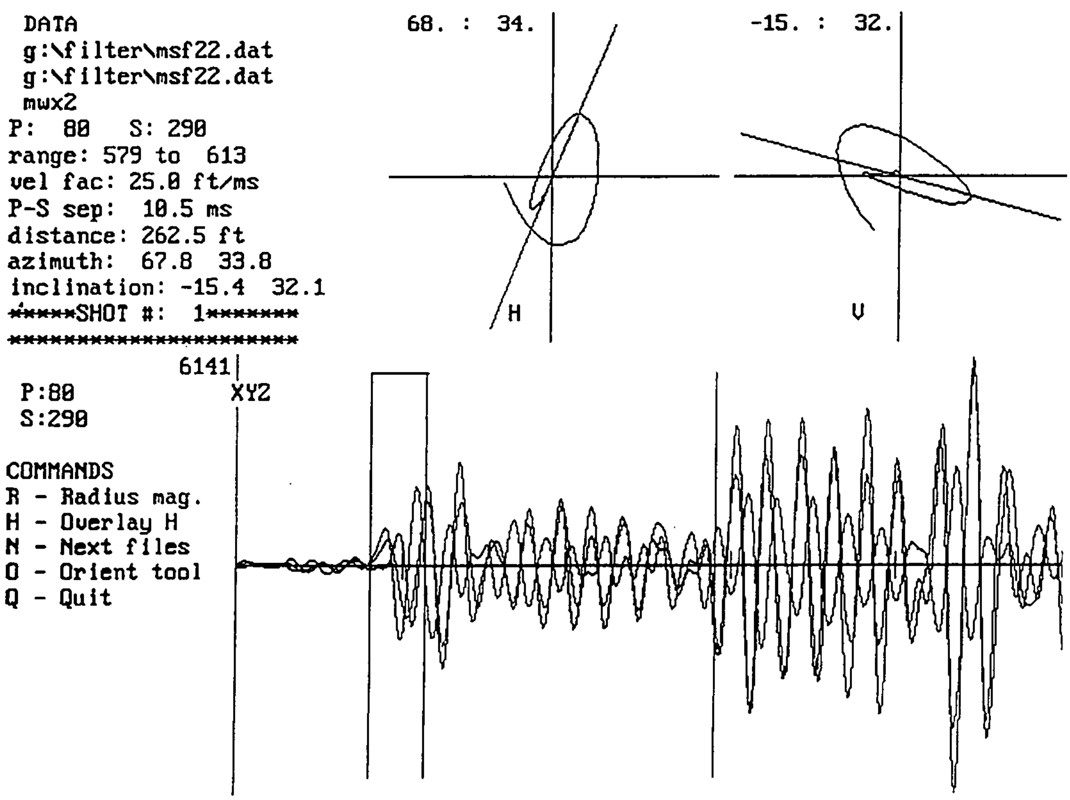

Figure A14 Event 22

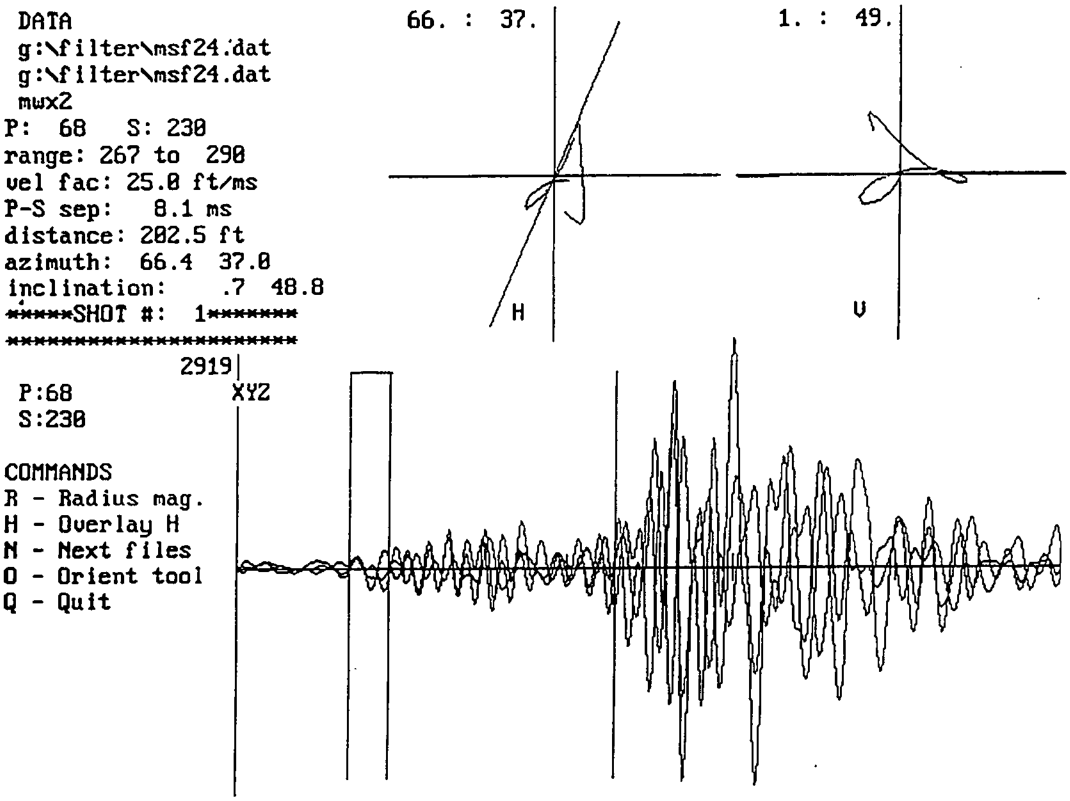

Figure A15 Event 24

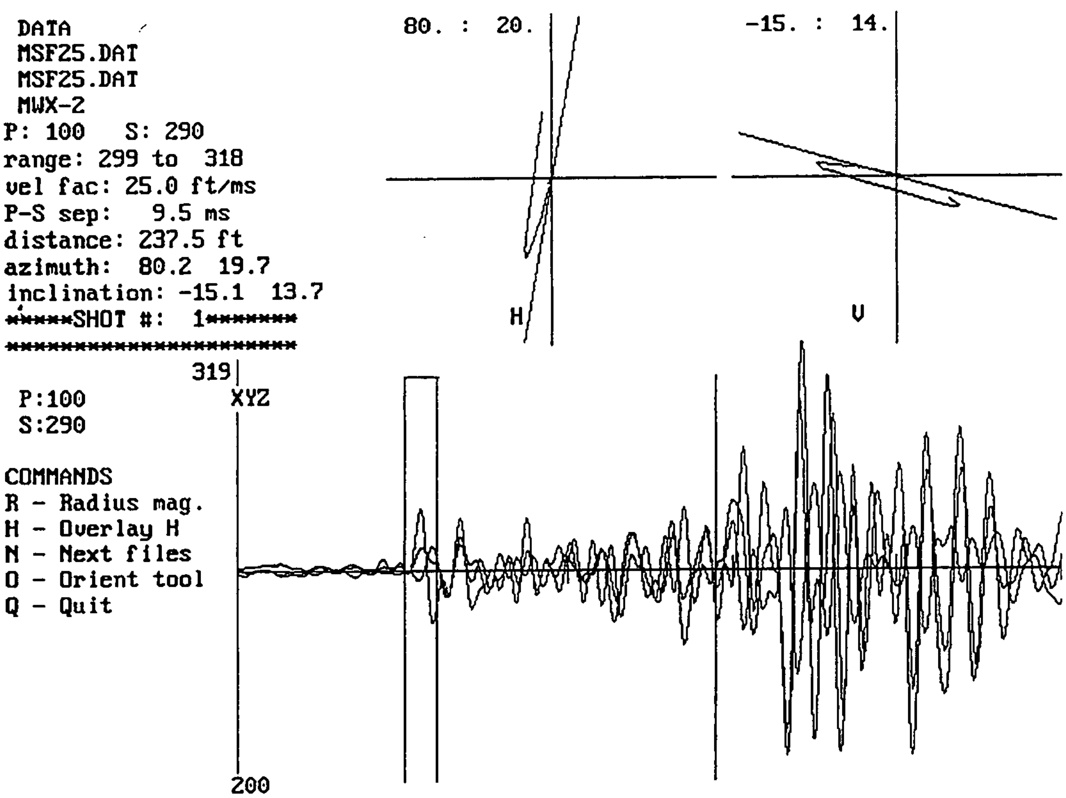

Figure A16 Event 25

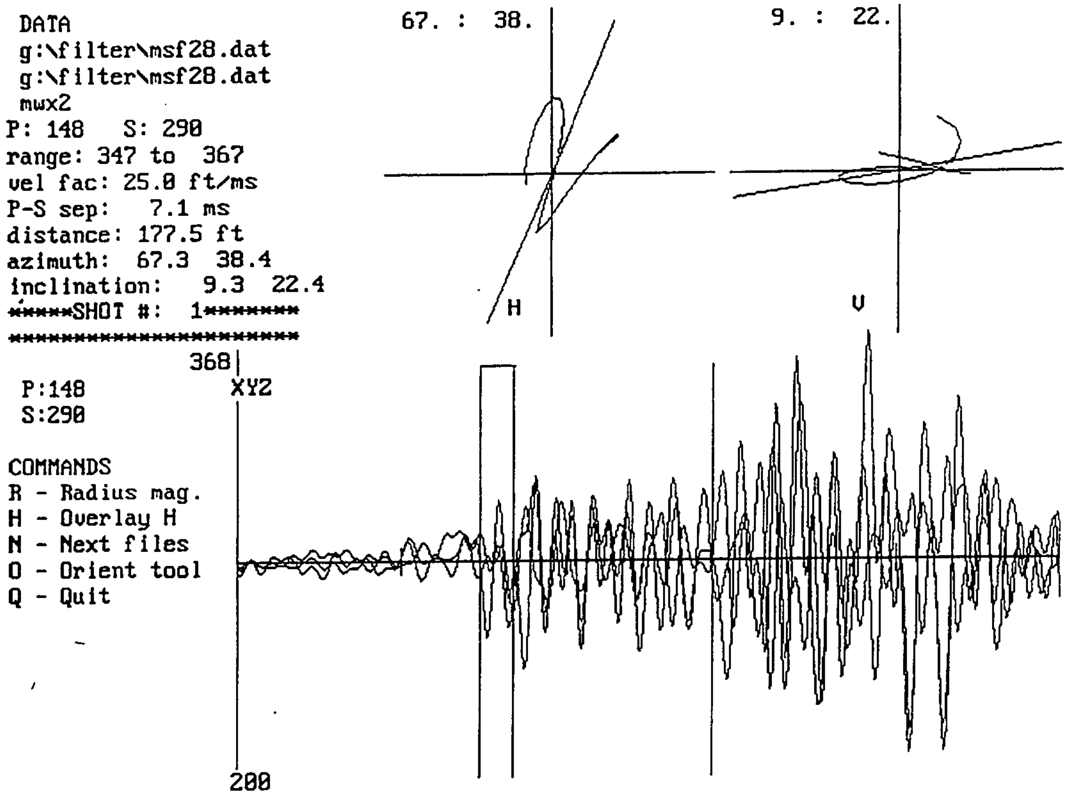

Figure A17 Event 28

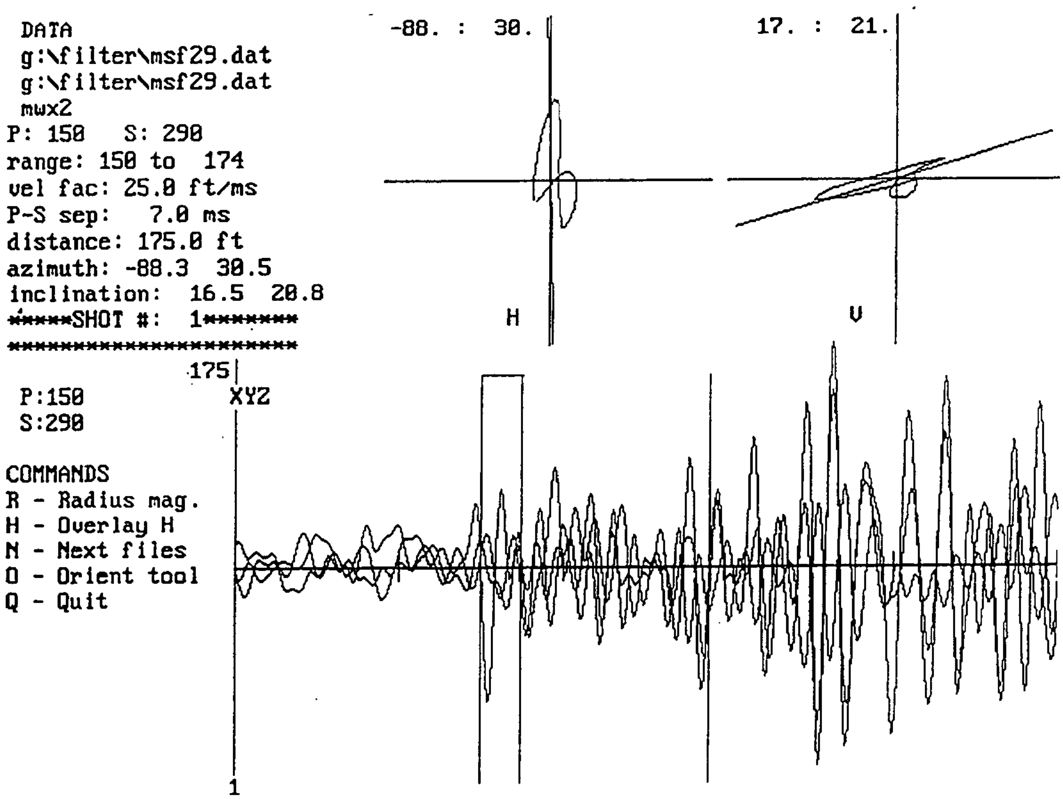

Figure A18 Event 29

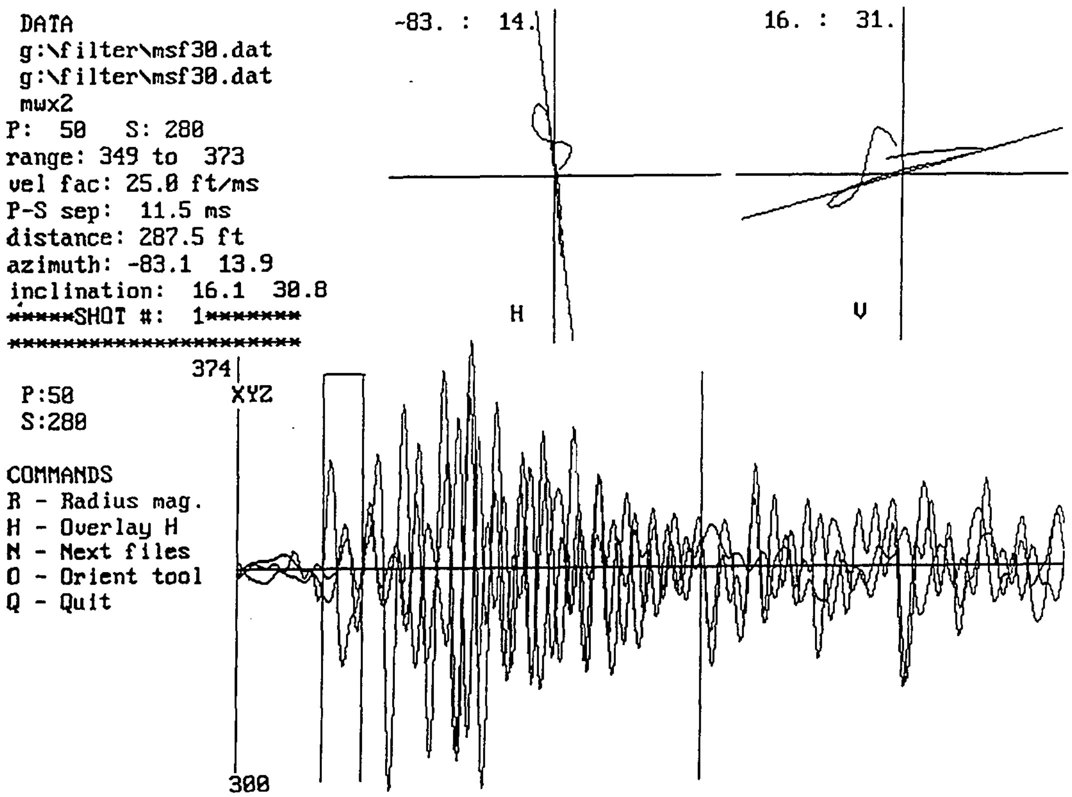

Figure A19 Event 30

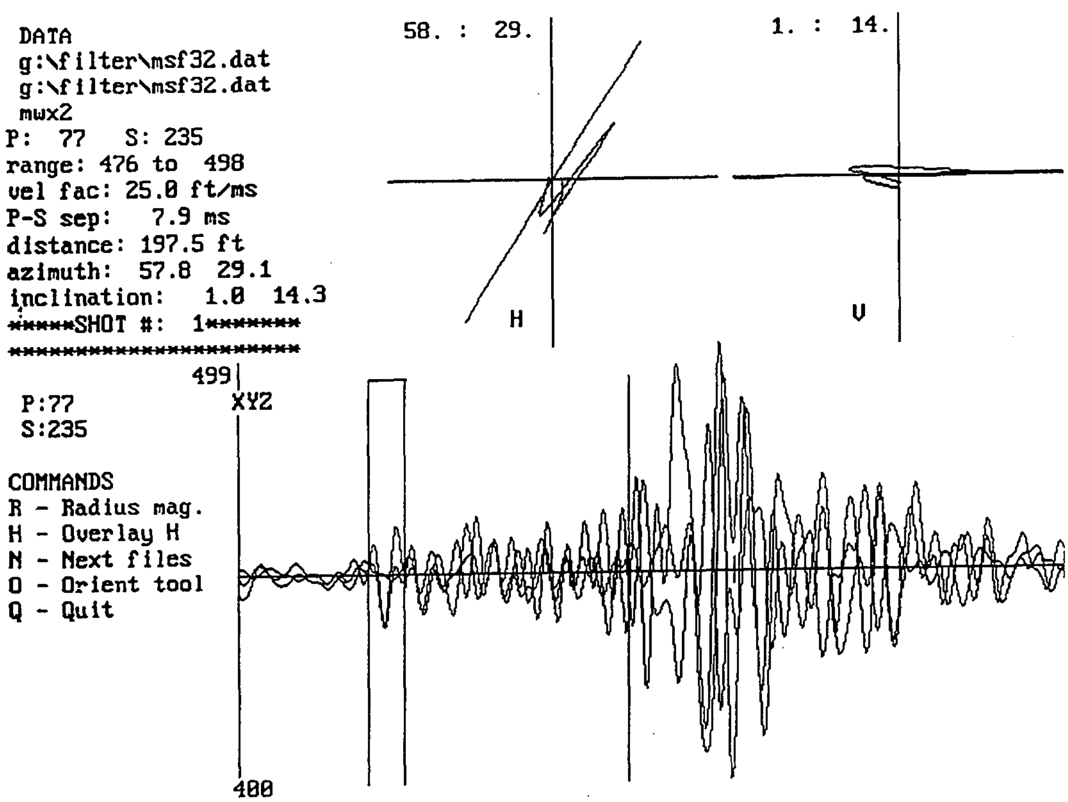

Figure A20 Event 32

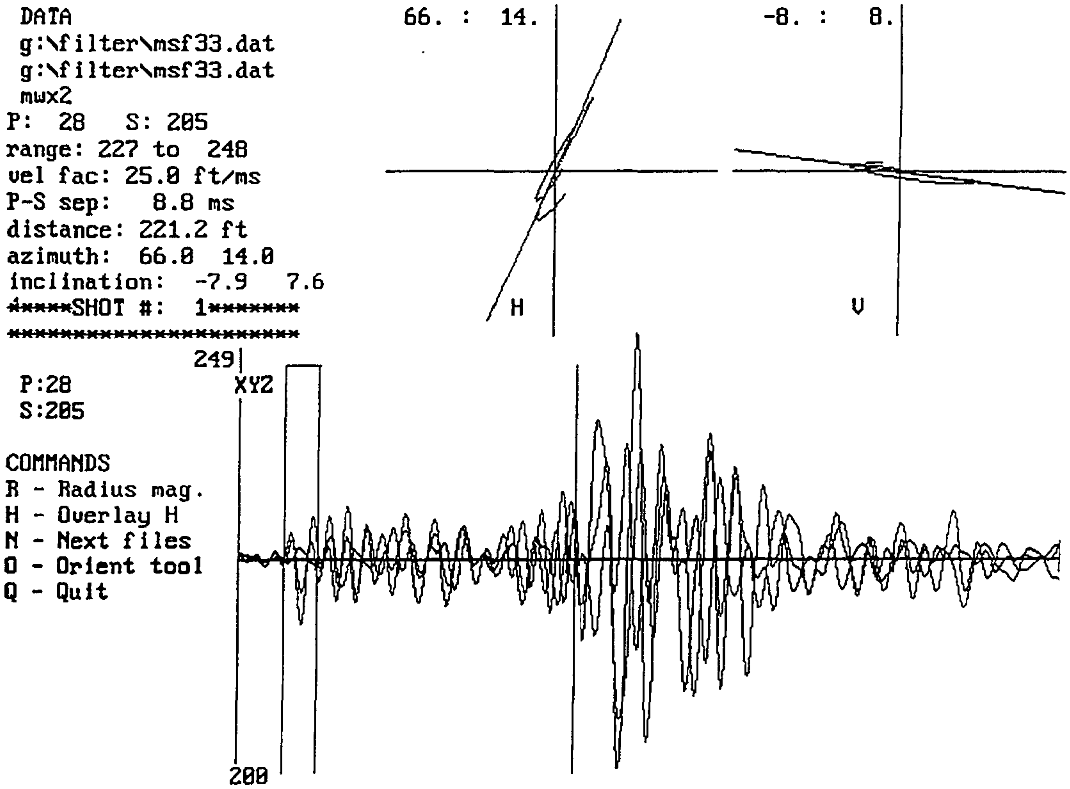

Figure A21 Event 33

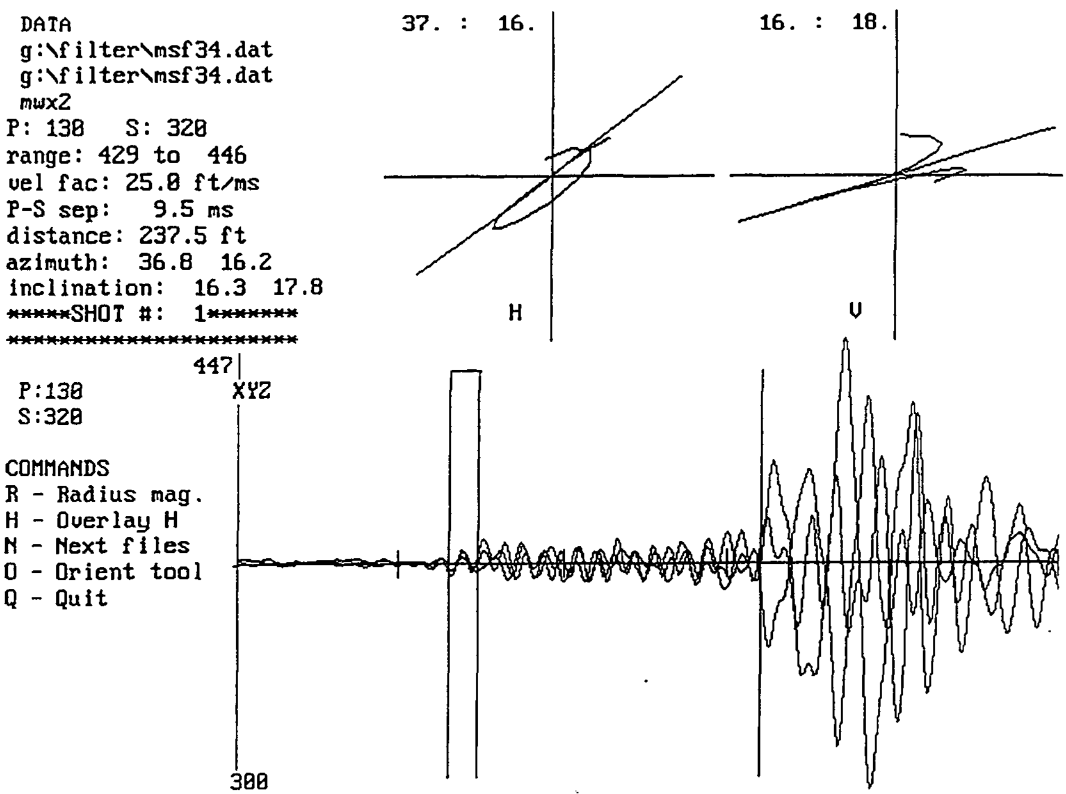

Figure A22 Event 34

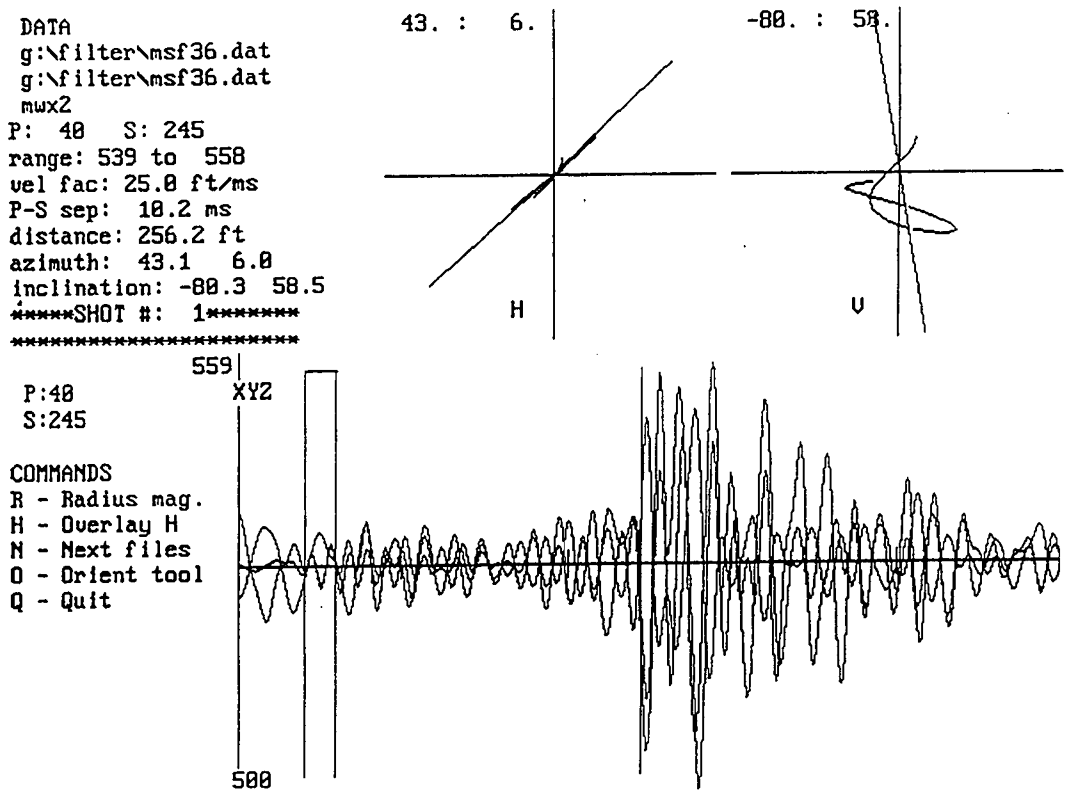

Figure A23 Event 36

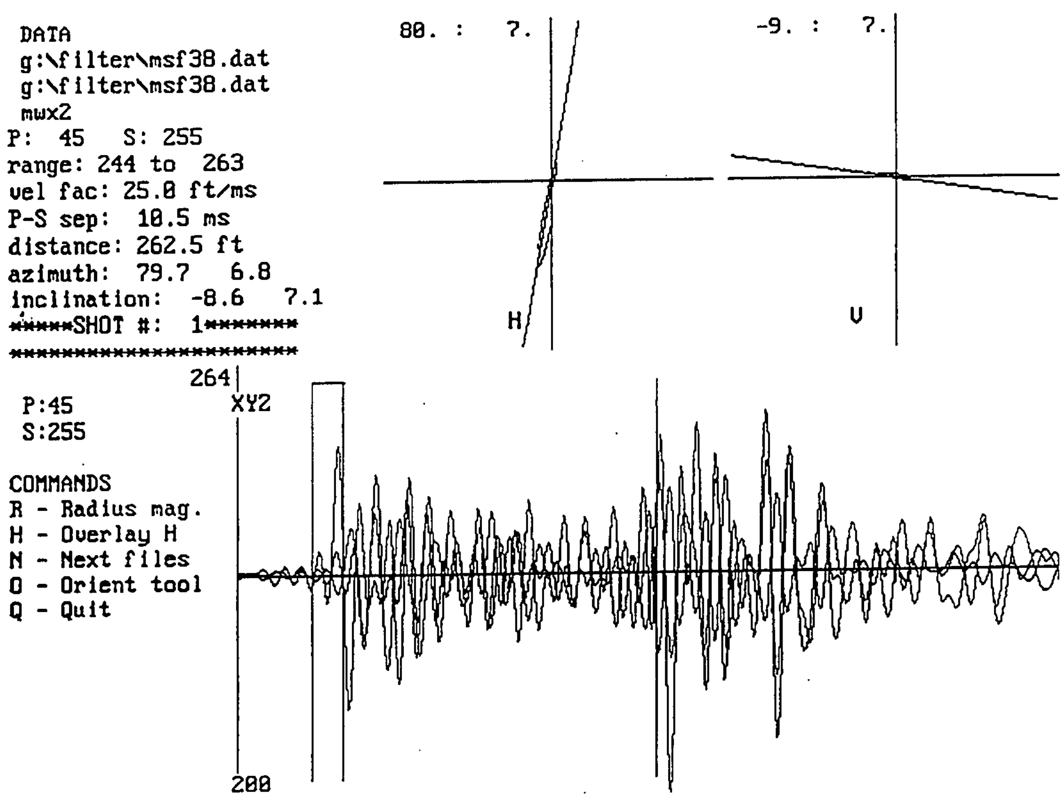

Figure A24 Event 38

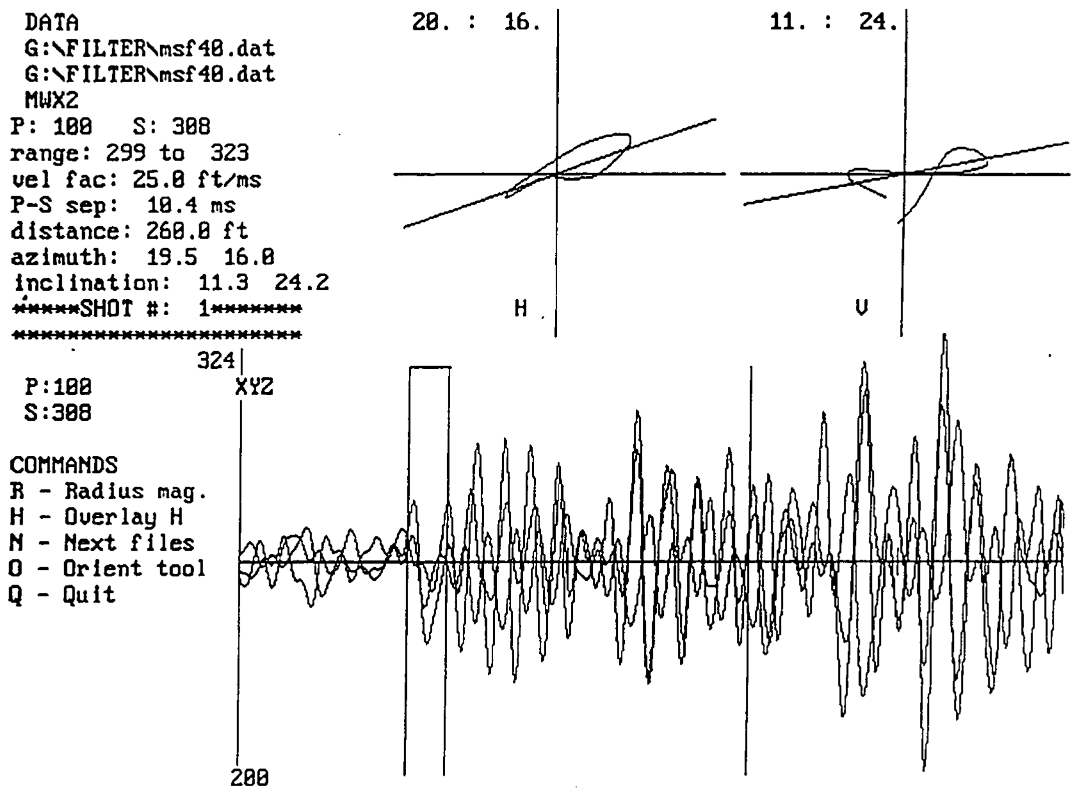

Figure A25 Event 40

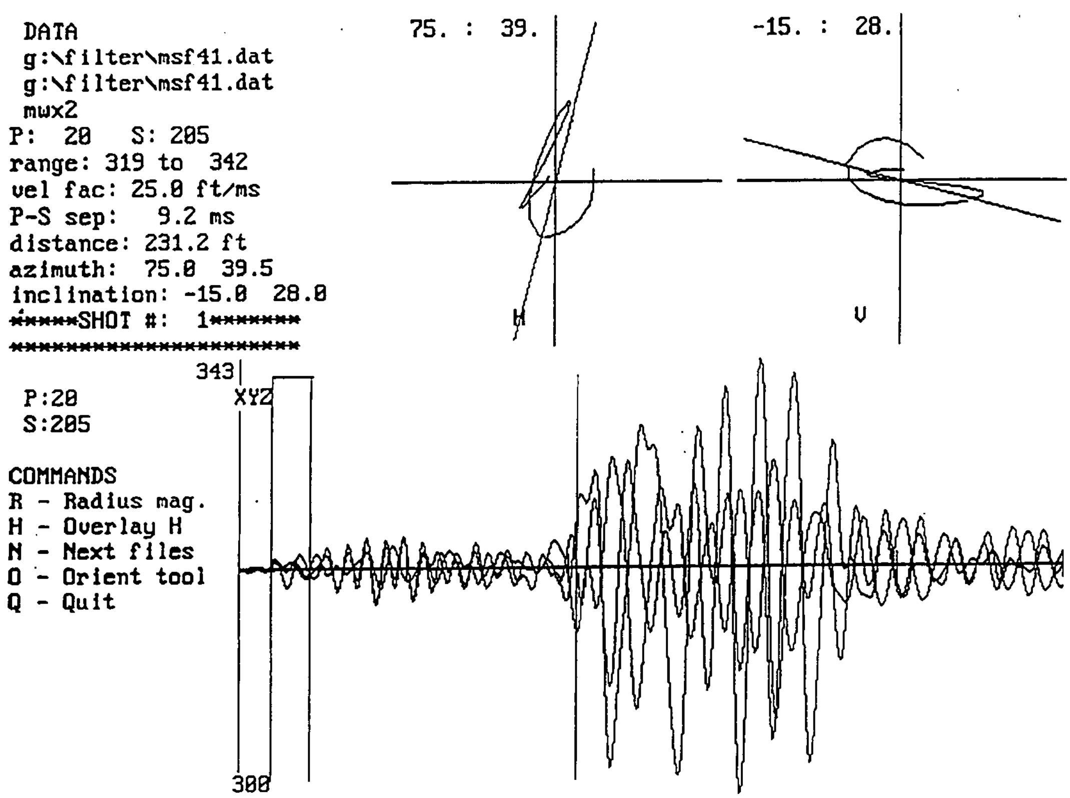

Figure A26 Event 41

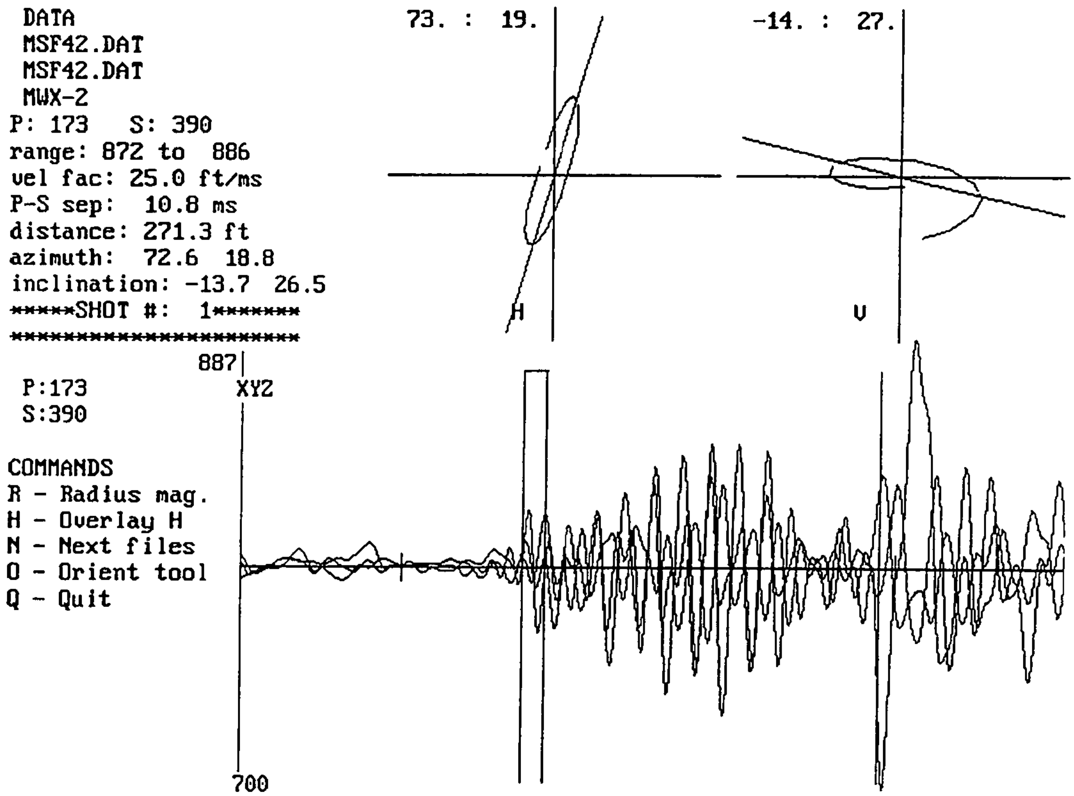

Figure A27 Event 42

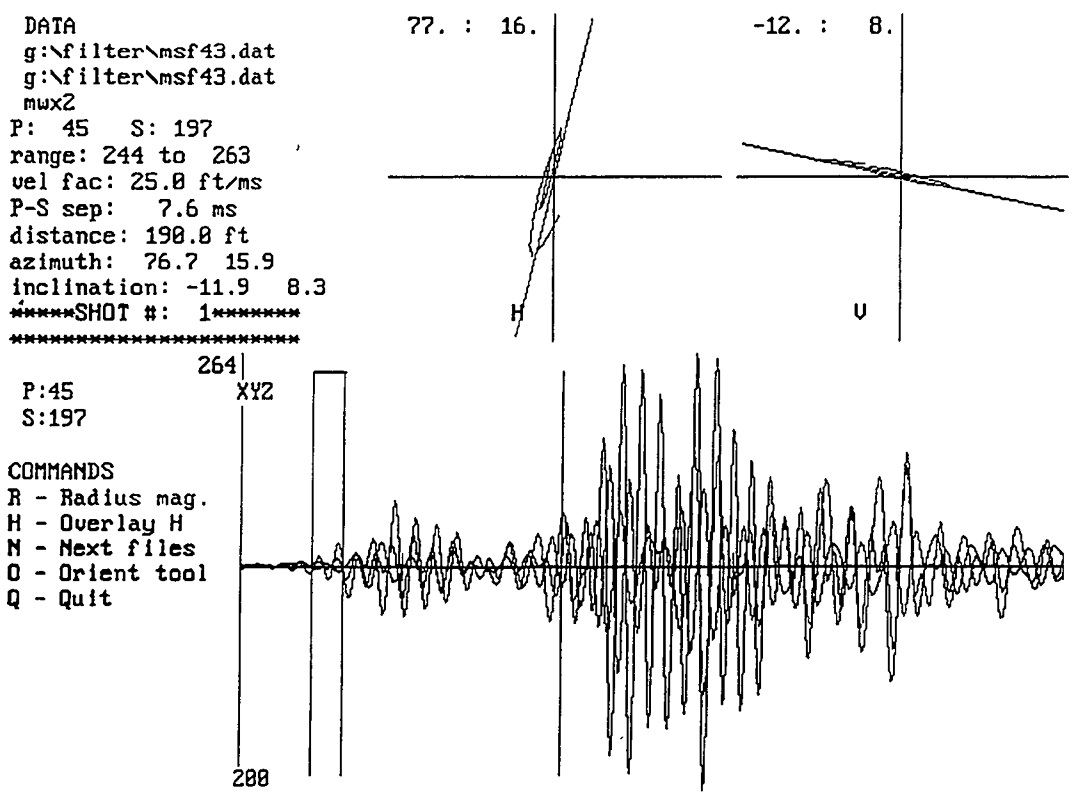

Figure A28 Event 43

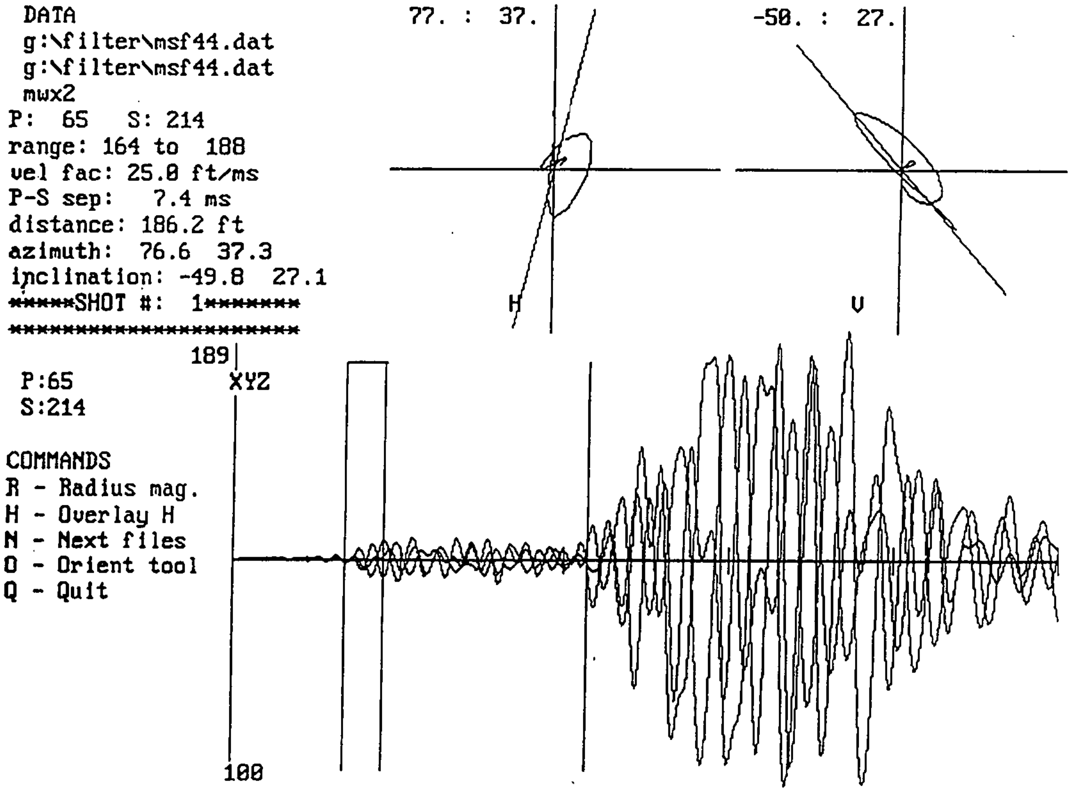

Figure A29 Event 44

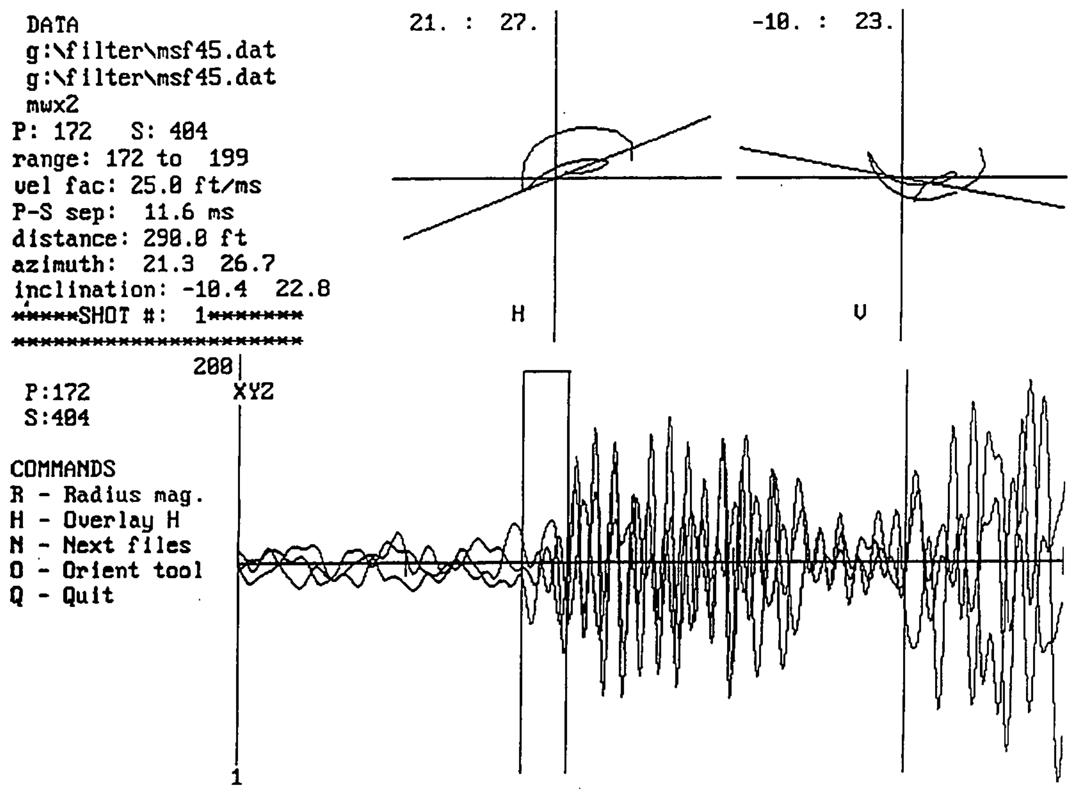

Figure A30 Event 45

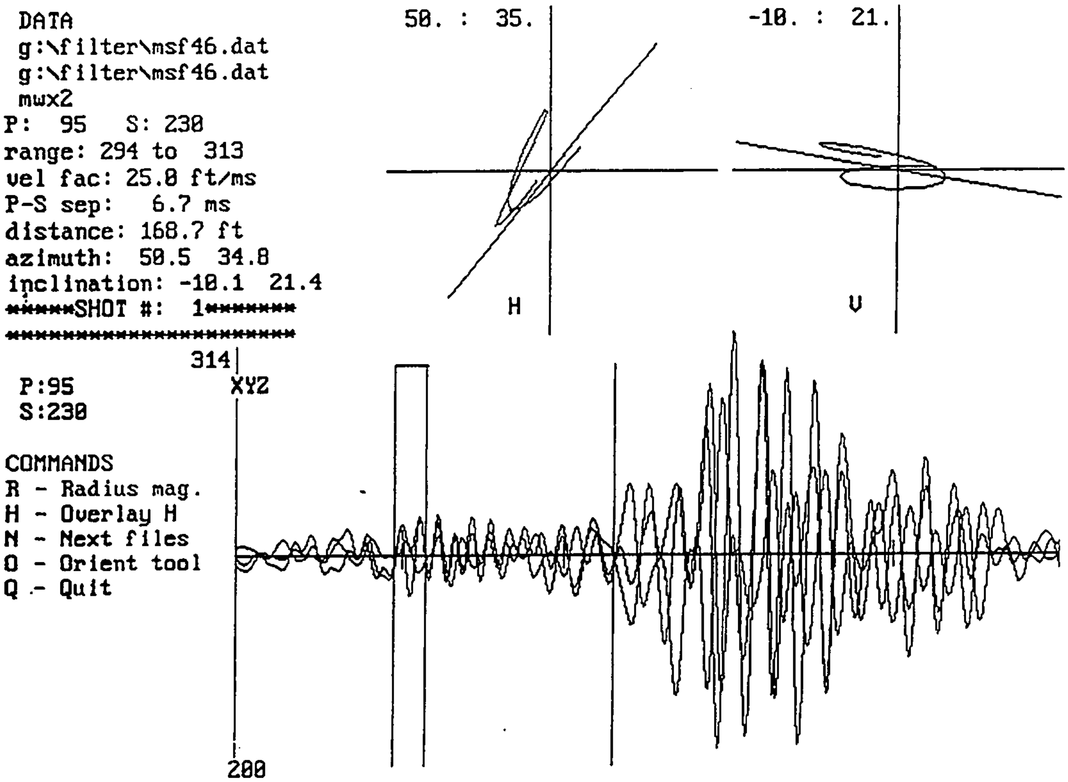

Figure A31 Event 46

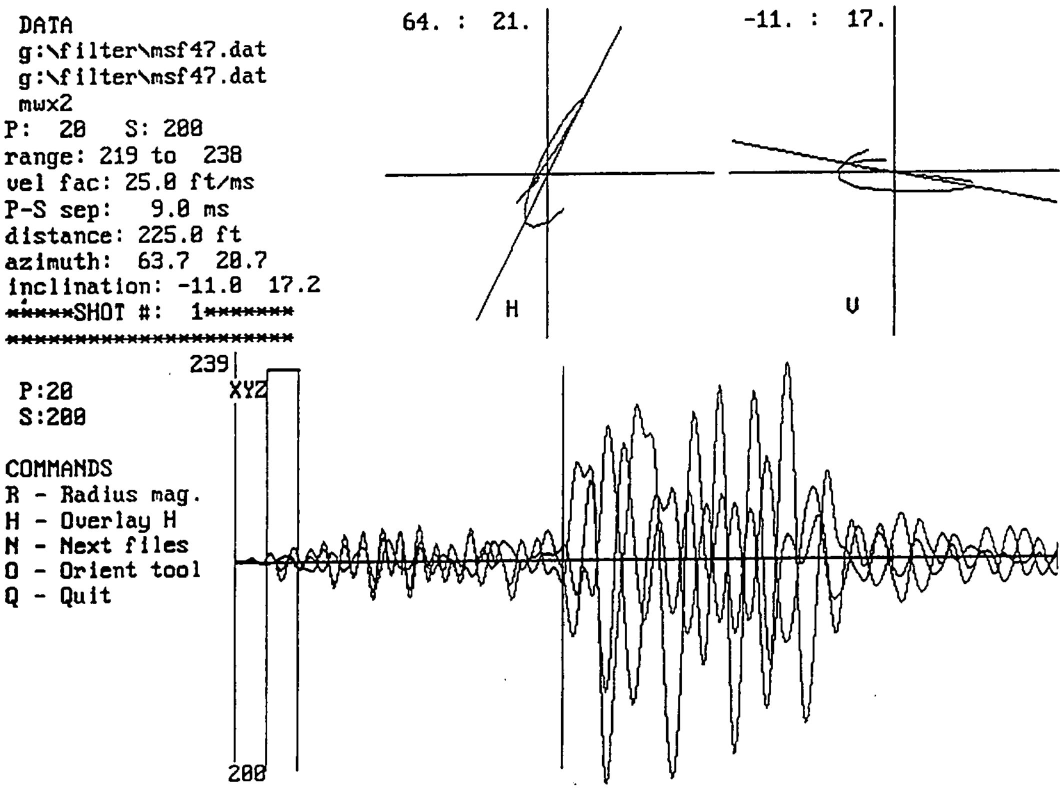

Figure A32 Event 47

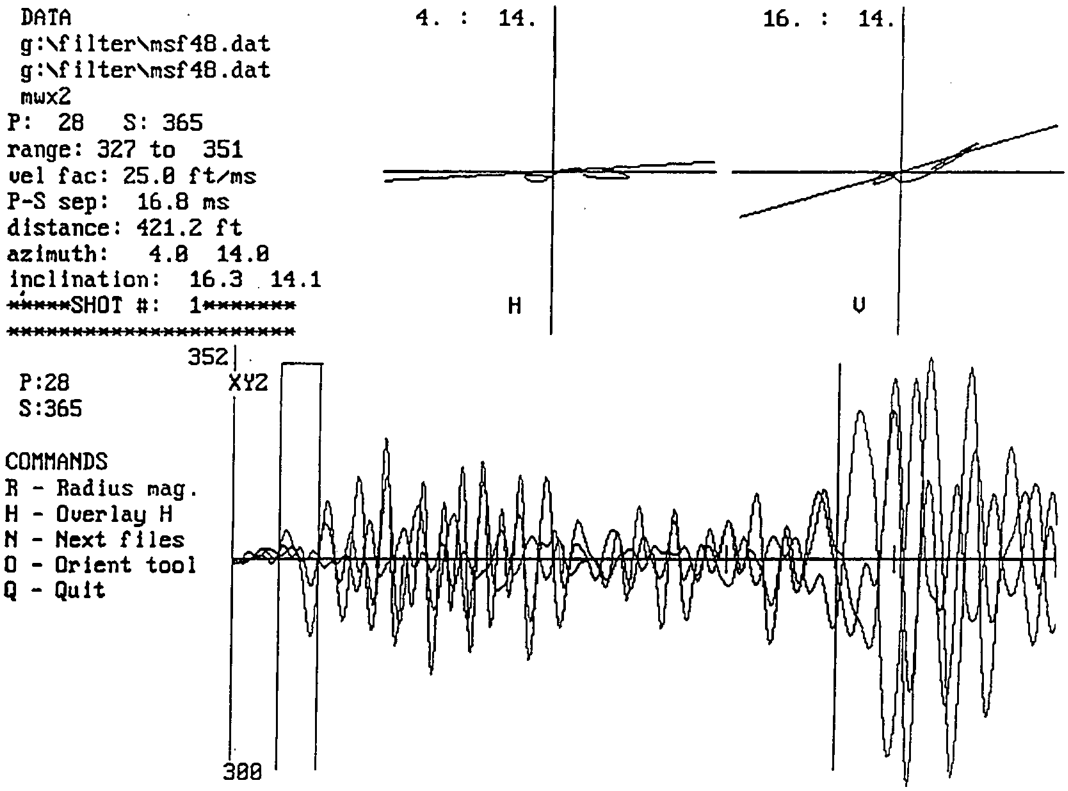

Figure A33 Event 48

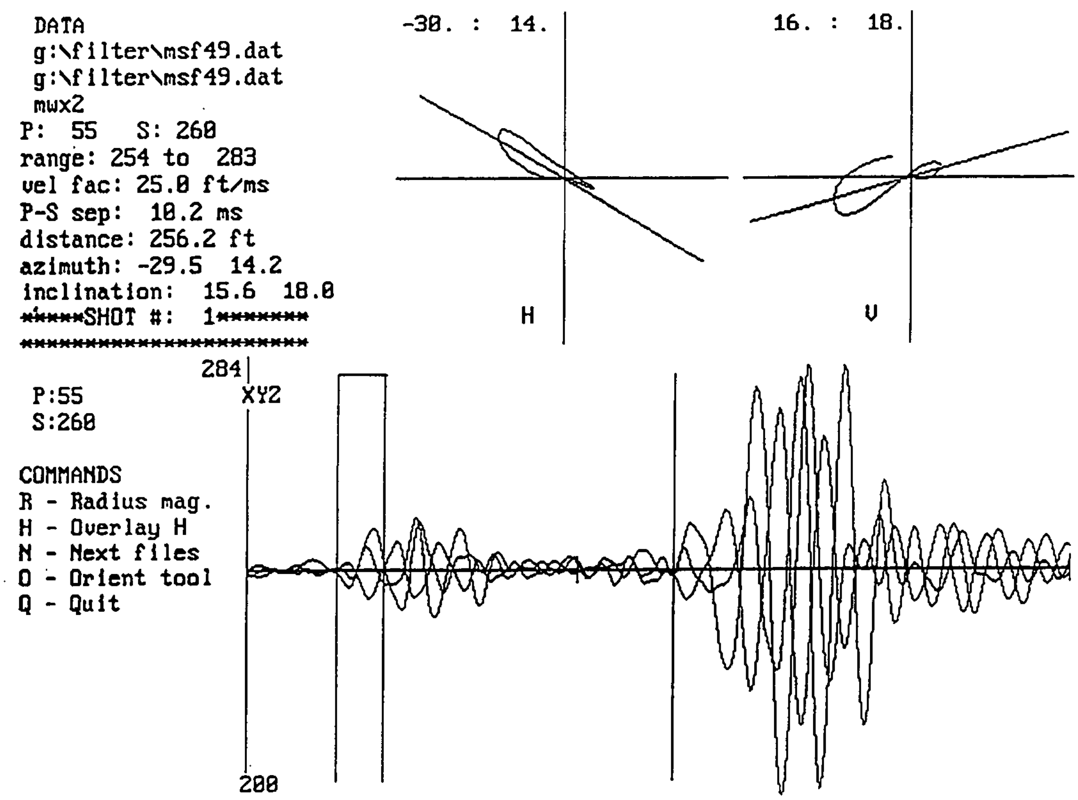

Figure A34 Event 49

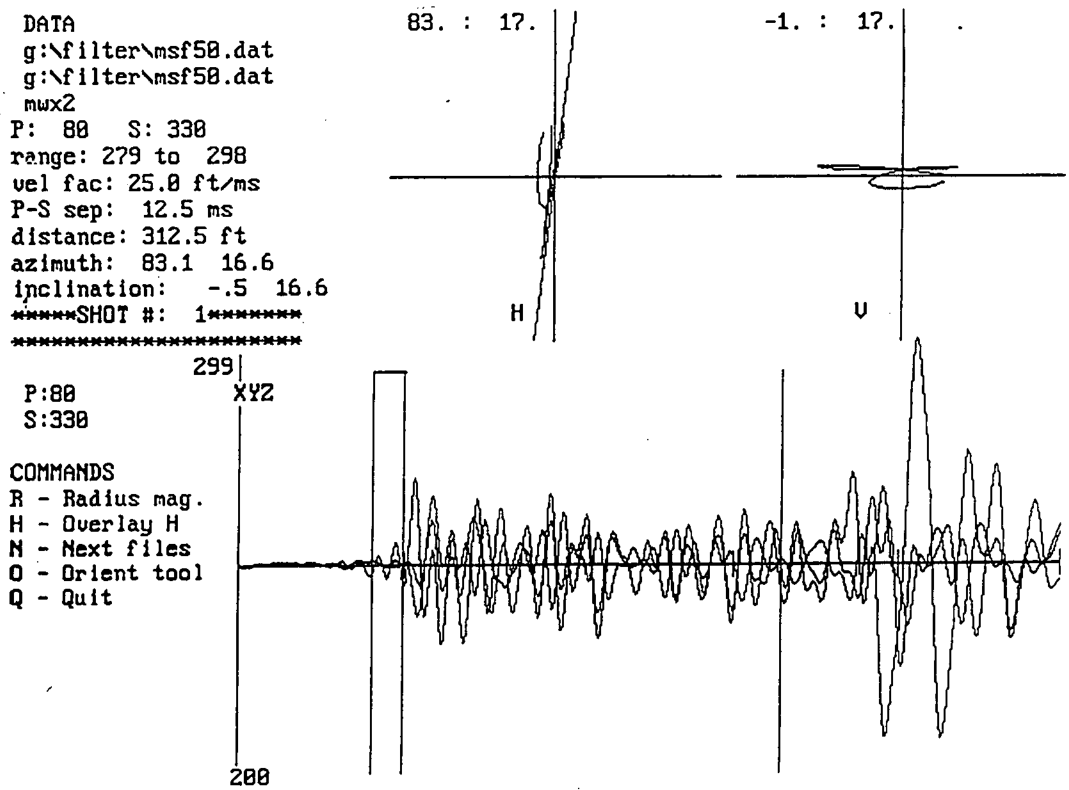

Figure A35 Event 50

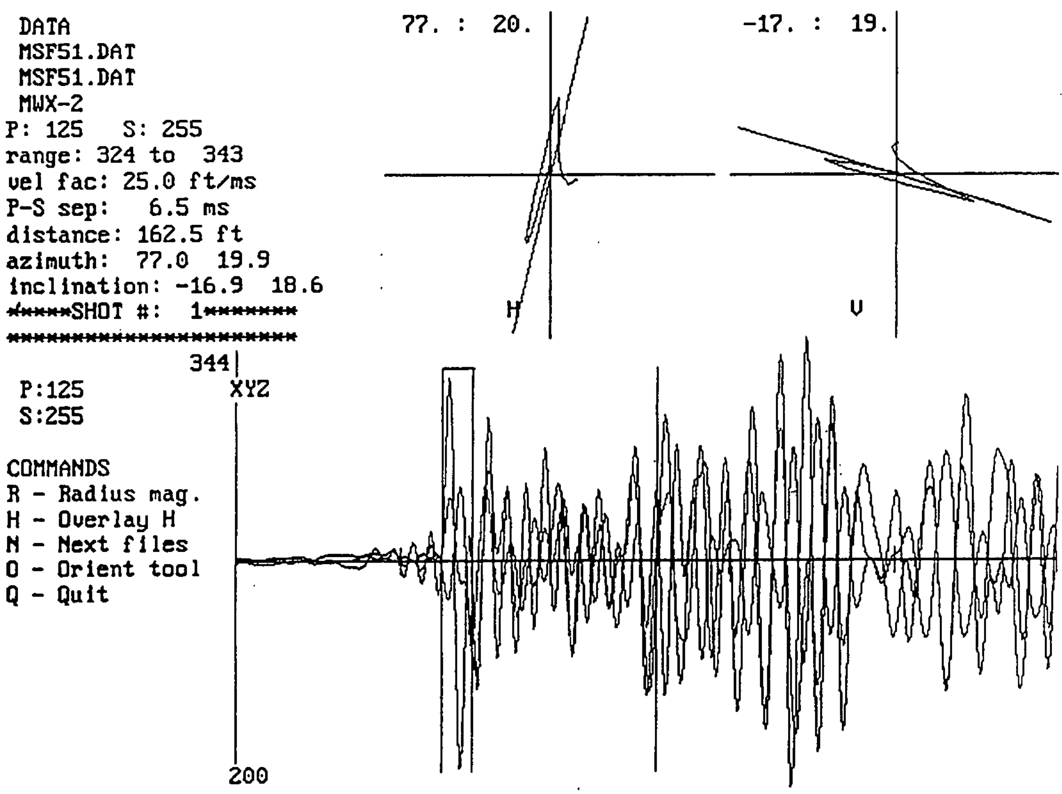

Figure A36 Event 51

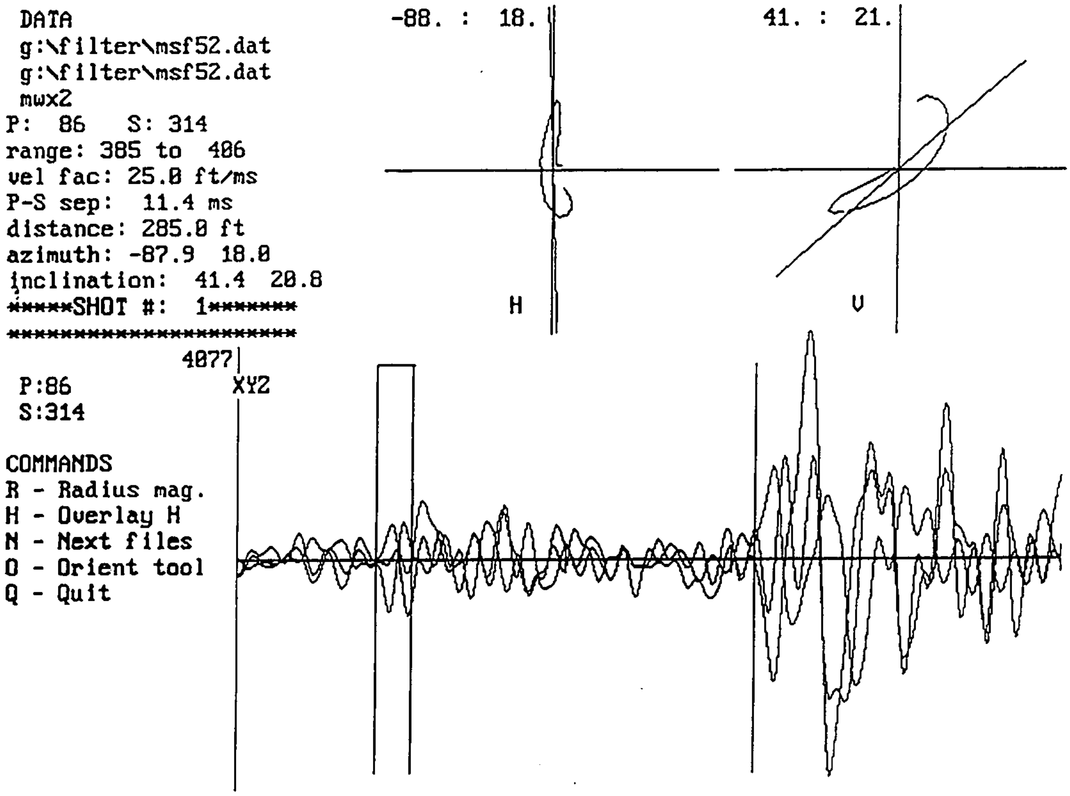

Figure A37 Event 52

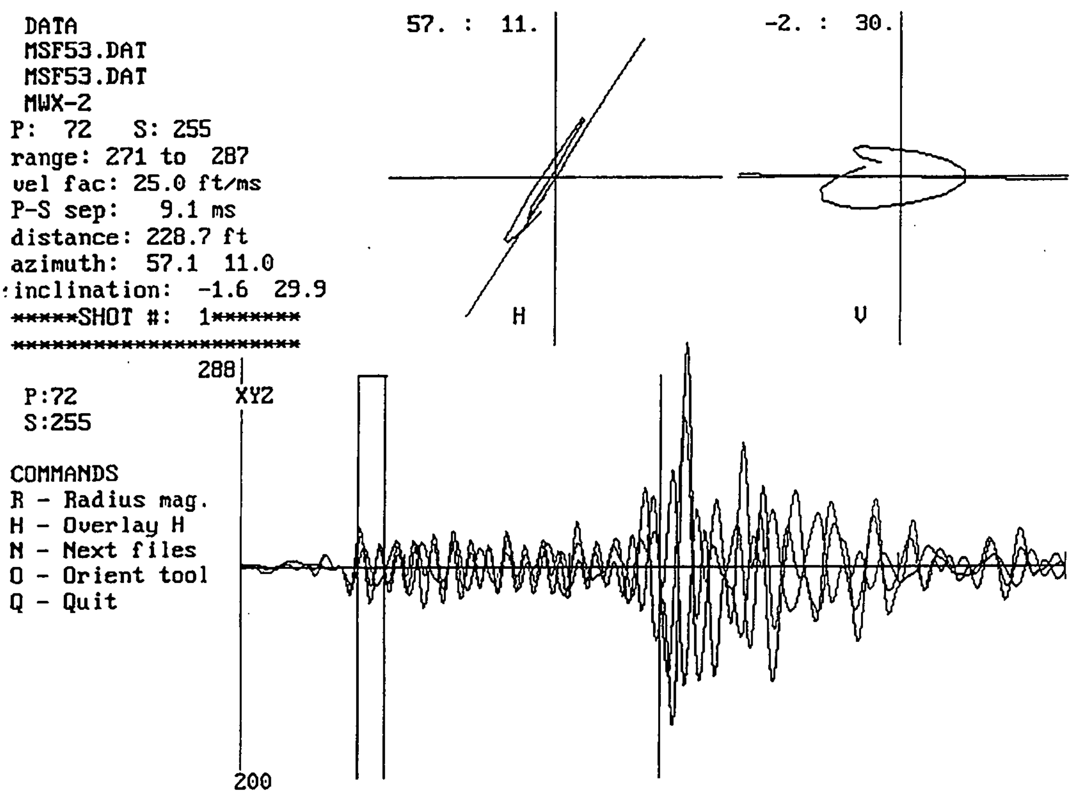

Figure A38 Event 53

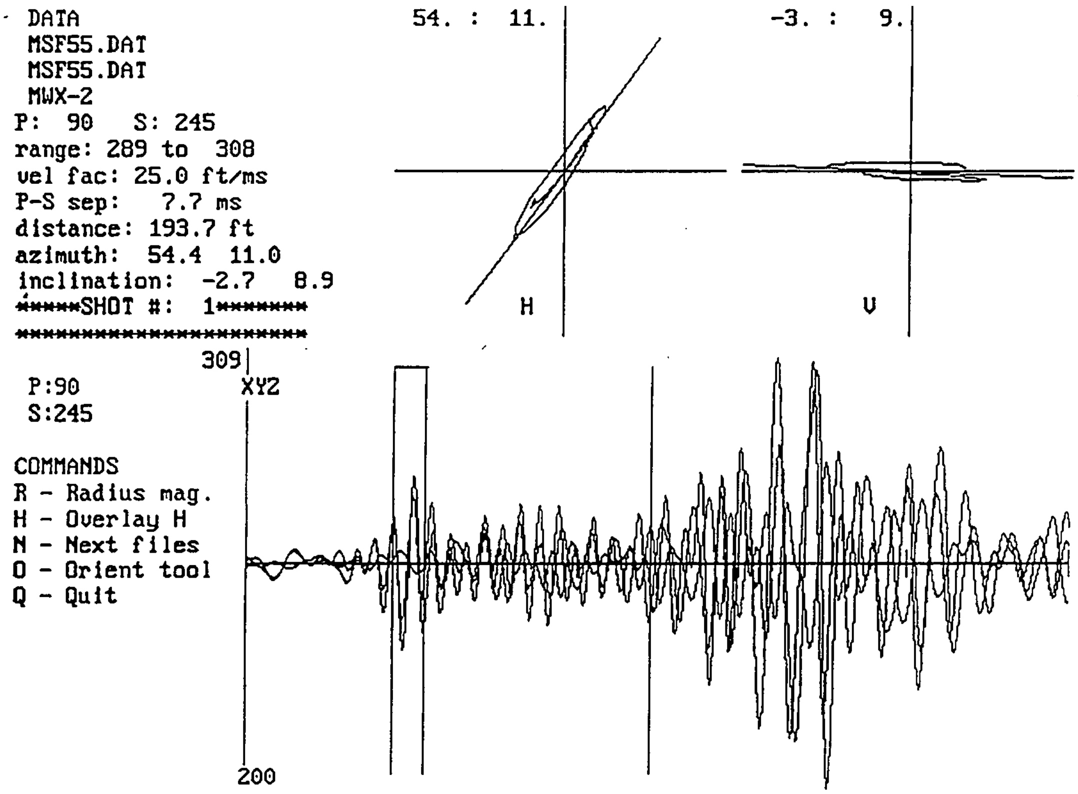

Figure A39 Event 55

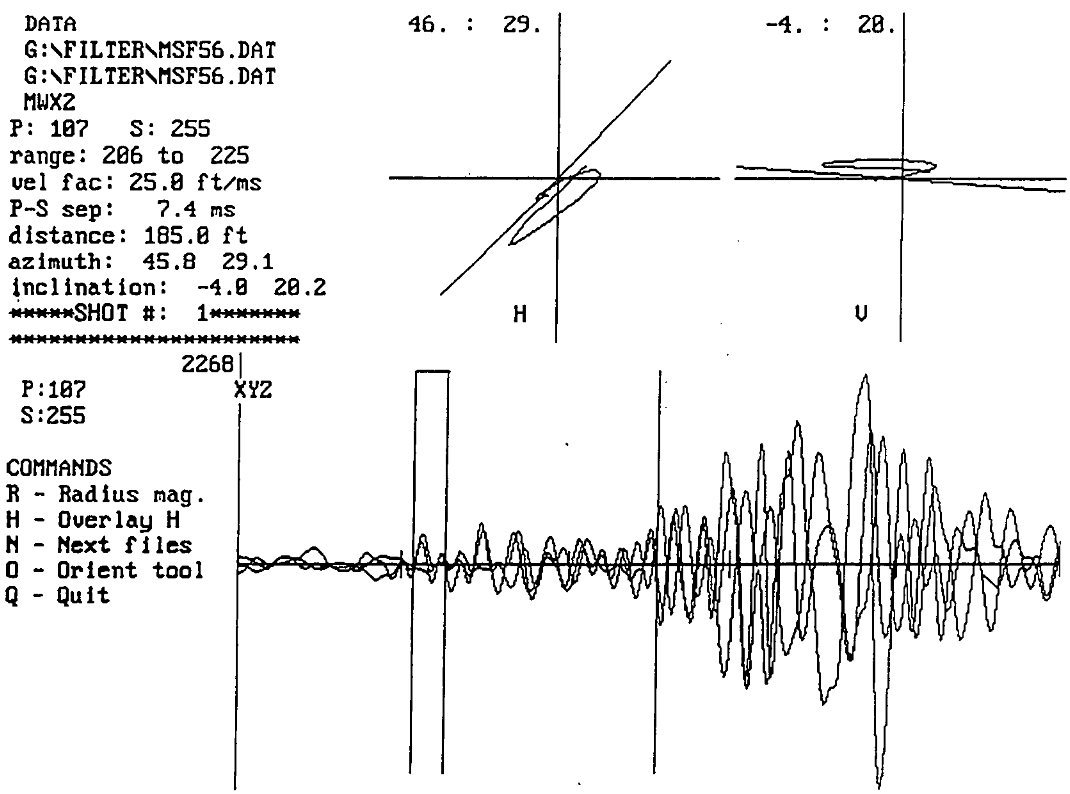

Figure A40 Event 56

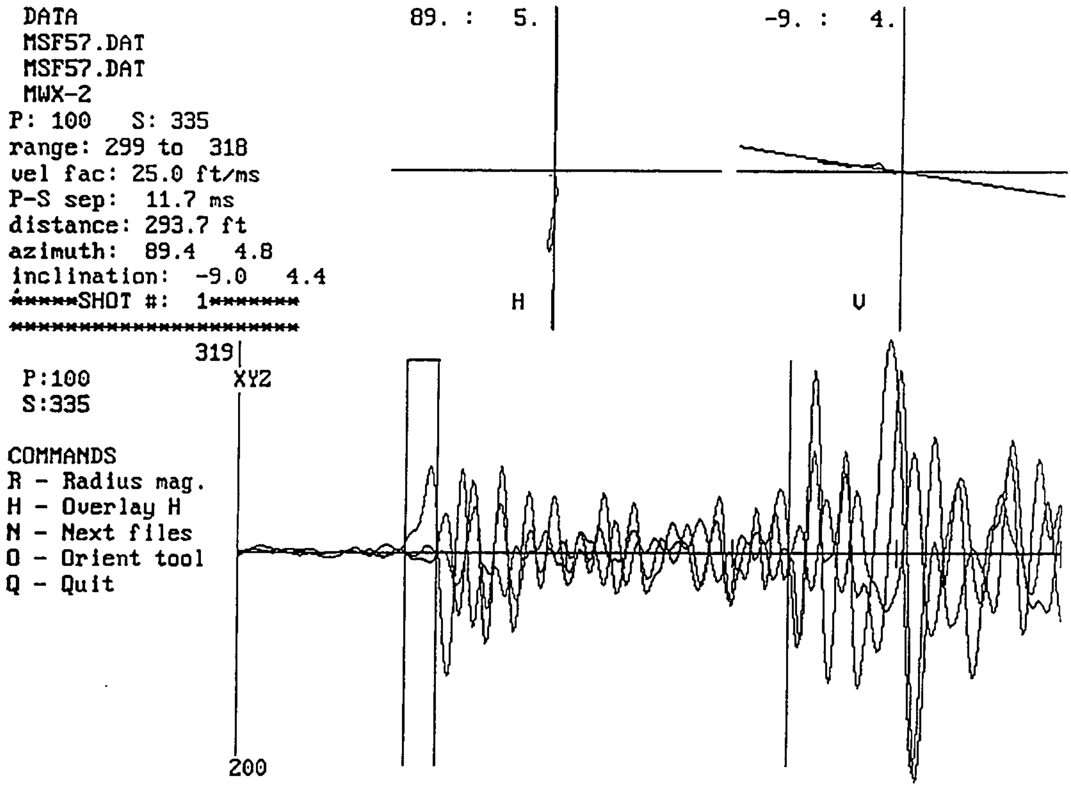

Figure A41 Event 57

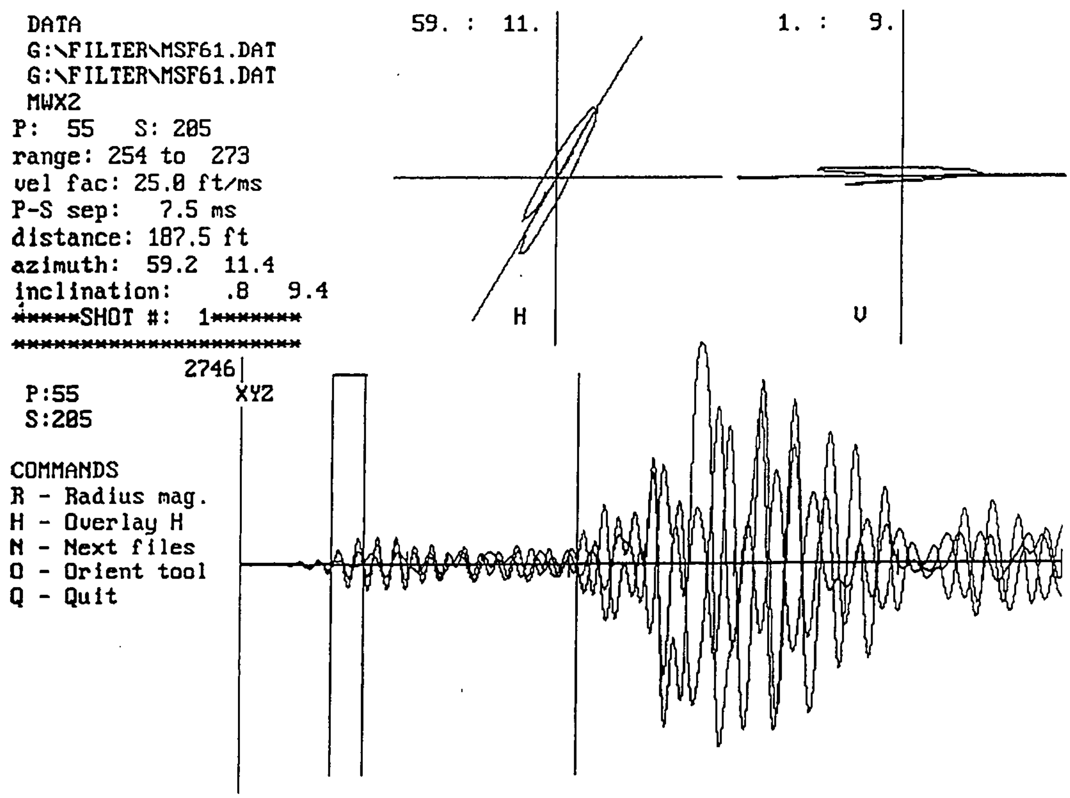

Figure A42 Event 61

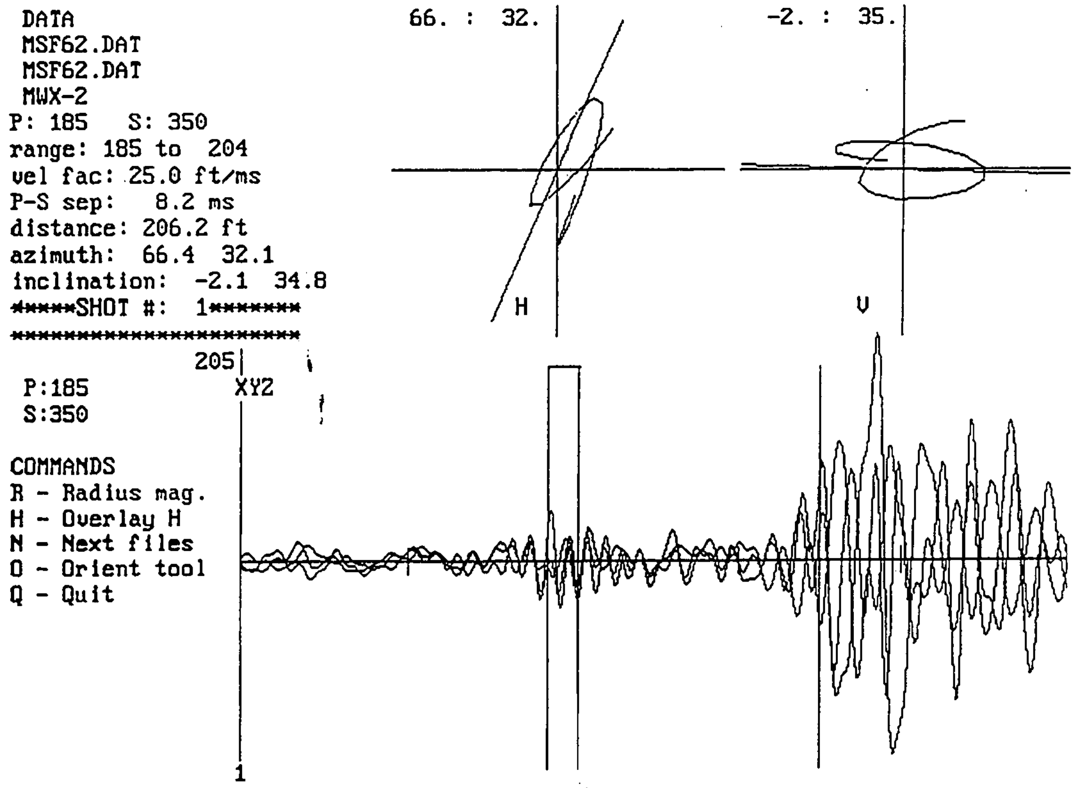

Figure A43 Event 62

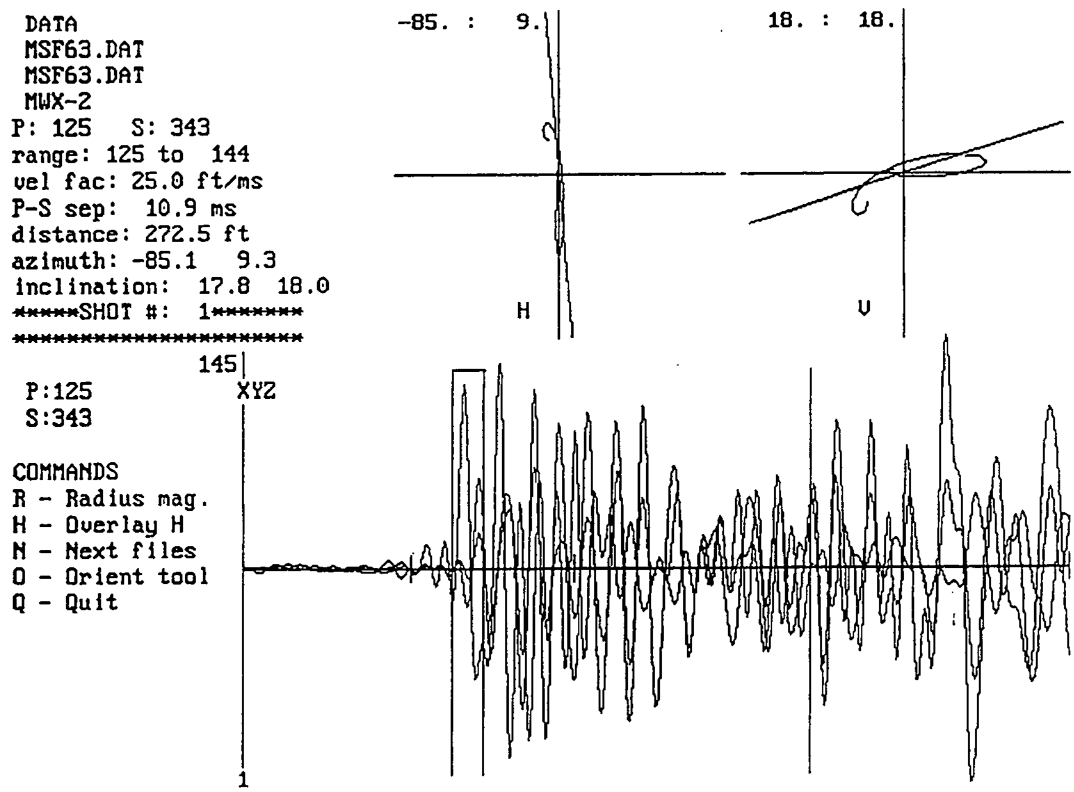

Figure A44 Event 63

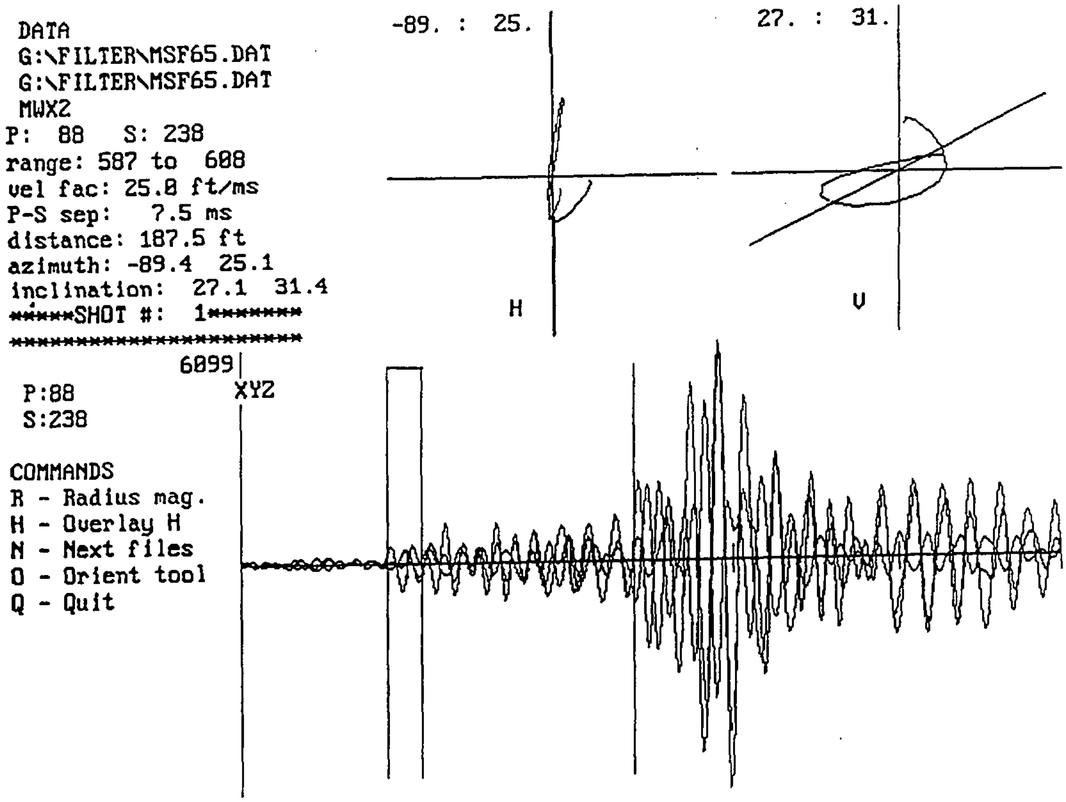

Figure A45 Event 65

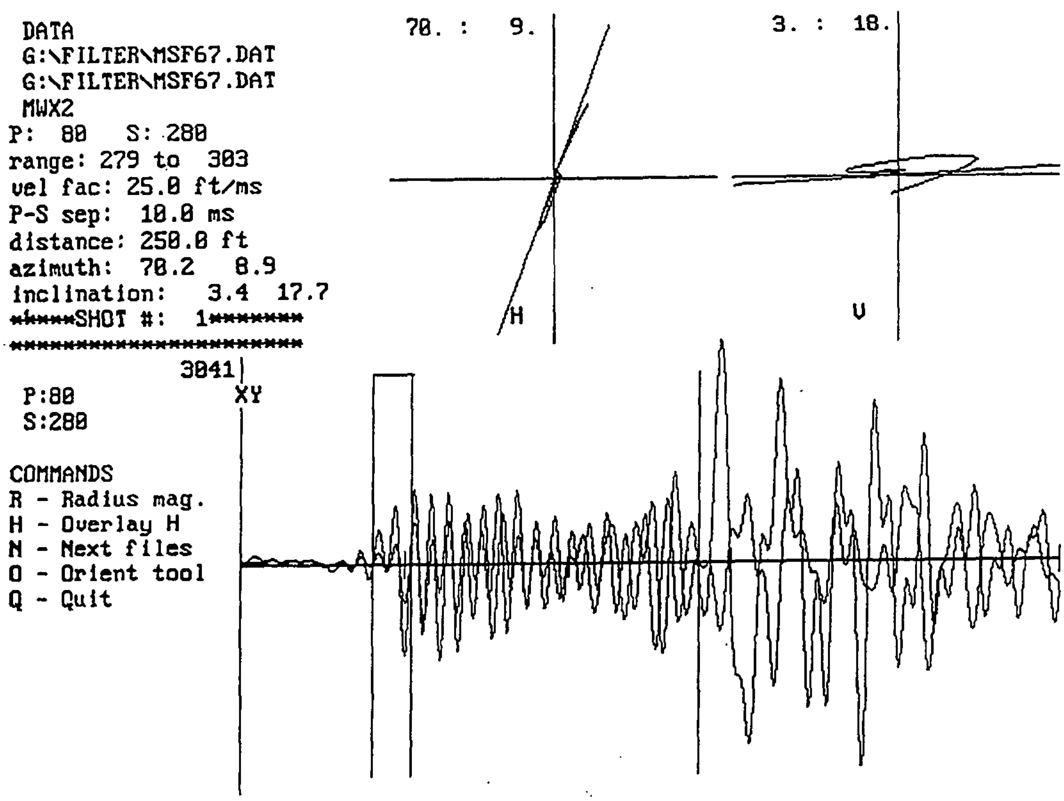

Figure A46 Event 67